1-1-2002

Polyolefin cubic silsesquioxane nanocomposites.

Lei Zheng
University of Massachusetts Amherst

POLYOLEFIN CUBIC SILSESQUIOXANE NANOCOMPOSITES

A Dissertation Presented

by

LEI ZHENG

Submitted to the Graduate School of the
University of Massachusetts Amherst in partial fulfillment
of the requirements for the degree of

DOCTOR OF PHILOSOPHY

September 2002

Polymer Science and Engineering

POLYOLEFIN CUBIC SILSESQUIOXANE NANOCOMPOSITES

A Dissertation Presented

by

LEI ZHENG

Approved as to style and content by:

E. Bryan Coughlin, Co-Chair

Richard J. Farris, Co-Chair

Thomas J. McCarthy, Member

Vincent M. Rotello, Member

Thomas J. McCarthy, Head
Department of Polymer Science & Engineering

DEDICATION

To my loving wife and parents.

ACKNOWLEDGMENTS

I would like to express my sincere gratitude to my advisors, Professor Coughlin and Professor Farris. Their generosity and encouragement have made my Ph.D. study an enjoyable journey. I would like to thank them for their continued help and their guidance throughout my graduate career. I feel honored to be the first Ph.D. student to graduate from Coughlin's group. I treasure memories of setting-up the lab and running the first few experiments together with him. I also feel fortunate to have Professor Farris as my advisor. I particularly appreciate his introduction of polymer engineering to me, which dramatically broadened my horizon and made my graduate research more fascinating and rewarding.

I would also like to thank Professor McCarthy and Professor Rotello for their time and interest in serving as members on my thesis committee. Their helpful suggestions are appreciated. I am also grateful to Dr. Alan Waddon, whose insightful knowledge of X-ray diffraction has contributed significantly to this project.

I also give my regards to Farris and Coughlin group members both past and present. Those who have worked on related aspects of this project include Rajeswari Kasi, Huiqing Zhang, Elisabeth Haley and Dr. Amiya Tripathy. I feel indebted to them for their contributions. I would also like to thank Dr. Sheng Hong, one of my best friends, for his efforts and help regarding TEM characterization of the synthesized materials.

The Polymer Science and Engineering Department at UMass has been a fun and stimulating place to study and learn for four years. It has been an exciting and pleasant experience for me. I appreciate the help that I have received from people including

faculty, staff and students, for example, the assistance of Dr. L. Charles Dickinson and Dr. Stephen J. Eyles on high-temp NMR and GPC instruments.

I want to thank the NSF-supported Material Research Science and Engineering Center on polymers at UMmass (MRSEC) for financial support, Edwards Air Force Research Laboratory and Hybrid Plastics, Inc., that provided POSS materials. I also appreciate the generous scholarship from the Society of Plastic Engineers.

Finally, I would like to thank my parents for the support and encouragement that they provided me throughout my academic studies. My deepest appreciation goes to my wife, Lin, for her continuous love and support. She has been the most wonderful person in my life and a constant inspiration and motivation for me to achieve excellence.

ABSTRACT

POLYOLEFIN CUBIC SILSESQUIOXANE NANOCOMPOSITES

SEPTEMBER 2002

LEI ZHENG, B.S., PEKING UNIVERSITY

M.S., THE PENNSYLVANIA STATE UNIVERSITY, UNIVERSITY PARK

Ph. D., UNIVERSITY OF MASSACHUSETTS AMHERST

Directed by: Professor E. Bryan Coughlin and Professor Richard J. Farris

This thesis focuses on the synthesis and characterization of polyolefin nanocomposites containing polyhedral oligomeric silsesquioxane (POSS) units. Two copolymerization methods were developed utilizing either ring-opening metathesis polymerization or metallocene-catalyzed reactions to incorporate cubic silsesquioxane into polyolefins. Ring-opening metathesis copolymerizations of cyclooctene and the POSS-norbornylene macromonomer have been performed using Grubbs' catalyst $RuCl_2(=CHPh)(PCy_3)_2$. Random copolymers have been prepared and characterized with POSS loadings as high as 55 wt%. Diimide reduction of these copolymers affords polyethylene-POSS random copolymers. Polyethylene (PE) and isotactic polypropylene (PP) copolymers incorporating POSS have also been prepared using a metallocene / methylaluminoxane (MAO) cocatalyst system. A wide range of POSS concentrations was obtained in these polyolefin POSS copolymers under mild conditions; up to 56 wt% for PE-POSS copolymers and 73 wt% for PP-POSS copolymers were prepared. Copolymerizations of styrene and the POSS-styryl macromonomer have been performed

using $CpTiCl_3$ in conjunction with MAO. Random copolymers of syndiotactic polystyrene and POSS copolymers have been formed and characterized.

Novel nanocomposites of PE-POSS have been characterized using Wide Angle X-ray Scattering (WAXS). From both line broadening of the diffraction maxima and also the oriented diffraction in a drawn sample, we conclude that POSS forms anisotropically shaped crystallites. On the basis of this result, a novel approach to obtain nanocomposites containing inorganic nanolayers is proposed. Cubic silsesquioxane (POSS) nanoparticles are used to achieve the nanolayered "clay-like" structure through controlled self-assembly. The organic polymer, covalently connected to POSS, is intended to regulate the POSS crystallization into a two-dimensional lattice. The concept is demonstrated by random copolymers of polybutadiene and POSS. The data from WAXS and transmission electron microscopy clearly show the formation of lamellar nanostructure of POSS aggregates, which bares the similarity at low POSS loadings to the morphology of exfoliated polymer clay nanocomposites. By taking the advantage of controlled interactions between polymer chains, we open the door to the design of polymeric materials at important nanometer length scales beyond their primary sequence length. Ultimately, this may provide materials with properties bridging the performance gap between polymer and ceramics.

TABLE OF CONTENTS

LIST OF TABLES

LIST OF FIGURES

CHAPTER 1

INTRODUCTION

1.1 Dissertation Overview

This thesis describes new processes for the synthesis of polyolefin nanocomposites that containing polyhedral oligomeric silsesquioxane (POSS)[1] nanoparticles as well as their properties and microstructures of these composite materials.

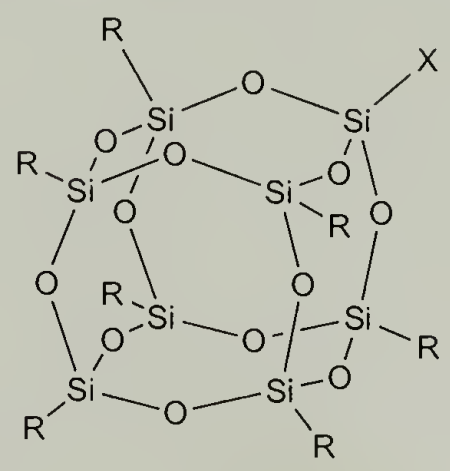

Figure 1.1 POSS Macromonomer Structure

Organic-inorganic nanocomposite materials[2-7] have drawn a great deal of attention due to their potential to bridge the gap between organic polymers and inorganic ceramics. In particular, the use of POSS macromonomers/nanoparticles (Figure 1.1) has been demonstrated to be an efficient method to design hybrid nanocomposite materials.[6,8-19] A typical POSS macromonomer has an inorganic Si_8O_{12} core surrounded by seven organic groups **R** (e.g. cyclopentyl or cycylohexyl) on the corners promoting solubility in conventional solvents and one unique corner group **X** capable of undergoing polymerization. Although a few POSS-containing polymers have been prepared previously, including polysiloxane,[9,16] poly(methyl methacrylate),[10] poly(4-methyl styrene),[11,13] epoxy,[12,14] polynorbornene,[15] and polyurethane,[18,19] no efficient methods to

synthesize polyolefin POSS copolymers have been developed prior to this study. Simple polymers, such as polyethylene-, polypropylene- and polybutadiene-POSS copolymers, were not readily available. These nanocomposites are important considering the large-scale industrial production of polyolefins. We have developed efficient synthetic routes to these materials.

This has been accomplished with two preparative routes. First, ring-opening metathesis copolymerization (ROMP) will be utilized for the preparation of polycyclooctenamer-POSS (Chapter 2), and polybutadiene-POSS copolymers (Chapter 6). Coupled with hydrogenation, this provides polyethylene-POSS copolymers. Second, metallocene-catalyzed reactions were employed to produce polyethylene-POSS and polypropylene-POSS copolymers (Chapter 3). POSS-containing copolymers were also extended to syndiotactic polystyrene (Chapter 4). The thermal and mechanical properties of polyethylene-POSS copolymers have been characterized (Chapter 3) and a microstructure of these materials has been proposed based on X-ray studies (Chapter 5). The strategy of self-assembly of POSS nanoparticles, to obtain a "clay-like" layered nanostructure, has been explored (Chapter 6). Polymer chains regulate the growth of POSS into a two-dimensional crystalline lattice. It is anticipated that one or more of these approaches will markedly advance the synthesis in nanocomposite science and technology, not only through the availability of polyolefin-POSS nanocomposites, but also through the efficient strategies, such as self-assembly, to synthesize them.

1.2 Nanocomposites

Composite materials are common in the production of modern plastics. A second component is often added to polymeric materials to enhance properties, such as thermal

stability and mechanical strength. Most of these systems are considered macro- or micro-composites according to the dimensional size of the second component, such as the well-known glass fiber. Their properties depend mainly on the interfacial interactions between the matrix and particles or fibers. Recently interests are been drawn to nanocomposite materials,[2-7] typically referring to discontinuous particulate inclusion with one major dimension on the length scale of 1-100 nanometers.[20] These materials have shown novel and often improved mechanical, thermal, electronic, magnetic, and optical properties.[21] It is recognized that behaviors at the nanoscale are not necessarily predictable from that observed at larger length scales. This is presumably due to the predominant interfacial interaction between ultrafine nanoparticles and polymer segments. Although the two-phase composite may be organic-organic, inorganic-inorganic, or organic-inorganic, the latter composite is more desirable from the standpoint of combined advantageous performance relative to either of the non-hybrid counterparts. For example, glass fibers can be introduced into a polymer matrix to obtain a composite with combined properties of improved mechanical strength from the glass fibers and easy of processing attributable to the polymer. It is envisaged that organic-inorganic nanocomposite materials have the potential to bridge the material performance gap between ceramics and polymers.

Organic-inorganic nanocomposites are also widespread in biological systems, for examples bones, cuticles, shells, and teeth. Detailed studies indicate that they are typically composed of alternating inorganic layers comprising carbonate, phosphate, or silica and organic layers of carbohydrate, lipid, or protein at the nanometer length scale.[22] The mechanism of "biomineralization" utilized by nature to efficiently produce well-defined nanocomposites is not entirely clear. It is generally believed that it is a templated

self-assembly process in which pre-organized organic surfaces regulate the nucleation, growth, morphology and orientation of inorganic crystals.[23] These materials offer superior strength, hardness and toughness. For example, the nacre of abalone shell, which is composed of alternating layers of aragonite ($CaCO_3$) and 1 vol.% of proteins and polysaccharides, is twice as hard and 1,000 times as tough as its constituent phases.[24]

Organic-inorganic nanocomposites are commonly synthesized by one of four strategies: sol-gel processing, host-guest inclusions, use of inorganic nanoparticles or clusters, or a "biomimetic" approach. A combination of these strategies is sometimes used. The sol-gel process involves condensation reactions of small inorganic precursors, such as $(RO)_3Si$-Y. (Here Y is an organic polymer chain or organic monomer that can be eventually polymerized to form a polymer.). Normally a silylalkoxide is allowed to undergo controlled hydrolysis to produce an inorganic network and incorporate the low molecular weight organic polymer in the inorganic matrix. The process can offer relatively homogenous composites with good control over particle size and morphology.[5] Fine tailoring of structural features, especially in the nanometer range, is a challenge for this approach. It is important to control and tune the beneficial phenomena associated with nanostructures. The use of structurally well-defined inorganic nanoparticles or clusters as building blocks provides a good strategy.[25] Although preparations of these nanoparticles requires some effort to establish a methodology to form covalently or ionically bonded nanoparticles, this approach can alleviate the problem of microphase separation through having the nanoparticles covalently bonded to the polymer. Host-guest inclusion chemistry refers to intercalation reactions of polymer chains into preformed host structures. Notable examples are the mesoporous zeolites as 3-D hosts[26-28]

and organo-clays as 2-D hosts[2,3,29]. Equivalently we can define nanoparticles as 0-D host and nanowires or nanotubes as 1-D host from consideration of their dimensional shapes. The problem associated with this approach is the difficulty of diffusing a polymer chain into the host due to unfavorable interactions between the hydrophilic surface of the host and hydrophobic organic polymers chains. The so-called "biomimetic" strategy involves "the study of biological structures, their functions and their synthetic pathways in order to stimulate new ideas and to develop these ideas into synthetic systems similar to those found in biological systems".[30] It includes crystallization beneath Langmuir monolayers,[31] crystallization on self-assembly monolyers,[32,33] surfactant templated self-assembly,[34-36] and sequential deposition.[37] Among them, only the latter two offer the ability to introduce periodic nanostructures. With regard to the surfactant templated self-assembly approach, the resulting structures are usually unstable and collapse upon surfactant removal.[38] Layer-by-layer deposition has also been used to produce nanocomposites.[37] However it is time-consuming due to the repeated deposition steps required to generate a practical coating, not to mention the production of bulk material. To my best knowledge, all the "biomimetic" approaches so far can produce only nanocomposite coatings. To obtain bulk composite materials with controlled nanostructures has not been achieved.

1.3 Polymer Clay Nanocomposites

Research, with potentials to apply nanocomposites as structure materials with good mechanical attributes, has been mainly focusing on either the use of organo-clay through guest-host chemistry, or the use of nanoparticles of polyhedral oligomeric silsesquioxane (POSS) nanoparticles. The key inorganic components of clays are layered

silicates such as montmorillonite, where each individual layer is composed of a central octahedral alumina sheet sandwiched in between two tetrahedral silica sheets.[2] The surfaces of clays are comprised of trivalent alunimium ions, some divalent magnesium ions or monovalent sodium or lithium ions exchanged from aluminum. A challenge to use clays to modify polymers is that their hydrophilic surfaces are not compatible with hydrophobic organic polymers. As a result, it is necessary to modify the clay surfaces. One of the earliest examples by Jordan and Williams in 1954 showed that organophilic bentonites could be to used to reinforce a latex through modification of bentonite surfaces using hydrolysis of $(RO)_3Si(CH_2)_3X$ (X is $CH{=}CH_2$, Cl, NH_2 or SH to interact with polymer).[39] Progress in this field developed quickly in recent years, stimulated by the results reported from a research group at Toyota in 1987 that using cation exchange with alkyl ammonium ions made the clay surface compatible with polymers.[40] Replacement of the inorganic exchange cations in the galleries of the native clay by alkyl ammonium surfactants followed by polymerization of ε-caprolactam in the interlayer gallery region of the organoclay, resulted in a true nylon-6 clay nanocomposites.[4] When the clays were exfoliated, well dispersed into each individual layer, dramatic changes of properties were observed. At a loading of 4.2 wt% clay, the modulus almost doubled and the strength increased by more than 50% while the distortion temperature increased by 80 °C compared with virgin polymer. Improved dimensional stability, barrier properties and flame retardant properties were also subsequently reported.[3] Although the use of organoclays to form nanocomposites have been extended to epoxys, polyurethanes, nitrile rubber, polyester, polypropylene, polystyrene and polysiloxanes, the true nanocomposites, in which the nanoclay are uniformly dispersed, are successful only in

selected systems.[41] The obstacle remains the unfavorable interfacial interaction between clays and polymers. Attempt to overcome it has been done by adding compatibilizers. For example, polypropylene clay nanocomposites are synthesized by adding maleic anhydride functionalized polypropylene oligomers as surface modifiers of clays.[42] The enhancement of properties are not as great as in nylon-6, possibly due to a lower degree of exfoliation and introduction of a large amount of oligomers (~20 wt%).

1.4 Polyhedral Oligomeric Silsesquioxane (POSS) and Polymer POSS Nanocomposites

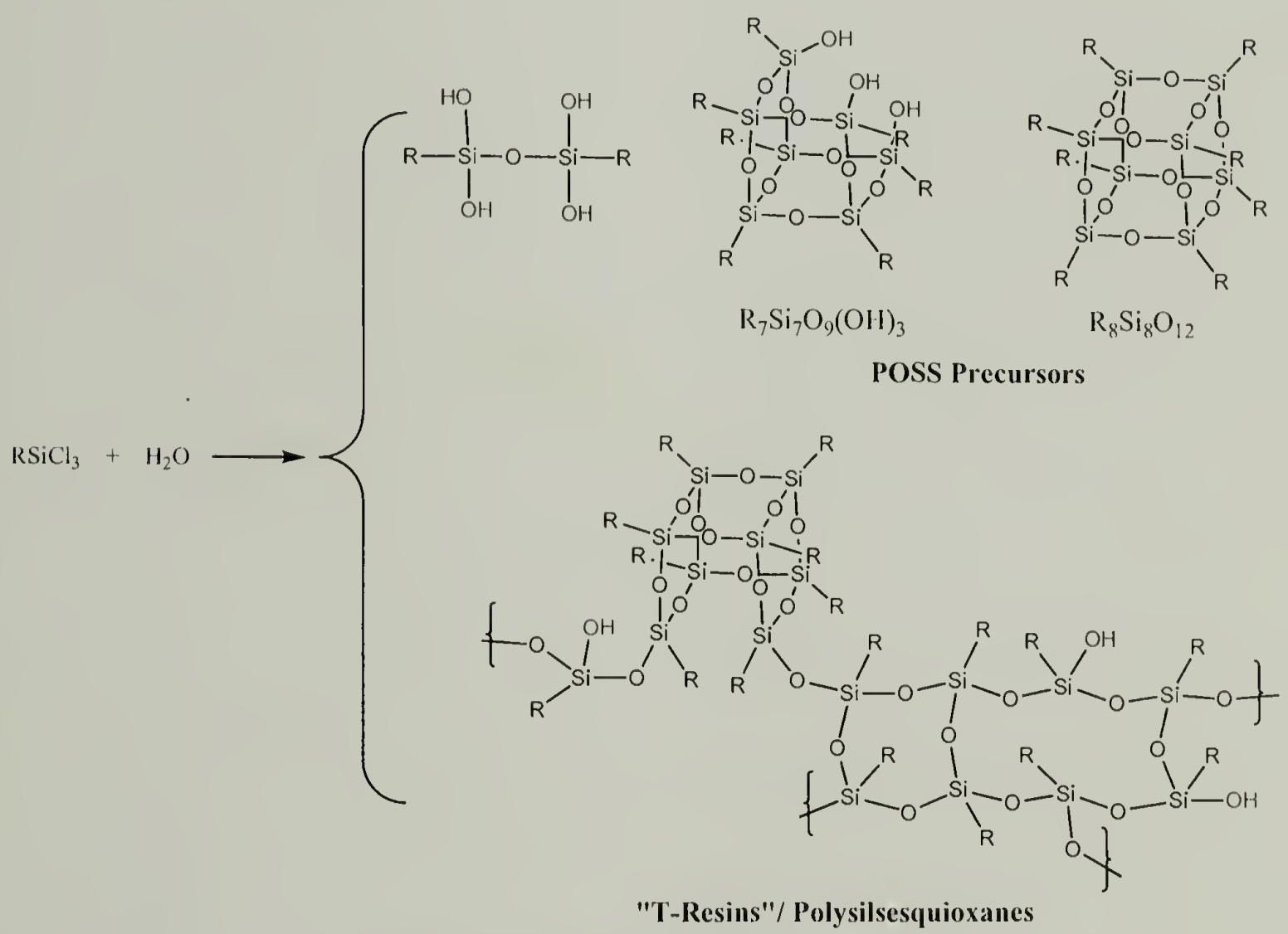

Figure 1.2 Synthesis of POSS Precursors

POSS and clays are similar since both are comprised of silicon oxygen frameworks. A typical cubic silsesquioxane unit contains an inorganic Si_8O_{12}

nanostructured skeleton surrounded by eight organic groups **R** (eg. isobutyl, cyclopentyl or cycylohexyl) on the corners to promote solubility in the conventional solvents and compatibility. Silsesquioxanes have the empirical formula $RSiO_{3/2}$, with their names derived from the one and one-half ratio (*sesqui*) between oxygen and silicon atoms. They were first reported by researchers at General Electric in 1965[43] and further studied by Feher *et. al.* in recent years.[44] It is discovered that kinetically hydrolytic condensation reaction of $RSiCl_3$ in aqueous acetone can yield two predominant stable structures: a fully condensed $R_8Si_8O_{12}$ cube and an incompletely condensed $R_7Si_7O_9(OH)_3$ trisilanol (Figure 1.2). Due to slow reaction times (typically days to years), the POSS nanoparticles were not commercialized until more efficient routes were further developed at Edward Air Force Research Lab in California and Hybrid Plastic, Inc. through hydrolysis of partially condensed oligomeric silsesquioxanes. Notable among the procedures is the ability to prepare macromonomers from $R_7Si_7O_9(OH)_3$ trisilanol with the inorganic core surrounded by seven hydrocarbyl groups, and a unique functional group capable of undergoing polymerization. For instance, the POSS-norbornylene, which has a polymerizable norbornene substitution on one silicon corner, can be synthesized according to the reaction in Figure 1.3.[15] A variety of functional groups, such as styrene, methacrylate and epoxide, have been attached in similar approaches.[10-12] This has provided the possibility to incorporate inorganic POSS cages into organic matrixes through copolymerization. The resulting nanocomposites, with nanosized silica covalently bonded to polymer matrixes, are otherwise difficult to synthesize. The use of POSS macromonomers, which are covalently connected to polymer chains, is superior to the use of POSS nanoparticles $R_8Si_8O_{12}$ for blending, since this prevents large phase

separation of POSS nanoparticles incompatible with the polymer matrix. In addition, the beneficial influence of chain dynamics can be shown only when POSS is covalently bonded to polymer chains. A variety of POSS-containing copolymers has been prepared using radical, both conventional and atom transfer protocols, condensation, and ring-opening metathesis polymerization techniques, including poly(methyl methacrylate), polystyrene, epoxy, polysiloxane and polynorbornene copolymers. A summary of these polymerizations is listed in Table 1.1.

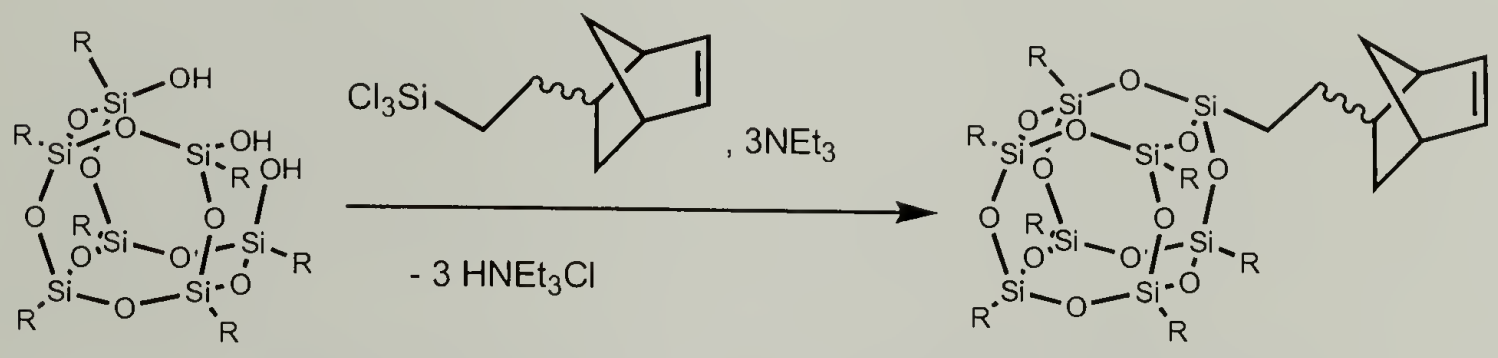

Figure 1.3 Synthesis of POSS-norbornylene Macromonomer

The physical aspects of POSS-containing copolymers are fascinating. Lee and Lichtenhan reported viscoelastic responses of POSS epoxy crosslinked system.[12] The glass transition temperature was observed to increase and broaden with increasing POSS loadings. This observation was attributed to the nanoscopic size of POSS particles, which hinder the motion of molecular chain network junctions. Rheological measurements on linear amorphous poly(4-methyl styrene)-co-POSS copolymers showed a high temperature rubbery plateau, which supported the argument that the interchain association interactions between POSS nanoparticles were responsible for the retardation of polymer chain motion.[13] Microstructural analysis based on mechanical relaxation of amorphous polynorbornene-co-POSS copolymers with different substituted groups on

POSS and WAXS data indicated a POSS aggregation at nanometer scale with better ordering in cyclopentyl substituted POSS than in cyclohexyl substituted POSS.[15]

Table 1.1 POSS Copolymers

Polymer	Monomer	Comonomer	Method to Polymerize	Reference
homopolymer	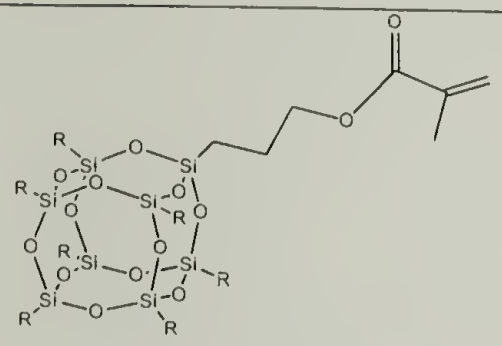	N.A.*	AIBN	10
homo and random copolymers	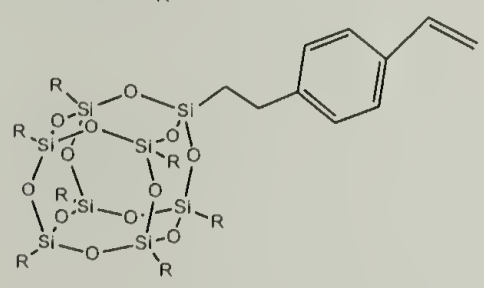	4-methyl styrene	AIBN	11
random copolymer	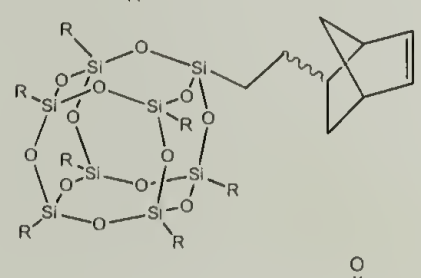	norbornene	ROMP	15
homo and block copolymer	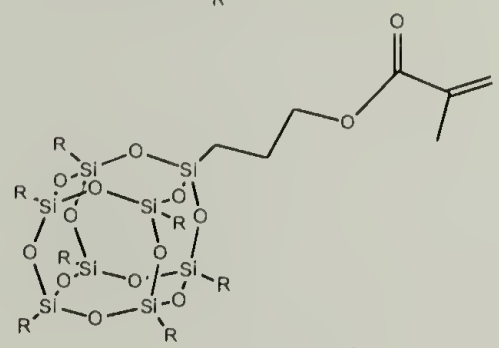	methyl acrylate	ATRP	45
N. A.	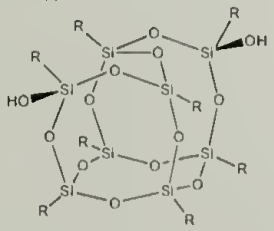	X-$SiMe_2$-X (X = Cl, NMe_2)	condensation	9
N. A.	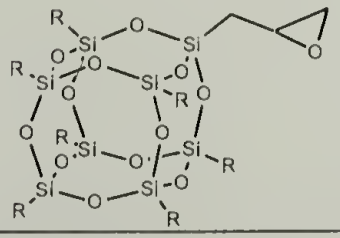	BDGE and Jeffamine D230**	condensation	12,14

*Not Applicable. ** BDGE: 1,4-butanediol diglycidyl ether; Jeffamine: diamine terminated poly(propylene oxide).

Interestingly, a report based on atomistic molecular dynamics simulations of the same system concluded that aggregation of the POSS nanoparticles was not required for the reinforcement effects such as the increase in glass transition temperature and retardation of chain dynamics. The lack of mobility of POSS nanoparticles, with an approximate spherical diameter of 1.5 nm, was reasoned to be the primary source for the beneficial effects.[46]

The POSS nanoparticles are different from organoclay nano-filler in many respects. First of all, it has a hydrophobic "coating". The peripheral groups **R** are typically isobutyl, cyclopentyl or cyclohexyl, due to available synthetic methods. Substitution groups such as methyl, ethyl, vinyl, and norbornenyl are also available. More groups can be obtained from further derivitization of vinyl groups. Since a variety of substituted groups are available, the POSS nanoparticles have the potential to be compatible with many hydrocarbon polymers. To the contrary, the surface modifications of organoclay are limited.

Another important distinction between POSS and clay is their shapes. Exfoliated clays have a large aspect ratio of 100-2000 with a thickness of 10 Å while POSS nanoparticles $Cp_8Si_8O_{12}$ (Cp = Cyclopentyl) are close to spherical with molecular diameter of about 15 Å and a Si-Si distance crossing the cube of 5.4 Å. POSS nanoparticles can be considered as a unit cell of or "molecular" silica while the nanoclay particles are silicate sheets. Because of the high aspect ratio, nanoclays impart anisotropy to the modified polymer system. Parallel to the length of the nanoclay particles, modulus, impact and toughness are improved. Perpendicular to the length of the nanoclay particles, modulus, impact and toughness are reduced. POSS nanoparticles should have the same

impact strength in all directions. In terms of the barrier property, it is well known that organoclay nanocomposites show enhanced impermeability due to an increased diffusional path. Whether or not POSS has similar effect is not clear. It is apparent that POSS nanoparticles will not have anisotropical effects unless layered assembly can be achieved.

Full comparisons of POSS, organoclay nanoparticles and traditional nanofillers can be found elsewhere.[47] A few of the advantages of POSS particles are noted. POSS particles are well defined, made of silicon, oxygen atoms and hydrocarbon peripheries. They have the potential of being biocompatible for medical applications. Their sizes are too small to diffract lights so that uses in optical devises are also possible. They also have the potential for electronic applications, for example the application as low dielectric constant materials. POSS particles have also been commercialized for coating application by Hybrid Plastics Inc. It is claimed that the coating has high flammability resistance, excellent dielectric properties and low moisture permeability.

From a nanoscience and nanotechnology point of view, two different approaches are taken to synthesize of organoclays and POSS nanocomposites. The synthesis of organoclay nanocomposites start with the clays aggregates and disperse them into individual layers, which is a top-down approach. In contrast, the well-defined POSS nanoparticles are synthesized from small molecule precursors. They can be further assembled into larger architectures based on the self-assembly mechanism. As a bottom-up approach, the POSS nanoparticles can be considered building blocks of larger hierarchical structures.

CHAPTER 2

SYNTHESIS OF POLYETHYLENE HYBRID COPOLYMERS CONTAINING CUBIC SILSESQUIOXANE PREPARED USING RING-OPENING METATHESIS COPOLYMERIZATION

2.1 Introduction

Hybrid materials with both an inorganic and organic component are of interest from the standpoint of increased performance capabilities relative to either of the non-hybrid counterparts. A variety of physical properties enhancements are expected to result from incorporation of an inorganic component into an organic polymer matrix, for example improved thermal stability. The use of polyhedral oligomeric silsesquioxanes (POSS) as modifiers of organic polymers has received a great deal of attention recently.[8] This is due, in part, to the development of efficient synthetic protocols for the preparation of the inorganic Si_8O_{12} core. Notable is the ability to prepare a unique group capable of undergoing polymerization on the inorganic core.[16] One special feature about POSS particles is that their size, ~ 15 Å in diameter, is comparable to that of polymer segments. By placing nanometer scale inorganic particles into organic polymers, we may dramatically enhance the physical properties of the resulting copolymers due to the sizable interfacial interactions between composite particles and polymer segments. For example, chain dynamics may be altered dramatically by incorporation of POSS nanoparticles on to the chain.

A variety of POSS containing amorphous polymers, including poly(methyl methacrylate),[10,45] polystyrene,[11] epoxide,[12] polysiloxane[9] and polynorbornene[15] copolymers, have been prepared using radical, conventional[10,11] and atom transfer

protocols,[45] condensation,[9,12] and ring opening metathesis (ROMP)[15] polymerization techniques. However, there are few reports of semi-crystalline copolymers.[19] Simple copolymers such as polyethylene-POSS have not been prepared in accordance with the development of more efficient routes to prepare POSS macromonomers. A preliminary report suggested that POSS macromonomers were not able of undergoing coordination polymerization using Ziegler-Natta catalysis, presumably due to their large dimensional size of POSS macromonomers.[16] The copolymers of polyethylene POSS are desired, since interesting rheology behavior as well as thermal and mechanical properties are expected. Noteworthy is that polyethylene clay nanocomposites, somewhat akin to polyethylene POSS nanocomposites, have failed to produce complete dispersal or exfoliation of clay nanolayers due to unfavorable interaction between hydrophilic clay and hydrophobic polyolefin.[41] Therefore, the synthesis of polyethylene POSS copolymers is crucial to develop an understanding of this type of hybrid material since the POSS nanoparticles have the potential to be well distributed into a polyethylene matrix through copolymerization or *via* modification of the POSS periphery.

Herein a two step synthetic route was described for preparing semi-crystalline polyethylene POSS copolymers that exhibit a large degree of control over the incorporation levels of the POSS comonomer. Our strategy involved a ring-opening metathesis copolymerization of cyclooctene and POSS monomer **1** containing one norbornylene, and seven cyclopentyl side groups. The initially formed copolymers are polycyclooctenamer-POSS random copolymers. Then diimide reduction was used to completely remove the unsaturated units from the polymer backbone to afford polyethylene-POSS copolymers.

2.2 Experimental

2.2.1 Materials

Cyclopentyl-POSS-norbornylene monomer 1-[2-(5-norbornen-2-yl)ethyl]-3,5,7,9,11,13,15-heptacyclopentylpentacyclo[9.5.1.$1^{3,9}$.$1^{5,15}$.$1^{7,13}$] octasiloxane (**1**) was provided by the Air Force Research Laboratory, Propulsion Directorate, AFRL/PRSM, Edwards Air Force Base, California. Other reagents were obtained from Aldrich and used as received unless otherwise indicated. Grubbs's catalyst[48] $RuCl_2(=CHPh)(PCy_3)_2$ was purchased from Strem Chemical. *cis*-Cyclooctene and tri-n-propyl amine were vacuum distilled from CaH_2 prior to use. Methylene chloride and xylenes were passed through columns of basic activated alumina prior to use.

2.2.2 Polymer Characterization

^{1}H spectra were obtained at 300 MHz and 500 MHz using Bruker DPX-300 and AMX-500 FT NMR spectrometers. ^{13}C NMR were recorded at 90 °C in toluene-d_8 or tetrachloroethane-d_2 with a Bruker AMX-500 FT NMR spectrometer operating at 125 MHz. Gel permeation chromatography was performed using a Polymer Lab LC1120 HPLC pump equipped with a Waters differential refractometer detector. The mobile phase was THF with a flow rate of 1 mL/min. Separations were performed using 10^5 Å, 10^4 Å and 10^3 Å Polymer Lab columns. Molecular weights were calibrated versus narrow molecular weight polystyrene standards.

Differential scanning calorimetry was performed on a TA Instruments DSC 2910 equipped with a liquid nitrogen cooling accessory (LNCA) unit under a continuous nitrogen purge (50 mL/min). Data were gathered on the second melt using a heating and

cooling scan rate of 10 °C/min unless otherwise noted. Thermogravimetric analysis was carried out using a TA Instruments TGA 2050 thermogravimetric analyzer with a heating rate of 20 °C/min from room temperature to 700 °C under a continuous nitrogen or air purge (nitrogen 100 mL/min, air 50 mL/min).

2.2.3 Procedures for Homopolymerization of POSS-norbornylene

4.87 mg (6 μmol) of $RuCl_2(=CHPh)(PCy_3)_2$ was dissolved in 1 mL of CH_2Cl_2 and added to a solution of 0.33 g **1** (0.32 mmol, 10 wt%) in 1.5 mL of CH_2Cl_2. The reaction mixture was stirred for 2 hours at room temperature. The reaction was stopped by injection of 5 mL CH_2Cl_2 containing a trace amount of ethyl vinyl ether. The polymer was precipitated in 50 mL methanol, recovered by filtration and dried overnight under vacuum at room temperature. The isolated yield was 0.29 g (88 %).

2.2.4 General Procedures for Copolymerizations of Cyclooctene and POSS-norbornylene

4.87 mg (6 μmol) of $RuCl_2(=CHPh)(PCy_3)_2$ was dissolved in 1 mL of CH_2Cl_2 and added to a solution of 0.33 g *cis*-cyclooctene (3 mmol, 500 equiv.) and 0.0367 g **1** (0.036 mmol, 10 wt%) in 1.5 mL of CH_2Cl_2. The reaction mixture was stirred for 2 hours at room temperature. The reaction was stopped by injection of 5 mL CH_2Cl_2 containing a trace amount of ethyl vinyl ether. The polymer was precipitated in 50 mL methanol, recovered by filtration and dried overnight under vacuum at room temperature. The polymerizations were repeated using varying amounts of **1**, 0-50 wt%, to prepare a range of copolymers. The isolated yields were generally above 90%.

2.2.5 General Procedures Hydrogenation of Polycyclooctenamer-POSS Copolymers

The polymer backbone was hydrogenated using p-toluenesulfonylhydrazide (TSH) in refluxing xylenes using a slight modification of a literature procedure.[49] To a solution of 0.30 g polycyclooctenamer-POSS copolymers in 20 mL xylenes was added p-toluenesulfonylhydrazide and tri-n-propyl amine. (A ratio of 2 mol of TSH and 2 mol of amine per mol of olefin on the backbones was used.) The solution was heated to reflux for 4 h under a positive pressure of nitrogen. The resulting polyethylene-POSS copolymers were isolated by cooling the xylenes solution to room temperature and precipitating in large excess of methanol. The copolymers were filtered and washed with methanol before being dried in a vacuum oven overnight at 60 °C. The extent of hydrogenation was judged, in all cases, to be greater than 99% based on ^{1}H NMR spectroscopy.

2.3 Results and Discussion

2.3.1 Homopolymerization of POSS-norbornylene

In spite of the large size of POSS cages, the ring-opening metathesis polymerization of POSS **1** went smoothly. Based on ^{1}H NMR, the reaction was complete in a few minutes. However a reaction time of two hours was used to obtain similar microstructure (e.g. trans/cis ratio of backbone double bonds) for comparison with the copolymers. The weight average molecular weight is estimated to be 41 kg/mol (DP = 41) with a polydispersity of 1.5 according GPC versus polystyrene standards. The polymer is soluble in most non-polar organic solvents, such as hexanes and ether. Interestingly, the ^{1}H NMR shows very broad olefinic peaks at room temperature (Figure

2.2a), which strongly indicates restricted backbone mobility in solution. Upon heating to 100 °C, the flexibility of polymer backbone is still relatively low with only partial resolution of the olefinic resonance in ^{1}H NMR (Figure 2.2b). The backbone of the homopolymer is very rigid in solution demonstrating that incorporation of POSS into polymer chains has dramatically retarded the chain movement and changed chain dynamics in solution due to its large dimensional size.

2.3.2 Copolymerizations of Cyclooctene and POSS-norbornylene

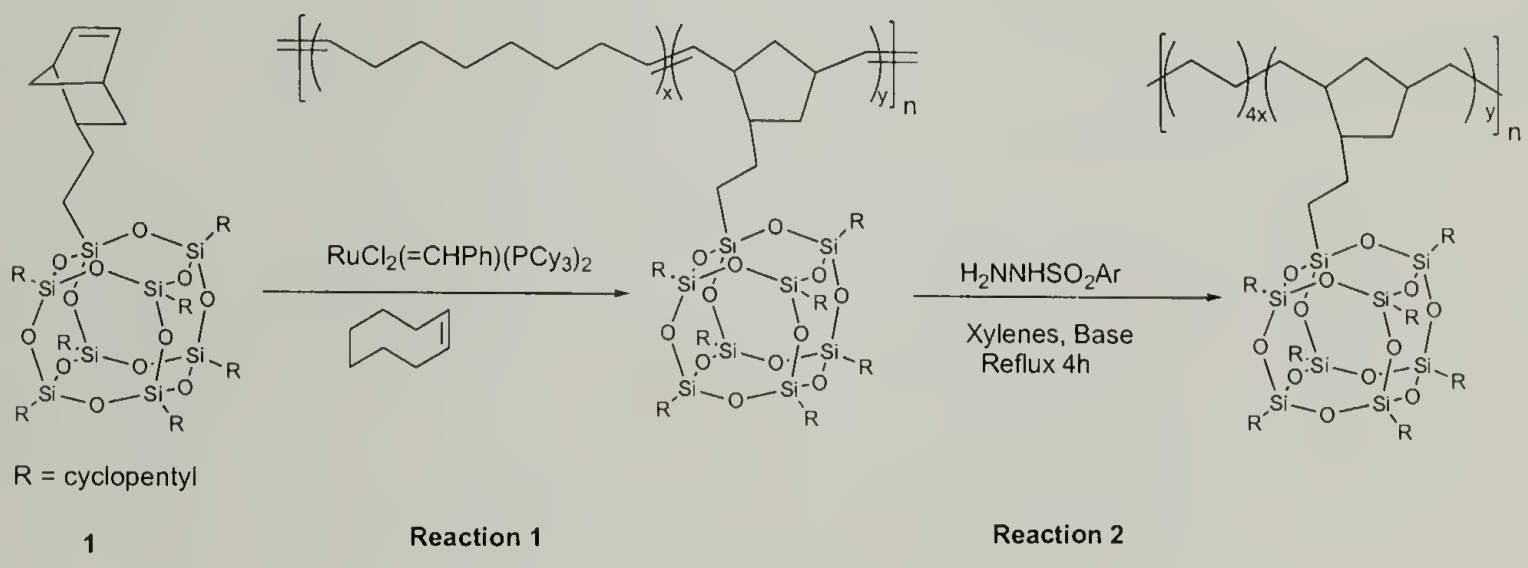

Figure 2.1 Copolymerization of Cyclooctene and POSS-norbornylene and Hydrogenation

Ring-opening metathesis polymerization has proven to be a versatile approach for the preparation of polymers with a wide range of functionalities and macromolecular architectures.[50] We have employed Grubbs' catalyst $RuCl_2(=CHPh)(PCy_3)_2$, for the copolymerization of cyclooctene and **1** to make the model copolymers for this study (Figure 2.1, reaction 1). The molar ratio of cyclooctene to catalyst was fixed at 500:1 to yield moderately high molecular weight polycyclooctenamer. For the various copolymerizations, **1** was added in the range of 10-50 wt%, relative to cyclooctene, prior to addition of catalyst. We were limited to a maximum of 50 wt% of **1** in the reaction

feed due to solubility limitations. The copolymerizations remained visibly homogenous throughout the entire reaction. The reactions were terminated by injection of a solution of ethyl vinyl ether in CH_2Cl_2, followed by precipitation into methanol. All isolated yields were greater than 90%. The level of incorporation of **1** in the copolymers was determined using ^{1}H NMR by monitoring the resonances for the cyclopentyl groups of POSS cages. A steady increase in the level of incorporation in the copolymers was seen as the amount of **1** in the feed increased (Figure 2.3). The calculated concentrations of POSS in the copolymers are consistent with the feed ratio. The molecular weight characterization data of the polycyclooctenamer-POSS copolymers are listed in Table 2.1. The molecular weight and polydispersity of the copolymers both increase with increasing comonomer incorporation.

From ^{1}H NMR reaction studies the addition of $RuCl_2(=CHPh)(PCy_3)_2$ to a mixture of **1** and cyclooctene in $CDCl_3$ shows very rapid consumption of **1**. The complete disappearance of the norbornylene vinyl resonances is seen in minutes, followed by a slower disappearance of the cyclooctene vinyl resonance. Rather than isolating a blocky copolymer, sufficiently long reaction times was chosen to allow for significant inter-chain cross metathesis to occur to ultimately afford a random copolymer. The ability to successfully perform this copolymerization relies on the tricyclohexylphosphine ligands of the catalyst to ensure that cross metathesis of norbornylene and the less strained cyclooctene will occur.[51] Further evidence for efficient cross metathesis comes from ^{1}H NMR studies of the final copolymers. The ^{1}H NMR of the copolymer with 55 wt% POSS (Entry 6, Table 2.1) at 100 °C in $C_2D_2Cl_4$ does not show any characteristic olefinic peaks

from homopolyer of POSS-norbornylene (Figure 2.4) and therefore no significant amount of POSS-norbornylene block segments are present in the copolymer.

Thermal analysis of the polycyclooctenamer-POSS copolymers clearly showed a decrease in melting temperature, and concomitant heat of fusion, as the concentration of POSS increased, Figure 2.5. This observation is consistent with random incorporation of POSS comonomer along the polycyclooctenamer main chain, which is disrupting crystallinity. The evidence from decreasing melting temperatures, and from ^{1}H NMR clearly support the assumption that random copolymers were obtained. No glass transition temperature was observed for these copolymers, presumably due to their semi-crystalline nature.

The backbone unsaturation in the polycyclooctenamer-POSS copolymers was removed using diimide reduction, as shown in Figure 2.1 reaction 2.[49] The isolated yields of the hydrogenated copolymers were all above 90%, ^{1}H NMR showed complete saturation of the backbone. ^{1}H and ^{13}C NMR spectra of the hydrogenated product confirmed that the inorganic POSS cage structure was unaffected while the double bonds were cleanly hydrogenated.

2.3.3 Thermal Properties of PE-POSS Copolymers

The resulting polyethylene-POSS copolymers all displayed a decrease in the observed peak melting point as the wt % of **1** increased. No T_g was observed for these copolymers as well. The thermal properties of the saturated copolymers are shown in Table 2.2. Our results indicated a moderate increase in the thermal stability of these PE-POSS copolymers, with the onset of decomposition temperature increasing 12-17 °C for all of the POSS containing samples relative to the polyethylene control sample (entries 8-

12 vs. entry 7). The slight increase in the onset of decomposition temperature under nitrogen might be due to crosslinking between scissioned polyethylene chains and the POSS silicon core. More interestingly, a dramatic improvement was observed in the thermo-oxidative resistance of these PE-POSS copolymers when air was used as the carrier gas during TGA, Figure 2.6. For example, at 5 % weight loss the temperature of the PE-POSS copolymer with 12 wt% POSS was 368 °C compared with 298 °C for the polyethylene control sample (entry 8 vs 7). This increase of 70 °C indicates that the polyethylene modified by incorporation of POSS improves the thermal degradation behavior towards oxygen and enhances overall thermal stability. One possible explanation is the formation of a silica layer on the surface of the polymer melt in the presence of oxygen, which is serving as a barrier preventing further degradation of underlying polymer.[52] However, this improvement decreases as the POSS concentrations exceeds 23 wt% (entry 10-12). Further investigation is currently underway.

2.4 Conclusions

In summary, a two step synthetic route for preparing polyolethylene-POSS copolymers has been described. The ring-opening metathesis copolymerization of cyclooctene and **1** afforded random copolymers. Subsequent diimide reduction of these copolymers gave hybrid polyethylene-POSS copolymers. Preliminary results point to improved thermal stability and oxidative resistance of these hybrid copolymers relative to polyethylene.

Table 2.1 Summary of Molecular Weight Data of Polycyclooctenamer-POSS Copolymers

Entry	Wt% POSS in Feed	Wt% POSS in Copolymer[a]	Mol % POSS in Copolymer[a]	M_w[b] x10^{-3} (g/mol)	M_n[b] x10^{-3} (g/mol)	PDI	T_m[c] (°C)	ΔH_f[c] (J/g)
1	0	0	0	100	56	1.79	46	56
2	10	12	1.39	105	57	1.84	43	45
3	20	23	3.06	143	69	2.06	38	36
4	30	31	4.62	144	68	2.13	36	28
5	40	45	7.96	151	66	2.37	33	24
6	50	56	11.9	168	68	2.47	30	19

[a] Mol% and wt% POSS in copolymers as determined by ^{1}H NMR.
[b] Weight and number average molecular weight as measured by GPC relative to polystyrene standards.
[c] Data were gathered on the second melt using a heating rate of 10 °C/min on thermally quenched samples (quenching rate ~ 30 °C/min).

Table 2.2 Summary of Thermal Characteristics of Polyethylene-POSS Copolymers

Entry	Wt% POSS	T_m[a] (°C)	Heat of Fusion ΔH_f[a](J/g)	Onset of Decomp. Temp[b] (°C)	Char Yield in N_2[b] (%)	5% wt. Loss in Air[b](°C)	Char Yield in Air[b] (%)
7	0	133	200	449	0	298	2
8	12	130	134	461	1	368	5
9	23	126	112	461	1	362	8
10	31	122	75	466	1	329	4
11	45	115	61	462	1	290	19
12	56	115	41	463	2	326	21

[a] Data were gathered on the second melt using a heating and cooling rate of 10 °C/min.
[b] Temperature ramp 20 °C/min under nitrogen or air.

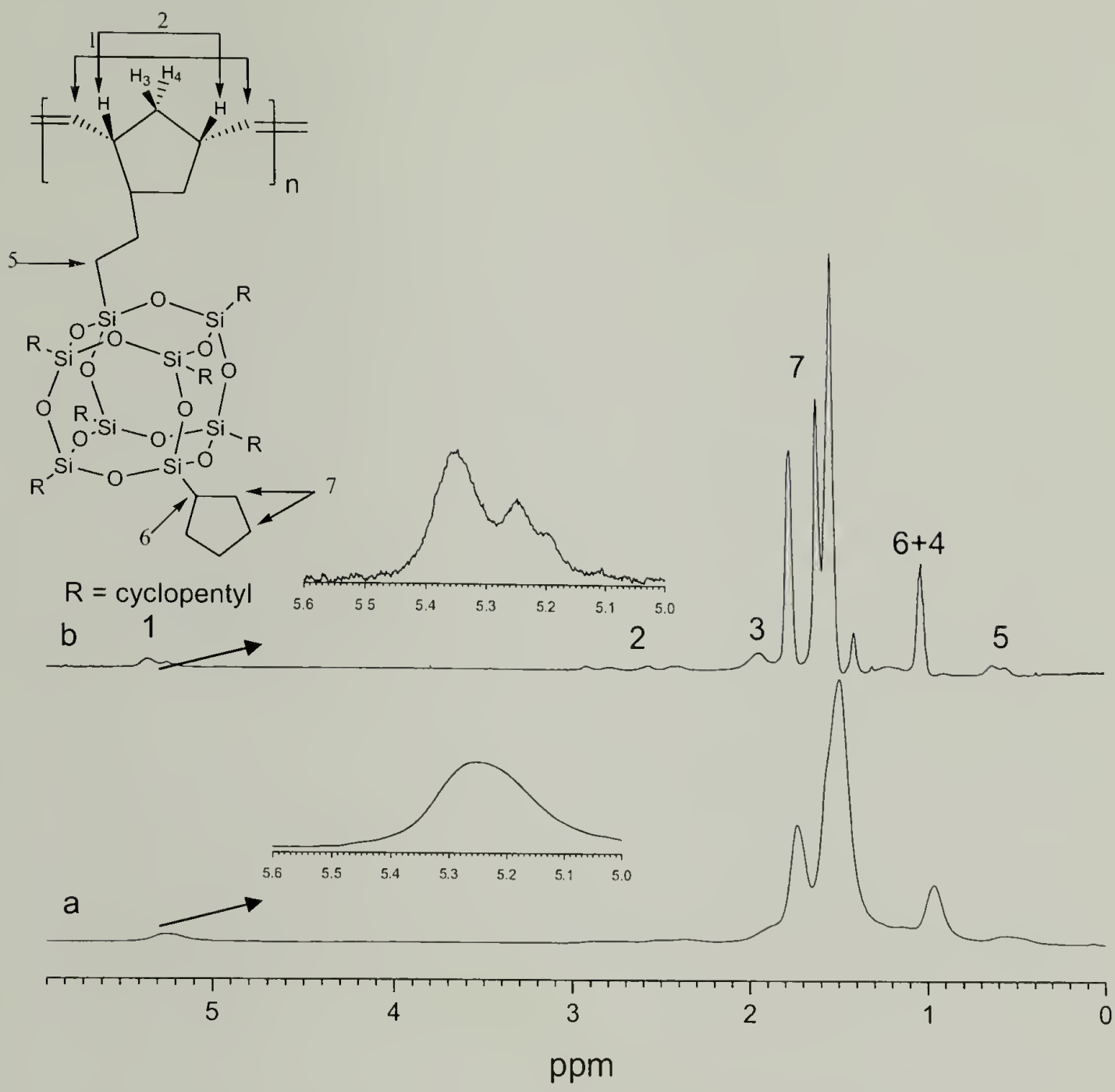

Figure 2.2 ^{1}H NMR Spectra of Homopolymer of POSS-norbornylene in (a) $CDCl_3$, at RT and (b) $C_2D_2Cl_4$ at 100 °C

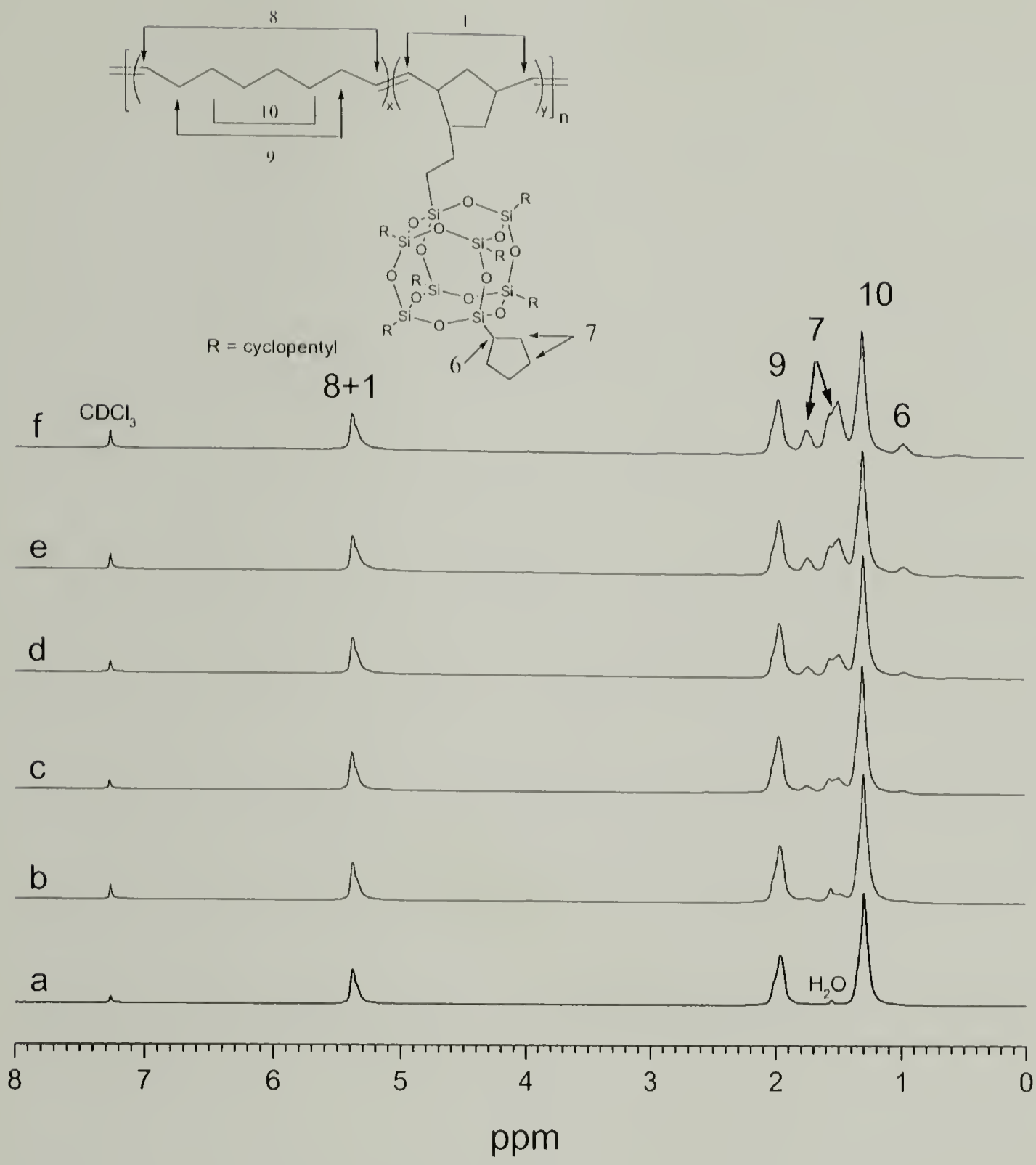

Figure 2.3 ^{1}H NMR Spectra of Polycyclooctenamer-POSS Copolymers in $CDCl_3$ (Entry 1-6, Table 2.1). POSS Concentration in Copolymers: (a) 0 mol%, 0 wt%, (b) 1.39 mol%, 12 wt%, (c) 3.06 mol%, 23 wt%, (d) 4.62 mol%, 31 wt%, (e) 7.96 mol%, 45 wt%, (f) 11.9 mol%, 56 wt%.

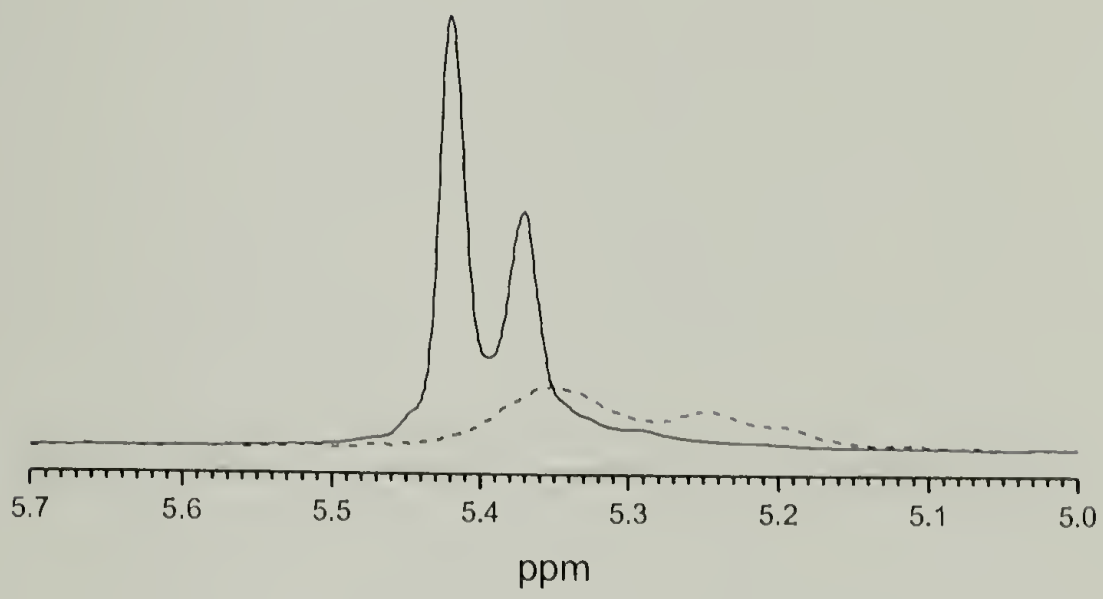

Figure 2.4 Olefinic Region ^{1}H NMR Spectra of Poly(cyclooctenamer-POSS) Copolymer (Entry 6 Table 2.1, solid line) and Poly(POSS-norbornylene) (dashed line) at 100 °C in $C_2D_2Cl_4$.

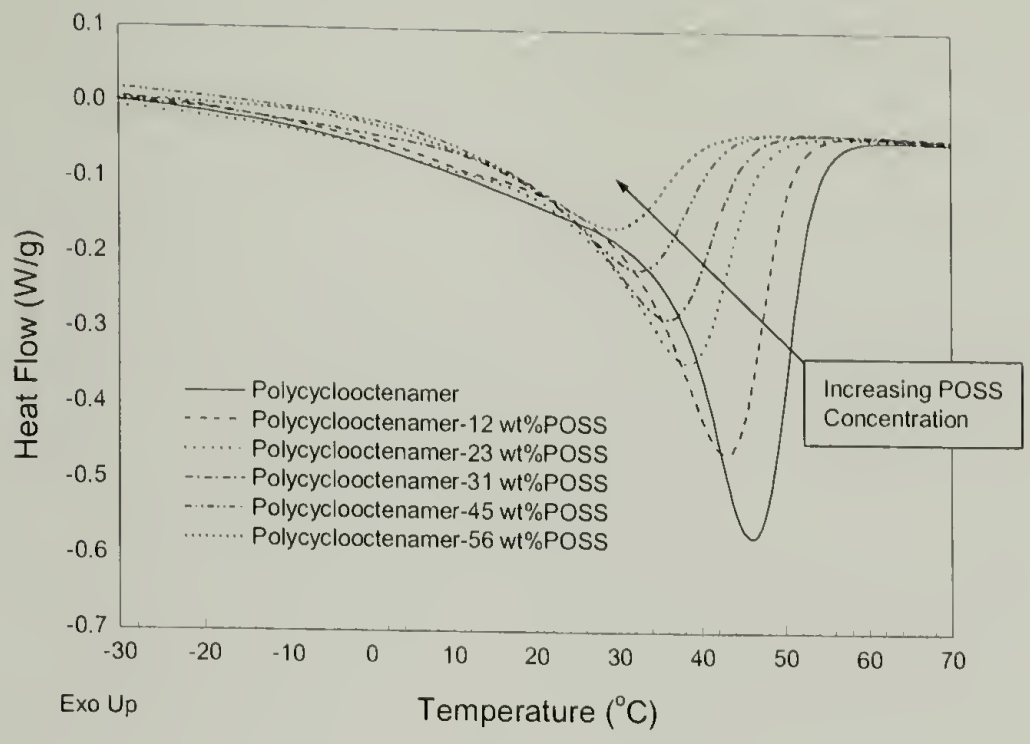

Figure 2.5 DSC Thermograms of Polycyclooctenamer-POSS Copolymers

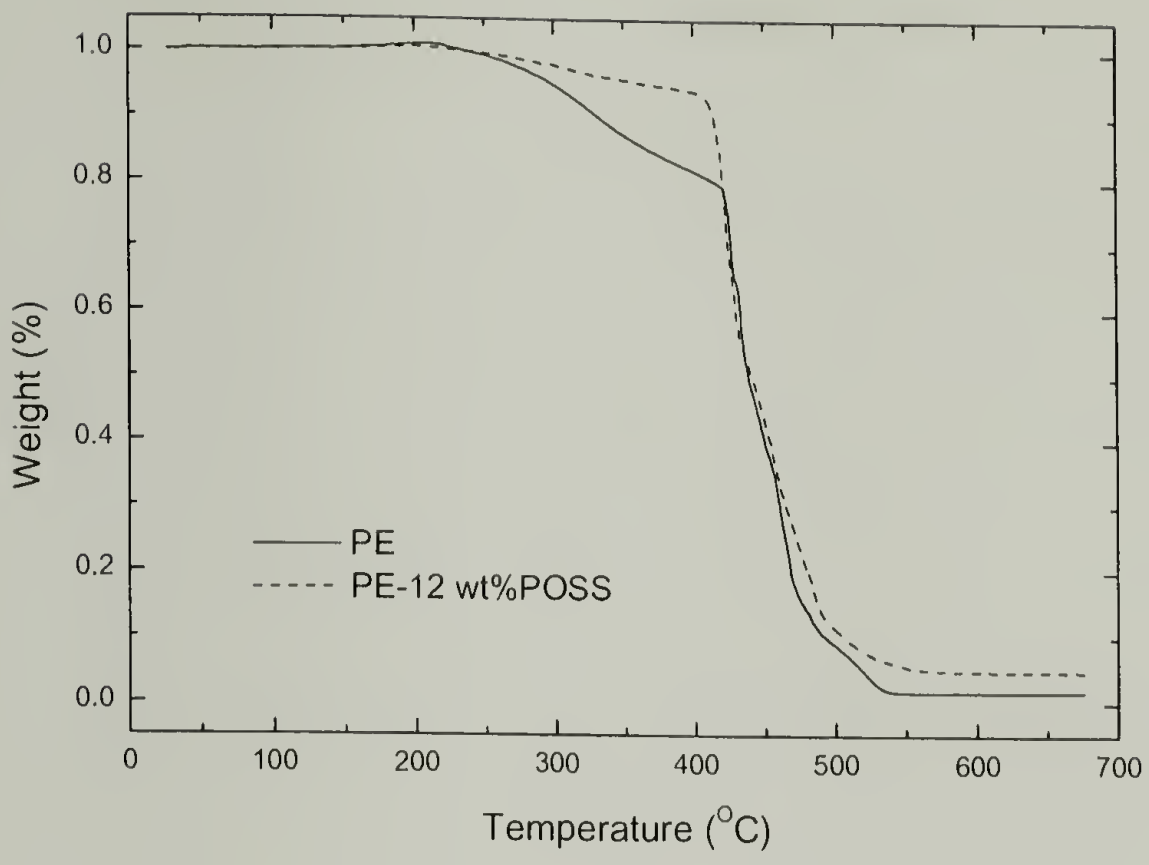

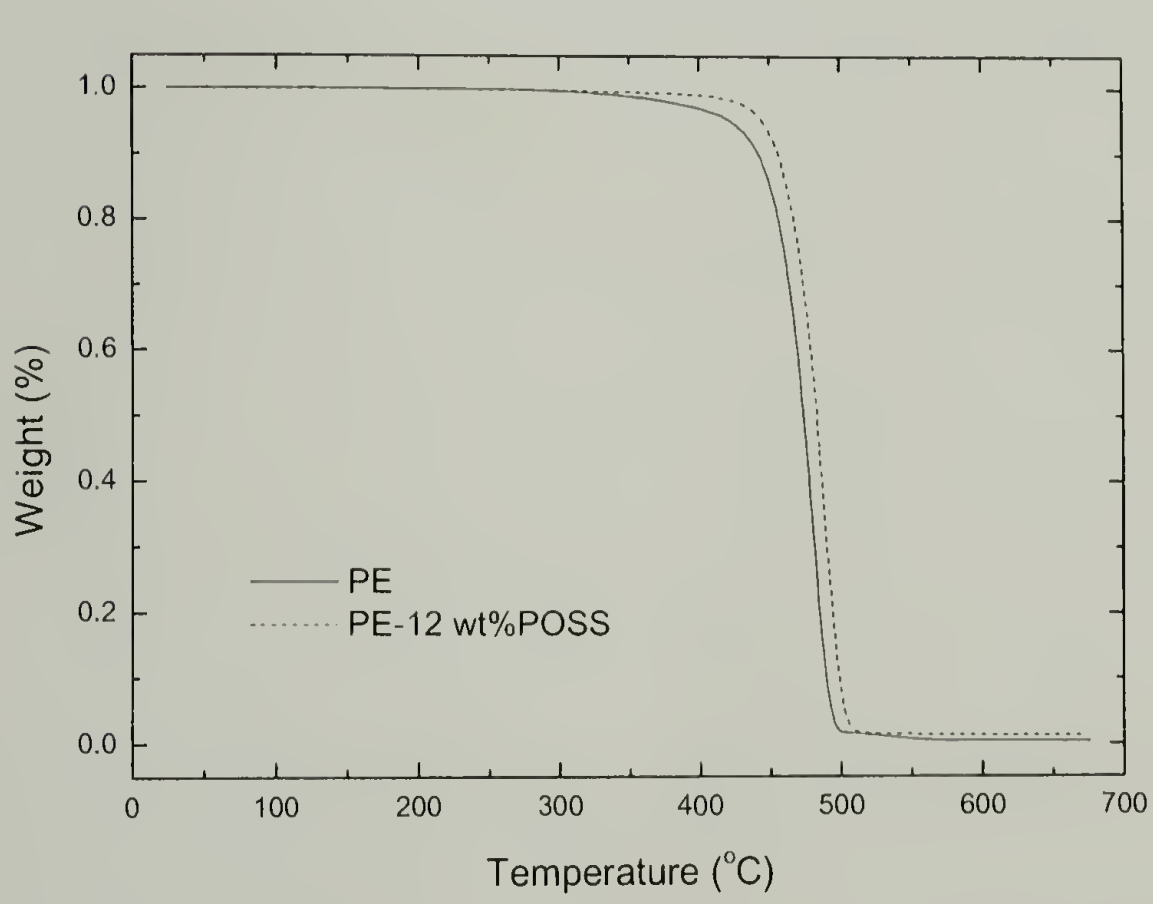

Figure 2.6 TGA traces of PE and PE-12 wt%POSS copolymers under air (top) and nitrogen (bottom)

CHAPTER 3

SYNTHESIS AND CHARACTERIZATIONS OF POLYOLEFIN POLYHEDRAL OLIGOMERIC SILSESQUIOXANE COPOLYMERS USING METALLOCENE CATALYZED REACTIONS

3.1 Introduction

Composite materials are common in the production of modern plastics. A second component is often added to polymeric materials to enhance properties, such as thermal stability and mechanical strength. Among composite materials, organic-inorganic hybrid materials have drawn great attention from the standpoint of advantageous performance relative to either of the non-hybrid counterparts.[53] With the developing interests in nanocomposite materials,[2-5,7,54] typically referring to discontinuous particulate inclusion with one major dimension on the scale of 1-100 nm, it is recognized that behaviors at the nanoscale are not necessarily predictable from that observed at larger length scale. Many studies have shown dramatic improvement of physical properties compared with pure materials by placing inorganic particles into an organic polymeric matrix at the nanometer scale. This is presumably due to the predominant interfacial interaction between nanoparticles and polymer segments. It is envisaged that nanocomposite materials have the potential to bridge the gap between ceramics and polymers.

In particular, the use of polyhedral oligomeric silsesquioxane (POSS) nanoparticles as modifiers of organic polymers has received a great deal of attention recently following the development of efficient synthetic protocols for the preparation of the inorganic Si_8O_{12} core.[6,43,44] Notable is the ability to introduce a functional group, for example a norbornene group, on the nano-cage of a POSS macromonomer.[16] In contrast

to organoclay fillers,[2-4] POSS nanoparticles have the advantages of being mono-disperse, lower in density, have high temperature stability and contain no trace metals. More importantly, it has tailorable interfacial properties and the potential for undergoing copolymerization reactions. These latter factors are especially noteworthy given that polyolefin-clay nanocomposites have failed to produce complete dispersal or exfoliation of clay nanolayers due to unfavorable interactions between hydrophilic clay surfaces and hydrophobic polyolefins.[42,55,56]

A variety of POSS containing copolymers have been prepared using radical, (both conventional[10,11] and atom transfer protocols[45]), condensation,[9] and ring opening methathesis[15,57] polymerization techniques. The ability to copolymerize POSS macromonomers with olefins using coordination polymerization is still at an early stage of development. Preliminary results showed that POSS macromonomers with seven cyclopentyl or cyclohexyl groups and one alkenyl group (approx. 1.5 nm in diameter), did not undergo Ziegler-Natta catalyzed copolymerization with 1-hexene.[16] Even a less sterically hindered ethyl-substituted POSS macromonomer with a long alkyl spacer between the pendant unsaturation group and the POSS core showed low activity and low incorporation of POSS when copolymerized with ethylene.[58] Furthermore, an attempt to obtain polypropylene copolymers resulted in only oligomeric atactic polypropylene copolymers (Mn ~2,200). In an earlier report, polyethylene POSS copolymers have been synthesized using a two-step procedure: ring-opening metathesis polymerization followed by hydrogenation.[57] Thermal studies on these model copolymers revealed substantial improvement in thermal oxidative stability. Therefore, a practical and direct method to synthesize polyolefin POSS copolymers was desired.

In this chapter, an efficient synthetic route is reported for the preparation of hydrocarbon POSS copolymers with control over the incorporation level of POSS macromonomer using metallocene catalysis. Ethylene was directly copolymerized with a POSS macromonomer containing seven cyclopentyl and one polymerizable norbornenyl group using classical metallocene catalysis to produce polyethylene POSS hybrid copolymers. Isotactic polypropylene POSS copolymers were also synthesized for the first time using a C_2 symmetric *ansa*-metallocene. To the best of our knowledge, this POSS macromonomer is to date the largest well-defined macromonomer copolymerized into polyolefins using metallocene catalysis.

3.2 Experimental

3.2.1 Materials

Cyclopentyl-POSS-norbornenyl macromonomer 1-[2-(5-norbornen-2-yl)ethyl]-3,5,7,9,11,13,15-heptacyclopentylpentacyclo [9.5.1.1^{3,9}.1^{5,15}.1^{7,13}] octasiloxane (**1**), cyclopentyl-POSS-vinyl macromonomer 1-vinyl-3,5,7,9,11,13,15-heptacyclopentylpentacyclo [9.5.1.1^{3,9}.1^{5,15}.1^{7,13}] octasiloxane (**2**) and cyclopentyl-POSS-allyl macromonomer 1-allyl-3,5,7,9,11,13,15-heptacyclopentylpentacyclo[9.5.1.1^{3,9}.1^{5,15}.1^{7,13}] octasiloxane (**3**) were provided by the Air Force Research Laboratory, Propulsion Directorate, AFRL/PRSM, Edwards Air Force Base, California. Other reagents were obtained from Aldrich and used as received unless otherwise indicated. Polymer grade ethylene and propylene were purchased from Matheson Gas Products and were passed though a Drierite® drying unit and a OxiClear® in-line gas purifier before use. Toluene was passed sequentially through columns of

activated alumina (LaRoche A-2) and Q-5 supported copper redox catalyst (Engelhard CU-0226S) under a prepurified nitrogen atmosphere. Methylaluminoxane (MAO) was obtained from Akzo Nobel Chemicals as a 10 wt% Al solution (3.36 M) in toluene.

3.2.2 Polymerization Procedures for Polyethylene POSS Copolymers

The ethylene POSS macromonomer copolymerizations were carried out in a 100 mL Schlenk flask equipped with a magnetic stirring bar, 0.51 g of **1** (0.5 mmol, 250 equiv. to Zr) and 19 mL toluene. The sealed flask was removed from the glovebox and charged with ethylene gas (1 atm). A solution of 0.84 mg (2 μmol) dichloro[*rac*-ethylenebis(indenyl)]zirconium in 1.0 mL toluene and 0.36 mL, 3.36 M MAO (1.2 mmol) were mixed, and then preactivated for 15 minutes prior to injection into the flask. Ethylene pressure was kept constant throughout the polymerization through use of a bubbler. The reaction temperature was controlled using a 20 °C water bath. The copolymer was observed to precipitate from solution during the reaction. After one hour, the reaction was terminated by addition of methanol. The polymers were precipitated in 100 mL of a 10% HCl/methanol solution. The polymers were recovered by filtration, washed with 2 × 10 mL hexanes to remove residual **1** and dried overnight under vacuum at 60 °C. The polymerizations were repeated using 0.5, 1.0, 1.5 and 2.0 mmol of **1**, to prepare a range of copolymers.

3.2.3 Polymerization Procedures for Polypropylene POSS Copolymers

The propylene POSS macromonomer copolymerizations were carried out in a 100 mL Schlenk flask equipped with a magnetic stirring bar, 0.51 g of **1** (0.5 mmol, 125 equiv. to Zr) and 18 mL toluene. The sealed flask was removed from the glovebox and charged

with propylene gas (1 atm). A solution of 1.68 mg (4 μmol) dichloro[*rac*-ethylenebis(indenyl)]zirconium in 2.0 mL toluene and 0.72 mL, 3.36 M MAO (2.4 mmol) were mixed, and then preactivated for 15 minutes prior to injection into the flask. Propylene pressure was kept constant throughout the polymerization through use of a bubbler. The reaction temperature was controlled using a 20 °C water bath. The polymer did not precipitate from solution during polymerization. After two hours, the reaction was terminated by addition of methanol. The polymers were precipitated in 100 mL of a 10% HCl/methanol solution. The polymers were recovered by filtration, washed with 2 × 10 mL hexanes to remove residual **1** and dried overnight under vacuum at 60 °C. The polymerizations were repeated using varying amounts of **1**, 0.5, 0.75 and 1.0 mmol, to prepare a range of copolymers. When 1.0 mmol of **1** was used, 1:1 hexane/ethanol was used to wash the polymer due to the copolymer being partial soluble in hexane.

3.2.4 Polymer Characterization

^{1}H NMR spectra were obtained at 300 MHz and 500 MHz using Bruker DPX-300 and AMX-500 FT NMR spectrometers. ^{13}C NMR were recorded at 100 °C in tetrachloroethane-d_2 with a Bruker AMX-500 FT NMR spectrometer operating at 125 MHz. The quantitative spectra were obtained using a standard inverse-gated proton decoupling pulse sequence and a relaxation delay of 6 s. Gel permeation chromatography was performed using a Polymer Laboratories high temperature GPC PL-220 equipped with a Wyatt high temperature light scattering detector miniDAWN (HTmD) at 135 °C in trichlorobenze. The miniDAWN detector contains a 690 nm diode laser. We used values of -0.104 for the dn/dc of polyethylene and -0.102 for polypropylene.[59]

Differential scanning calorimetry was performed under a continuous nitrogen purge (50 mL/min) on a TA Instruments DSC 2910 equipped with a liquid nitrogen cooling accessory (LNCA) unit. Data were gathered on the second heating cycle using a heating and cooling scan rate of 10 °C/min. Thermogravimetric analysis was carried out using a TA Instruments TGA 2050 thermogravimetric analyzer with a heating rate of 20 °C/min from room temperature to 700 °C under a continuous nitrogen or air purge (nitrogen 100 mL/min, air 50 mL/min).

Samples for mechanical tests are made from the synthesized polymer powders, which were preheated in a Carver press at 180 °C for 10 mins between two Kapton® films before being pressed into thin films. The press was then cooled to room temperature by circulating tap water through the two hot plates.

Dynamic mechanical thermal analysis was collected on a Rheometric Scientific DMTA Mark IV running in tensile mode at an oscillation frequency of 1 Hz. Rectangular samples were used with approximate length of 5 mm, width of 2 mm and thickness of 0.2 mm. The strain amplitude was set to 0.1 % strain, well within the linear viscoelastic range. A gaseous nitrogen purge and a heating rate of 5 °C per minute were used.

3.3 Results and Discussion

3.3.1 Copolymerization of Ethylene and POSS-norbornenyl

The low activity observed for previous copolymerizations of POSS macromonomers was presumably due to its steric bulkiness. Our experimental data from attempted copolymerization of ethylene with POSS-vinyl **2** or POSS-allyl **3** showed an order of magnitude decrease in activity with only homo-polyethylene being obtained.

Likewise, attempts to use the spacing strategy of placing long methylene units, such as $-(CH_2)_8-$, between the vinyl groups and the POSS core also resulted in low or no incorporation of POSS at all.[16,58] These results suggest that electron pairs from the oxygen of POSS core may play a role through reversibly coordinating to the zirconium catalysts in spite of the cyclopentyl "coating". In order to increase the activity, norbornene was chosen as the polymerizable linkage. There are a number of advantages to doing so. First of all, the rigid structure of norbornene prevents the simultaneous interaction of a zirconium catalyst with the double bond and lone pair of electrons on oxygen, which makes the oxygen atom inaccessible during polymerization. A similar strategy was adopted in the copolymerizations of 5-norbornen-2-yl esters with olefins using vanadium based Ziegler-Natta catalysts.[60] Secondly, norbornene has higher reactivity than α-olefin in copolymerizations with ethylene. It has been demonstrated that norbornene can be copolymerized with ethylene using dichloro[*rac*-ethylenebis(indenyl)]zirconium / MAO to generate cyclic olefin copolymers with norbornene concentration up to 30 mol%.[61-63] This relatively high reactivity, due to the ring strain on norbornene, should be applicable to POSS-norbornenyl macromonomers. In addition, POSS-norbornenyl macromonomer **1** is much simpler to synthesize and commercially available.

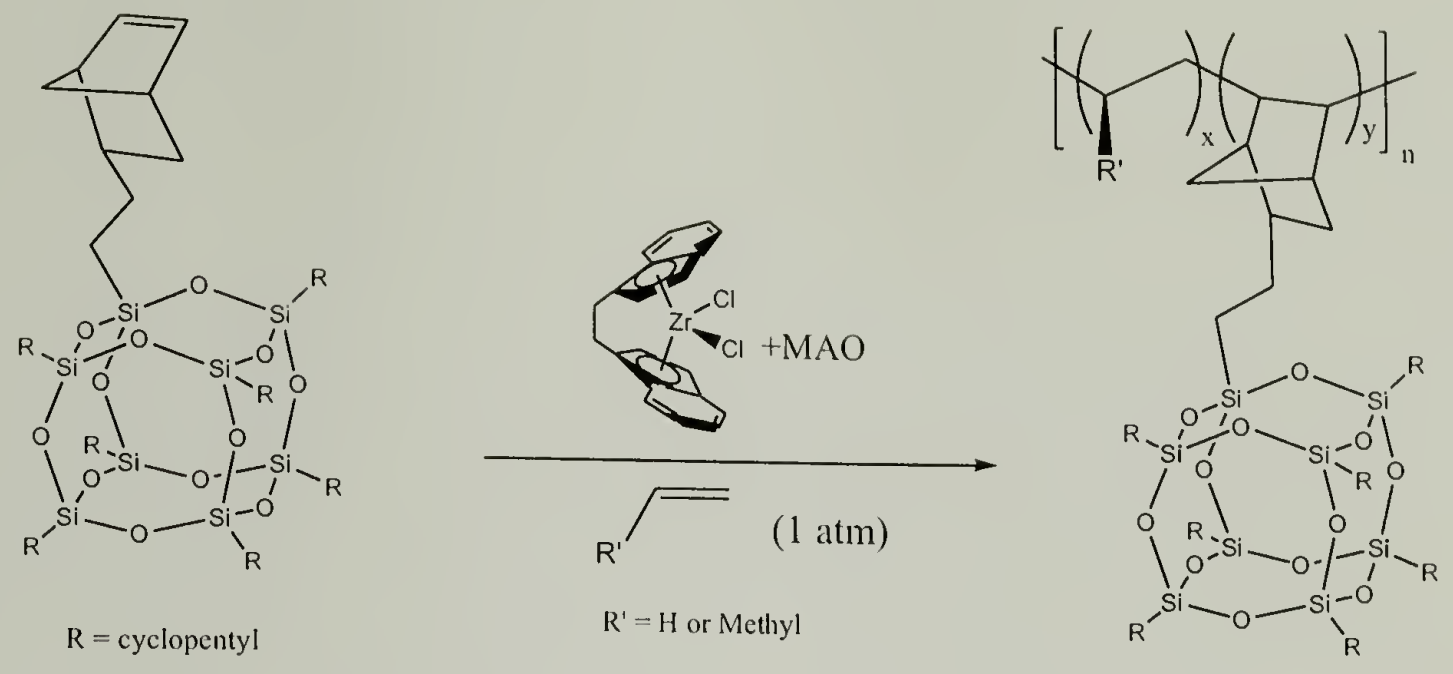

Figure 3.1 Copolymerization of Ethylene or Propylene with POSS-norbornenyl

According to our strategy, we have successfully prepared a series of ethylene copolymers with varying amounts of **1** (Figure 3.1, R' = H) using a metallocene polymerization catalyst. The reaction conditions, yield of copolymer obtained, and the determination of the extent of POSS incorporation are shown in Table 3.1. The reactivity of **1** is sufficiently comparable to ethylene at 1 atmosphere pressure to afford the possibility of adjusting the POSS concentration in the copolymer by simply changing the feed ratio. A broad range of POSS containing copolymers have been prepared (from 18 to 58 wt%). These values are much higher than that achieved using a vinyl POSS macromonomer with ethyl side groups and a long alkyl spacer, that was copolymerized with ethylene using either metallocene, or constrained geometry catalysts.[58] The absolute molecular data obtained by light scattering indicated no significant change at low POSS loadings (entries 2 and 3 vs. 1, Table 3.1). The extremely high molecular weight measured at high POSS loadings may be exaggerated since a dn/dc value of homo-

polyethylene was used in the calculations. Nevertheless, the copolymerization of POSS macromonomer with ethylene has no adverse effect on molecular weight.

In an independent experiment, **1** was found to be unaffected by an excess of MAO after one week in solution. The peripheral cyclopentyl groups are presumably shielding the siloxane core from cleavage by the aluminum alkyls. These results bode well for the use of POSS macromonomers in copolymerization with olefins using single site catalyst / MAO cocatalyst systems.

3.3.2 Copolymerization of Propylene and POSS-norbornenyl

We were also interested in extending our copolymerization method to α-olefin. Polymerization of an α-olefin is more challenging due to both stereo- and region-regular concerns. One advantage of our method is the use of the well studied metallocene catalyst dichloro[*rac*-ethylenebis(indenyl)]zirconium, which is known to control tacticity as well as molecular weight.[64] Propylene was used in our experiment to demonstrate the feasibility of this approach (Figure 3.1, R' = Methyl). The copolymerizations were quite successful. A wide concentration range of polypropylene POSS copolymers was obtained with up to 73 wt %, or 10 mol %, of POSS macromonomers. The polymerization conditions and results are listed in Table 3.2. Since the relative reactivity between propylene and POSS-norbornenyl is higher than that between ethylene and POSS-norbornenyl, a much lower POSS feed concentration was used to produce the copolymers with the same POSS molar concentration (entry 7 vs. entry 3). The molecular weight decreased moderately with increasing POSS concentration. The molecular weight can be fine tuned by altering experiment conditions (entry 10 vs. 7). The copolymers have moderately high isotacticities with [*mmmm*] pentad sequences comparable to that of a

propylene homopolymer (entries 7 and 8 vs. 6). Optimization of molecular weight and activity should be achievable using any of a number of more efficient metallocene catalysts developed recently.[65]

3.3.3 Thermal Properties of PE-POSS Copolymers

A summary of the thermal characterization of PE-POSS copolymers is listed in Table 3.3. A gradual decrease in the melting temperature and heat of fusion of the polymers was observed with an increase in the POSS content of the copolymer, which clearly indicates a random copolymer structure (entries 2-5 vs. 1). An interesting observation is that the PE-POSS sample with the highest POSS concentration (entry 5) has fewer polyethylene crystalline domains detectable under standard DSC conditions. This sample was partially soluble at room temperature in hexanes while all of the others of this series were not. It is also noted that the thermal stability was improved in these copolymers. A slight increase in the onset of decomposition temperature was observed similar to our previous report.[57] Again, a significant improvement of the thermal oxidative resistance in the PE-POSS copolymers was noted. The temperature of 5% weight loss of all the samples increased 90-104 °C compared with a PE control sample (Figure 3.2). The char yields, however, were low (less than 10%) under both nitrogen and air. Since polyethylene decomposition in air is through random chain scission to generate free radicals,[66] a crosslinking mechanism around the silicon core was speculated as an explanation for the improved thermal stability. The existence of POSS nanoparticles facilitates recombination of the free radicals and raises stable temperature regime close to 400 °C. Another possible explanation for the improvement of thermal oxidative stability is the formation of a silica layer on the surface of the polymer melt in the presence of

oxygen, which serves as a barrier preventing further degradation of the underlying polymer.[52] Further investigation is currently underway.

3.3.4 Thermal Properties of PP-POSS Copolymers

Similar to the PE-POSS copolymers, the PP-POSS copolymers had a slightly decreased melting temperature compared to homo-polypropylene prepared with the same metallocene catalyst. However, the thermal decomposition behavior was apparently different. The 5 % weight loss in air did not increase until high POSS concentration even though the PP-POSS copolymers have a much slower decomposition rate compared with homo-polypropylene (Figure 3.3). The onset of decomposition temperature in nitrogen increased moderately (Table 3.4). Similar to polyethylene, polypropylene also decomposes by a mechanism of random chain scission. However, due to the existence of tertiary carbons, which are more susceptible to degradation, the existence of POSS nanoparticles merely slows down the degradation process.

3.3.5 Mechanical Properties of PE-POSS Copolymers

The PE-POSS copolymers can be easily pressed at 180 °C into thin, transparent, tough films. Dynamic mechanical thermal analysis was carried out to probe the mechanical properties of these films. Since mechanical properties (small-strain tensile deformation properties, Young's modulus, yield stress and yield strain) of polyethylene primarily depend on percent crystallinity,[67] a dramatic decrease of modulus was expected due to disruption of crystallinity from the presence of bulky POSS sidegroups. However, the storage modulus E' of the unorientated PE-POSS sample (19 wt% POSS) was almost unchanged compared with the PE control sample in temperature range from –50 to 50 °C

(Figure 3.4). This indicated the tensile properties were maintained even though the crystallinity of polyethylene was decreased in the copolymer with 19 wt % POSS loading (56% to 39%). We believe that this result is due to the beneficial effect of POSS nanoparticles enhancing mechanical properties countering the adverse effect of disrupting polyethylene crystallization. The storage modulus decreased with higher POSS loadings. In order to prevent disruption of crystallization, polyethylene-block-poly(POSS) copolymers might be more desirable.

The mechanical relaxation of PE-POSS copolymers was also examined. Even though the assignments of these relaxation processes are controversial, they can provide some information into the microstructure of PE-POSS copolymers. The γ-relaxation, a localized conformational transition, possibly due to a "crankshaft" motion in PE amorphous domain, was at the same temperature in PE-POSS copolymers (Figure 3.4). The α-relaxation, a mechanism involving the 180° rotational jump followed by translation of the chain along the crystallographic *c*-axis by one methylene group, shifted to lower temperature due to thinner crystal thickness in the PE-POSS copolymer. This result is consistent with the observed depression of melting temperature. Although the crystallinity of PE-POSS copolymers is lower, the β-relaxation (about –20 °C), commonly believed to be the glass transition, was not observed with increasing percent of amorphous domains. Apparently, it was suppressed in the PE-POSS copolymer due to the existence of POSS nanoparticles.

The salient feature of this test was the extension of rubbery plateau for the PE-POSS sample (Figure 3.4). The behavior of a polyethylene melt starting to flow above its melting temperature was suppressed. This observation of a rubbery plateau at

temperatures above 175 °C likely indicates improved impact and toughness properties for these materials. In addition, the storage modulus of PE-POSS sample is slightly higher in the rubbery region, which suggests better enhancement from POSS nanoparticles in elastomeric materials. This observation agrees well with the mechanical results from polyurethane polymers containing POSS cages.[19] At this time, we believe these phenomena are attributable to the formation of nanocrystals of POSS nanoparticles on the basis of our X-ray and TEM studies.[68] These nanocrystals, functioning as physical crosslinking points inside polyethylene, result in the extension of the rubbery plateau. Their existence also explains the confinement of polyethylene chains for β-relaxation. Similar associative interactions of POSS nanoparticles was observed in other systems.[13,15] However, it was reported recently that the aggregation of POSS was not required for these effects to occur On the basis of molecular dynamic simulations.[46] It was concluded that the chief source of reinforcement arises from the POSS nanoparticles behaving as strong anchor points in the polymeric matrix.

3.4 Conclusions

An efficient synthetic route for preparing polyolefin POSS copolymers has been described. The method involves the direct copolymerization of a POSS macromonomer having a polymerizable norbornene linkage and ethylene or propylene using metallocene catalysis. PE-POSS and PP-POSS copolymers were obtained with a wide concentration range of POSS incorporation. The hybrid copolymers showed substantial improvement in thermal oxidative decomposition with promising high temperature applications. On the basis of dynamic mechanical thermal analysis, the tensile properties of the copolymers

were maintained at low POSS loadings. These results bode well for the use of polymerizable POSS macromonomers in copolymerization with olefin using metallocene catalysis to synthesize novel polyolefin nanocomposites.

Table 3.1 Copolymerization of Ethylene with POSS-norbornylene[a]

Entry	POSS Conc. (mol/L)	Yield (g)	Activity[c] (kg/mol·h)	POSS wt %[d]	POSS mol %[d]	M_w $\times 10^{-3}$ (g/mol)[e]	PDI[e]
1	0	0.86[b]	3440	0	0	328	1.26
2	0.025	1.85	925	19	0.64	315	1.43
3	0.050	0.93	465	27	1.0	315	1.67
4	0.075	0.66	330	37	1.6	516	1.73
5	0.10	1.02	510	56	3.4	446	2.07

[a] Experimental Conditions: 2 μmol dichloro[*rac*-ethylenebis(indenyl)] zirconium (0.84 mg) and 1.2 mmol MAO, total 20 mL toluene and 1 atm of ethylene. Reaction time: 1h.

[b] 1 μmol dichloro[rac-ethylenebis(indenyl)]zirconium (0.42 mg) and 0.6 mmol MAO, total 20 mL toluene and 1 atm of ethylene. Reaction time: 15 min.

[c] Activity in [kg polymer/(mol catalyst·h reaction time)]

[d] as determined by ^{13}C-NMR.

[e] as determined by GPC coupled with light scattering detectors in trichlorobenzene(TCB) at 135 °C.

Table 3.2 Copolymerization of Propylene with POSS-norbornylene[a]

Entry	POSS Conc. (mol/L)	Yield (g)	Activity[c] (kg/ mol·h)	POSS wt %[d]	POSS mol %[d]	M_w $\times 10^{-3}$ (g/mol)[e]	PDI[e]	[*mmmm*][d]
6	0	2.23[b]	1100	0	0	24.9	1.54	90
7	0.025	2.29	290	20	1.0	15.7	1.44	89
8	0.0375	1.68	210	58	5.4	13.3	1.54	88
9	0.050	0.62	78	73	10.4	11.0	1.42	n.d.
10[f]	0.025	0.24	2.5	4.6	0.2	28.8	2.03	84

[a] Experimental Conditions: 4 μmol dichloro[*rac*-ethylenebis(indenyl)] zirconium (1.67 mg) and 2.4 mmol MAO, 1 atm of propylene, total toluene 20 mL. Reaction time: 2h.

[b] 2 μmol dichloro[rac-ethylenebis(indenyl)] zirconium and 1.2 mmol MAO, 1 atm of propylene, total toluene 20 mL. Reaction time: 1h.

[c] Activity in [kg polymer/(mol catalyst·h reaction time)]

[d] as determined by ^{13}C-NMR.

[e] determined by GPC coupled with light scattering detectors in TCB at 135 °C.

[f] reaction temp –10 °C, reaction time 24 hrs.

Table 3.3 Summary of Thermal Characterization of PE-POSS Copolymers

Entry	Wt % POSS	T_m[a] (°C)	Heat of Fusion[a] ΔH_f (J/g)	Onset of Decomp. Temp[b] (°C)	Char Yield in N_2[b] (%)	5% wt. Loss in Air[b](°C)	Char Yield in Air[b] (%)
1	0	136	161	437	0.5	283	0
2	19	126	112	448	2	373	7
3	27	125	91	456	2	397	9
4	37	116	65	457	2	387	10
5	56	--	--	458	4	388	7

[a] Data were gathered on the second melt using a heating and cooling rate of 10 oC/min.

[b] Temperature ramp 20 °C/min in nitrogen or air.

Table 3.4 Summary of Thermal Characterization of PP-POSS Copolymers

Entry	Wt % POSS	T_m[a] (°C)	Heat of Fusion[a] ΔH_f (J/g)	Onset of Decomp. Temp[b] (°C)	Char Yield in N_2[b] (%)	5% wt. Loss in Air[b] (°C)	Char Yield in Air[b] (%)
6	0	140	84	382	0.03	257	0
7	20	134	69	405	1	256	8
8	58	130	55	421	1	259	12
9	73	119	23	427	3	309	24

[a] Data were gathered on the second melt using a heating and cooling rate of 10 °C/min.

[b] Temperature ramp 20 °C/min in nitrogen or air.

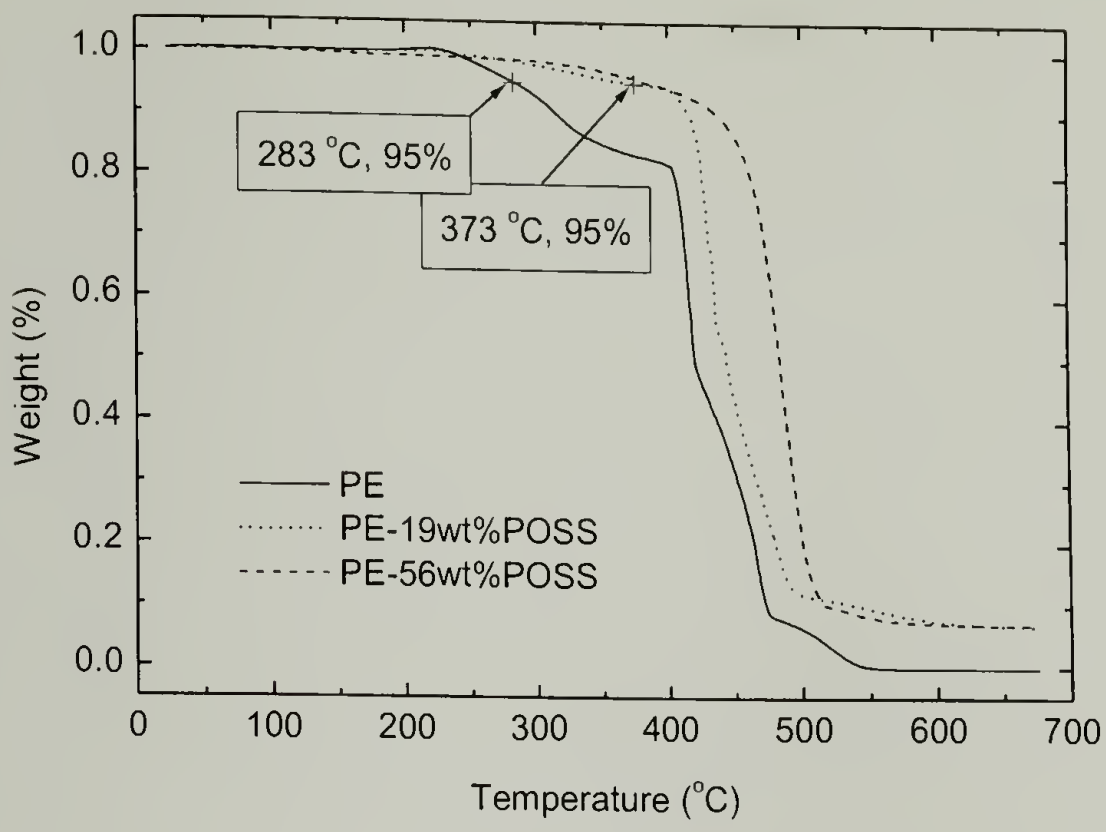

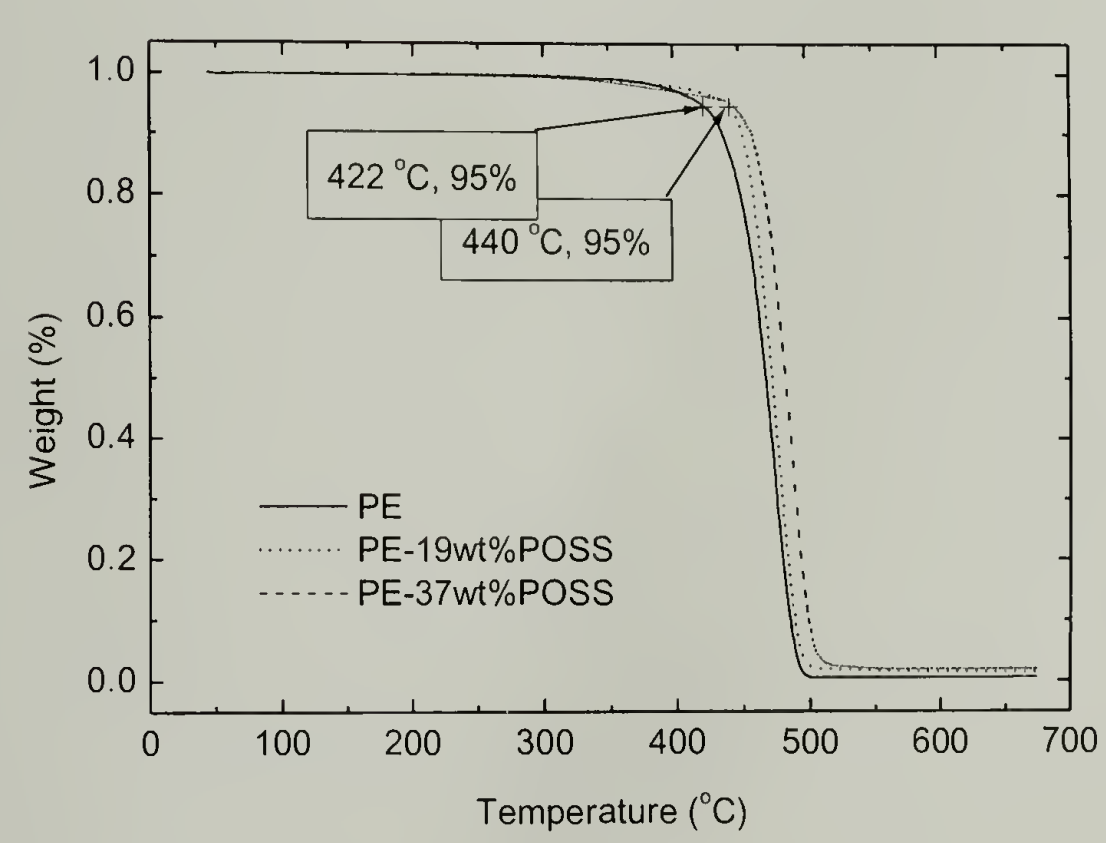

Figure 3.2 TGA Traces of PE-POSS Copolymers under Air (top) and Nitrogen (bottom).

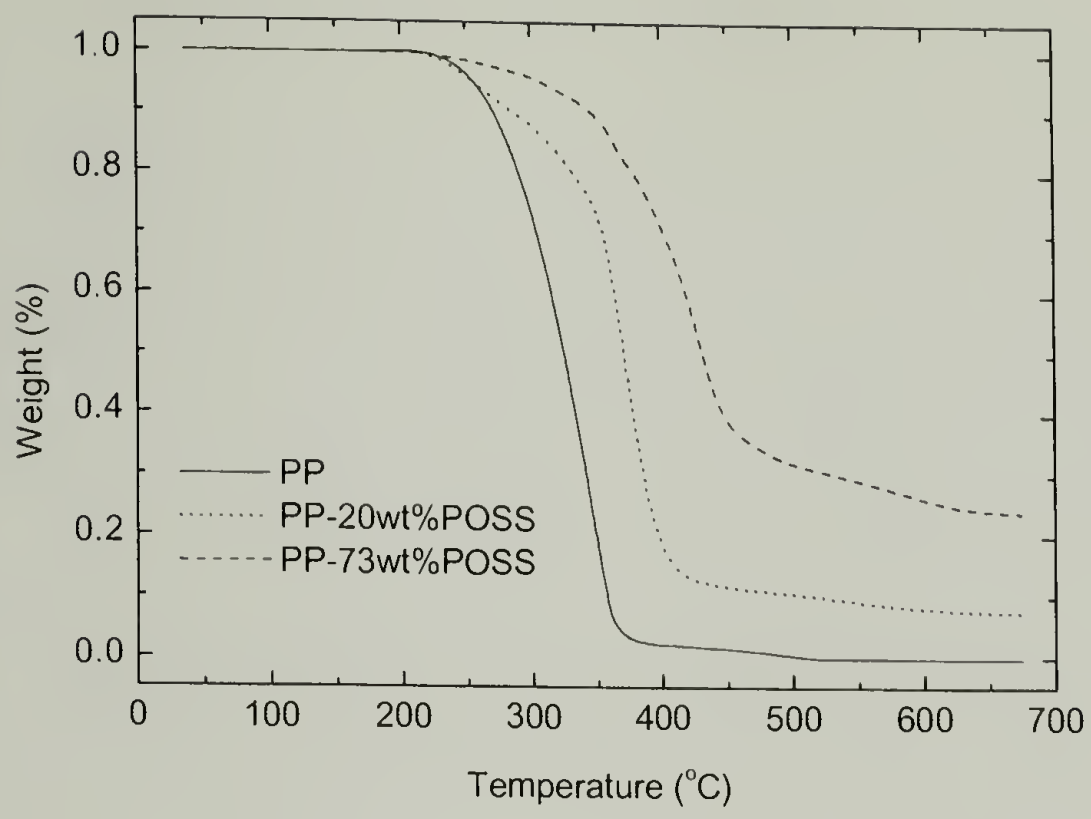

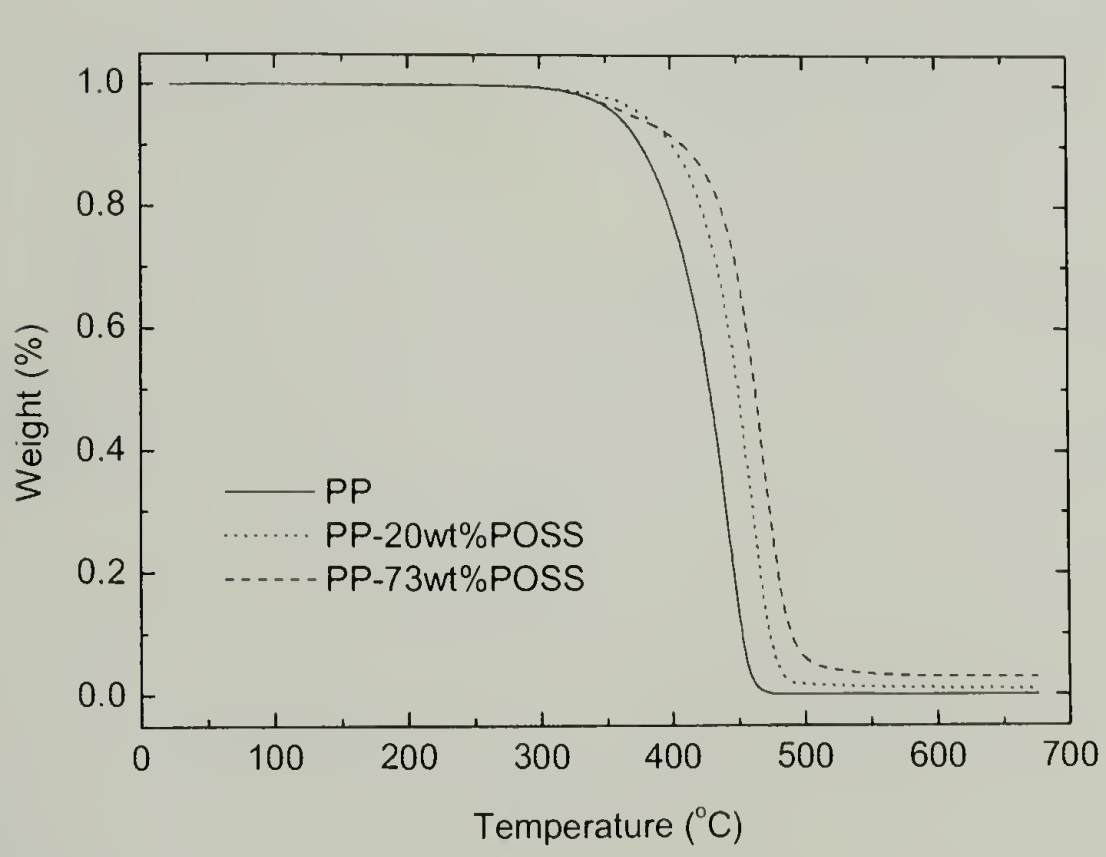

Figure 3.3 TGA Traces of PP-POSS Copolymers under Air (top) and Nitrogen (bottom).

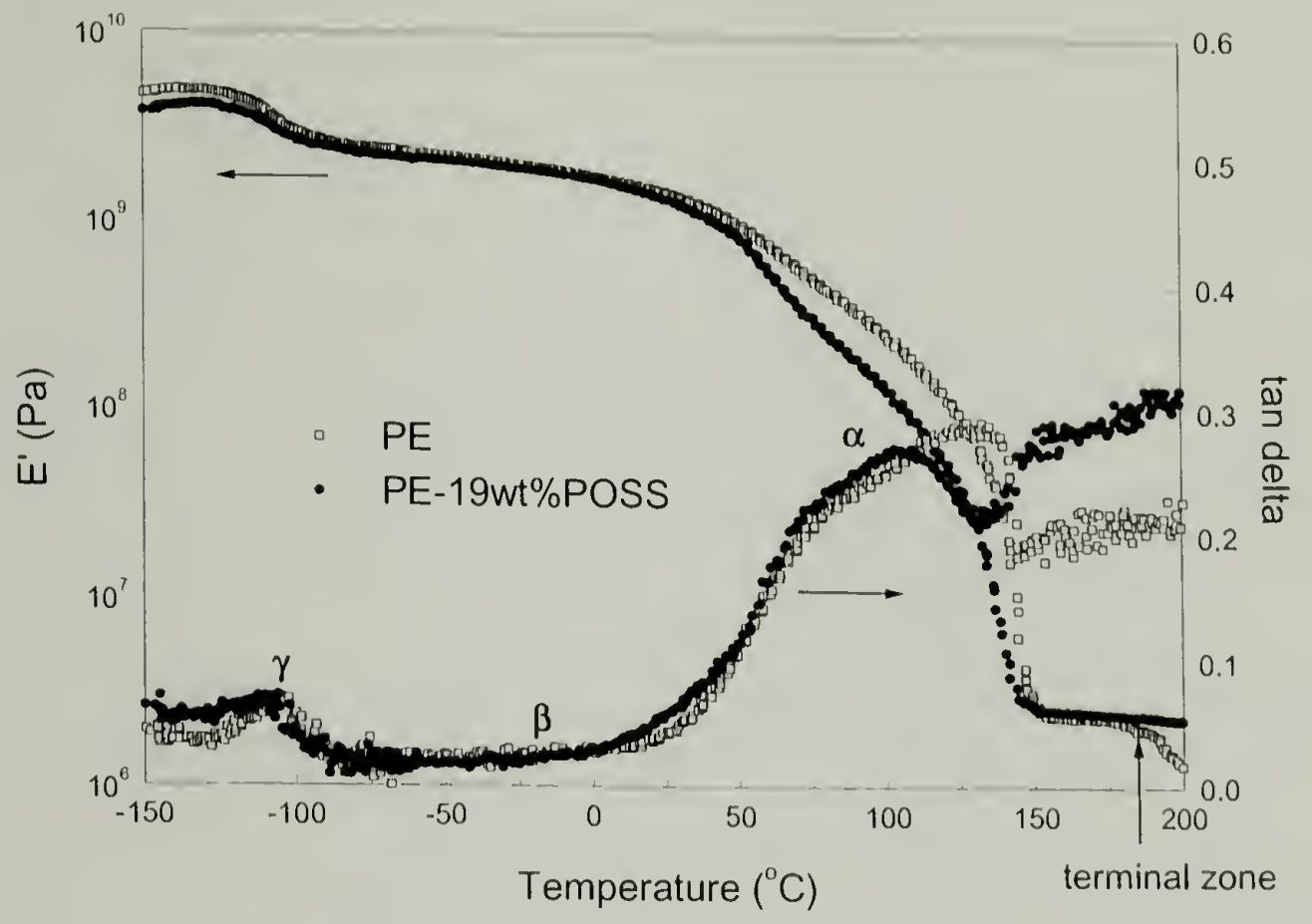

Figure 3.4. Dynamic Mechanical Spectroscopy of PE and PE-19 wt% POSS

CHAPTER 4

SYNTHESIS AND THERMAL PROPERTIES OF HYBRID COPOLYMERS OF SYNDIOTACTIC POLYSTYRENE AND POLYHEDRAL OLIGOMERIC SILSESQUIOXANE

4.1 Introduction

Recently a great deal of attention has been focused on nanocomposite materials, typically referring to discontinuous particulate inclusions having one major dimension on the scale of 1-100 nanometers. These materials have shown novel and often improved mechanical, thermal, electronic, magnetic, and optical properties.[21] Although the two-phase composite may be organic-organic, inorganic-inorganic, or organic-inorganic, the latter is more desirable from the standpoint of combined advantageous performance relative to either of the non-hybrid counterparts. Among the many synthetic approaches to obtain nanocomposites, the use of structurally well-defined inorganic nanoparticles or clusters is becoming an increasingly important strategy.[25] Despite the effort required to establish methods to form covalently or ionically bonded nanoparticles from suitable precursors, this approach has the advantage that it can control and tune the beneficial phenomena associated with nanostructures over a range of length scales. Furthermore, the problem associated with microphase separation in organic-inorganic composites can be alleviated either through the nanoparticles being covalently bound to a polymer backbone or through modification of their surface properties.

In particular, the use of polyhedral oligomeric silsesquioxane (POSS) nanoparticles has been demonstrated to be an efficient method to design hybrid nanocomposite materials.[6] A typical POSS nanoparticles contains an inorganic Si_8O_{12}

nanostructured skeleton surrounded by eight organic groups R (eg. isobutyl, cyclopentyl or cycylohexyl) on the corners to promote solubility in conventional solvents and compatibility with a host polymer matrix. These are generally synthesized through kinetically controlled hydrolytic condensation reactions of $RsiCl_3$ in aqueous acetone. Two predominant stable structures can be obtained: a fully condensed $R_8Si_8O_{12}$ cube and an incompletely condensed $R_7Si_7O_9(OH)_3$ trisilanol.[43,44,69] POSS macromonomers (Figure 4.1) can be prepared from $R_7Si_7O_9(OH)_3$ trisilanol and a $R'SiCl_3$ (R': functional group) in a corner capping reaction.[11] The resulting inorganic core is thus surrounded by seven hydrocarbyl groups and a unique group capable of undergoing polymerization. A variety of functional groups, such as styrene,[11] methacrylate,[10] epoxide[12] and norbornene,[15] have all been prepared. This has afforded the opportunity to incorporate inorganic POSS cages into organic matrices through copolymerizations. This class of organic-inorganic nanocomposites, with nanosized silica covalently bonded to the polymer matrix, are difficult to synthesize otherwise. A variety of POSS containing copolymers have been prepared using radical, both conventional[10,11] and atom transfer protocols,[45,70] condensation,[9] ring opening metathesis polymerization[15,57] and metallocence catalysis techniques.[58,71] Materials prepared include poly(methyl-methacrylate),[10,45,70] polystyrene,[11] epoxy,[12] polysiloxane,[16] polynorbornene,[15] polyethylene and polypropylene copolymers.[71]

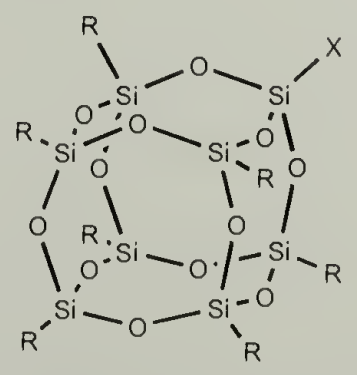

Figure 4.1 POSS Macromonomer Structure

The research interests in this thesis have focused on the polyolefin POSS copolymers. Although these hybrid materials are desirable considering the vast scale of production and wide range of applications for polyolefins, the ability to copolymerize polyolefin with POSS macromonomers using coordination polymerization (Ziegler-Natta or single site catalysis) is at an early stage of development. Efficient synthetic methods to produce polyethylene and polypropylene POSS copolymers have not been reported until recently from our group.[71] In this study, we extend POSS containing copolymers to syndiotactic polystyrene (sPS). Since the initial report from Ishihara,[72,73] sPS has become an attractive engineering thermoplastic due to its high melting temperature (270 °C), fast crystallization kinetics, high modulus and good resistance to water and organic solvents. This work addresses a method to synthesize nanocomposites of syndiotactic polystyrene and POSS, and their resulting thermal properties. The composite matrix of syndiotactic polystyrene is a semi-crystalline material, in contrast to the conventional amorphous atactic polystyrene synthesized by radical polymerization.[11] Different microstructures and thus novel properties are expected due to this crystalline nature.[68]

4.2 Experimental

4.2.1 Materials

Cyclopentyl-POSS-styryl macromonomer 1-(4-vinylphenyl)-3,5,7,9,11,13,15-heptacyclopentylpentacyclo [9.5.1.1^{3,9}.1^{5,15}.1^{7,13}] octasiloxane (**4**) was provided by the Air Force Research Laboratory, Propulsion Directorate, AFRL/PRSM, Edwards Air Force Base, California. $CpTiCl_3$ was obtained from Strem. Styrene was obtained from

Aldrich and distilled from calcium hydride before use. Methylaluminoxane (MAO) was obtained from Albemarle as a 30 wt% solution in toluene. Toluene was passed sequentially through columns of activated alumina (LaRoche A-2) and Q-5 supported copper redox catalyst (Engelhard CU-0226S) under a prepurified nitrogen atmosphere.[74]

4.2.2 Polymerization Procedures for Syndiotactic Polystyrene POSS Copolymers

The styrene POSS copolymerizations were carried out in a 100 mL round bottom flask equipped with a magnetic stirring bar, 3.12 g (0.03 mol) styrene, 1.7 ml of a 4.77 M MAO solution (8 mmol), 0.30 g (0.3 mmol, styrene:POSS = 100: 1) POSS-styryl monomer **4** and toluene. The sealed flask was removed from the glovebox and heated to 50 °C in an oil bath. A toluene solution of 10 μmol $CpTiCl_3$ was injected. The total volume of toluene was 20 mL. The polymer was observed to precipitate from the solution during the course of polymerization. After a certain reaction time (see Table 4.1), polymerization was terminated by addition of methanol. The copolymers were fully precipitated in 100 mL of a 10% HCl/methanol solution. The copolymer was recovered by filtration, washed with a copious amount of hexanes to remove residual **4** and dried overnight under vacuum at 60 °C. The polymerization protocol was repeated using varying amounts of **4** (0.3-, 0.9-,1.5-, or 3.0 g) to prepare a range of copolymers. The copolymers were then extracted with refluxing 2-butanone for 24 h in a Soxhlet extractor to remove atactic copolymers and possible residual POSS macromonomer.

^{1}H NMR: 7.0 (br, phenyl-para and ortho positions), 6.5 (br, phenyl-meta position), 1.8 (br, C*H* of the backbone), 1.3 (br, CH_2 of the backbone), 1.6-1.5 (m, CH_2 of cyclopentyl) and 1.0-0.9 (m, C*H* of cyclopentyl). ^{13}C NMR sPS-POSS copolymers: 143.2 (ipso-C of phenyl), 125.9 (phenyl-meta position), 125.6 (phenyl-ortho position), 123.6

(phenyl-para position), 41.5 (*C*H of sPS backbone), 38.4 (*C*H_2 of backbone), 25.2, 25.1 (*C*H_2 of cyclopentyl), 20.1 (*C*H of cyclopentyl).

4.2.3 Polymer Characterizations

^{1}H and ^{13}C NMR spectra were obtained on a Bruker AMX 500 FT NMR spectrometer using tetrachloroethane-d_2 $CDCl_2CDCl_2$ as the solvent. The residual proton resonance from the solvent at 5.95 ppm was used as the internal reference for ^{1}H NMR and hexamethyldisiloxane was used as the reference at 0 ppm for ^{13}C NMR. Quantitative spectra were obtained using a standard inverse-gated proton decoupling pulse sequence and a relaxation delay of 6 s. Gel permeation chromatography was performed using a Polymer Laboratories high temperature GPC PL-220 equipped with a Wyatt high temperature light scattering detector miniDAWN (HTmD) and a refractive index detector at 135 °C using 1,2,4-trichlorobenzene solvent. The miniDAWN detector contains a 690 nm diode laser. The value of 0.047 ml/g for the dn/dc of polystyrene was used. Differential Scanning Calorimetry was performed on a TA instrument DSC 2910 equipped with a liquid nitrogen cooling accessory (LNCA) unit under continuous nitrogen purge (50mL/min). Data reported were gathered for the second melt using a heating and cooling scan of 10°C/min. The thermogravimetric analysis was carried out using a TA instrument TGA 2050 thermogravimetric analyzer with a heating rate of 20°C/min over a range from RT to 700°C under continuous nitrogen (100mL/min) or air (50mL/min) purge.

4.3 Results and Discussion

4.3.1 Synthesis of Syndiotactic Polystyrene POSS Copolymers.

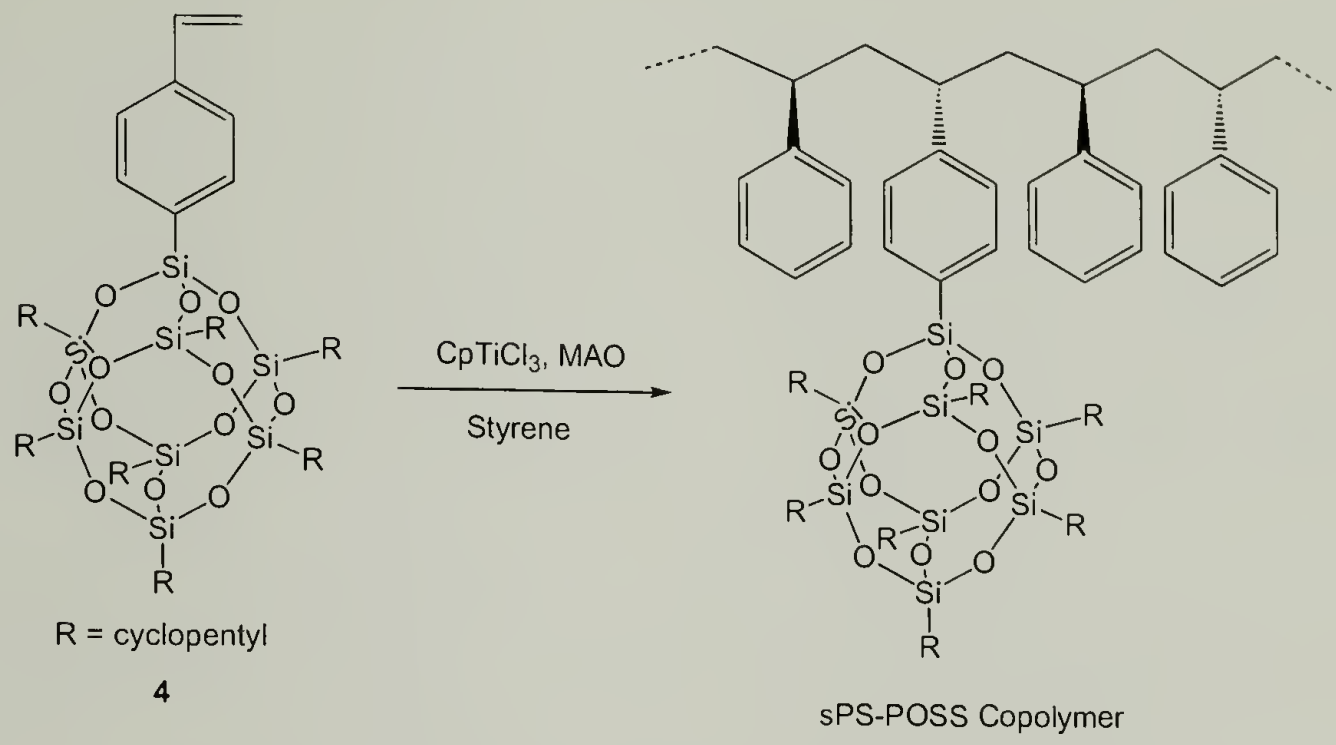

Figure 4.2 Copolymerization of Styrene and POSS-styryl

Copolymers of syndiotactic polystyrene and POSS were synthesized using cyclopentadienyl titanium (IV) trichloride, in conjunction with MAO (Figure 4.2).[72] The reaction conditions, yields, POSS concentration and molecular weight data are shown in Table 4.1. It was noted that on increasing the POSS concentration, the yields of the copolymers dropped considerably. This observation is in contrast to the trend observed by Haddad *et al.* for the synthesis of atactic poly(4-methyl styrene) POSS copolymers by a free radical mechanism,[11] where no significant influence on yield was reported. The observed decrease in the yield of the copolymers with the increase in POSS contents can be attributed to the coordination polymerization mechanism. The polymers are formed by the coordination of the styrene unit to the cationic titanium metal center, followed by 2,1 insertion of subsequent styrene units in the propagation step.[75] Hence in the copolymers, due to the presence of a very bulky POSS-styryl units and possible polar interaction

between oxygen of the POSS cage and the titanium catalyst center, the propagation rate is much slower than that for styrene. The molecular weights of these copolymers are similar to the control homopolymer except sPS-POSS-3, which decreased from 33 to 18 kg/mol. No significant change, or trend, was observed for the polydispersity indices. All were within a range of 1.5-1.8. These polymerizations were all run to moderate levels of conversion to preserve random copolymer structures, thus avoiding the formation of sPS homopolymer. In general, POSS-styryl **4** is less readily incorporated than styrene in the copolymers, inspection of Table 4.1 reveals a relative reactivity ratio of approximate 1:300.

Ketones are commonly used to extract atactic polystyrene from a mixture of atactic and syndiotactic polystyrene as a semi-quantitative means to measure tacticity. In our case, the Soxhlet extraction of the copolymers was carried out for a day using refluxing 2-butanone as the extraction solvent, followed by recovery of the insoluble material. It was observed that the percentage of copolymer insoluble of the copolymers in refluxing 2-butanone decreased as the POSS content was increased. It was first assumed that the increased solubility with increase in POSS content was due to the decrease in tacticity of the copolymers. However, ^{13}C NMR of the copolymers has proved otherwise (Figure 4.3). The carbon peak at 143.2 ppm of the ipso-carbon has been used as a reference for the tacticity determination in syndiotactic polystyrene. In the case of our syndiotactic styrene POSS copolymers, a single peak at 143.2 ppm has been observed for all the copolymers both before and after extraction. This demonstrates that the POSS incorporation does not decrease the tacticity of the copolymers, instead the loss of crystallinity accounts for the increased solubility (*vide infra*). The ^{13}C NMR has also

provided information of the extent of the POSS incorporation in the copolymers. As expected, upon increasing the POSS content in the feed, the extent of the POSS concentration in the copolymers also increased proportionally. The highest concentration obtained in the copolymers was 3.2 mol % (24 wt %).

4.3.2 Thermal Characterization of Syndiotactic Polystyrene POSS Copolymers

The thermal properties of the syndiotactic polystyrene POSS copolymers are shown in Table 4.2 Thermal analysis of the syndiotactic polystyrene POSS copolymers revealed that the glass transition temperatures (T_g) of the copolymers have a minor increase from 98 to102 °C corresponding to 0-3.2 mole% POSS. This is not surprising since Haddad *et. al.* have reported a dramatic increase in the T_g when the mole% of POSS was increased above 7.8 mole% in atactic poly(4-methyl styrene) POSS copolymers.[11] We also observed a melting point depression of the semi-crystalline syndiotactic polystyrene components upon incorporation of POSS. The melting point of sPS homopolymer was determined to be 259 °C, while the melting temperature of sPS-POSS-3 drops to 237 °C for 1.9 mol% of POSS. The heat of fusion data reveal that the degree of crystallinity also drops with increasing the POSS content. Interestingly, the sample sPS-POSS-4 with 3.2 mol% of POSS does not show a melting peak on the second scan under standard DSC experimental conditions. Disruption of the crystallization process of sPS due to random incorporation of POSS is attributed to this observation.

Thermal degradation data from thermogravimetric analysis (TGA) demonstrate that inclusion of the inorganic POSS nanoparticles makes the organic polymer matrix more thermally robust. TGA of the copolymers was performed both under an atmosphere of nitrogen or air and the temperatures of 5% wt loss (T_{dec}) were recorded. The T_{dec}

recorded from the TGA analysis in nitrogen as the carrier gas remained in the range of 387-394 °C. Comparing this set of data to that obtained from Haddad *et al.*, [11] it was seen that the value of T_{dec} for sPS-POSS copolymers was higher than that obtained in the case of atactic poly(4-methyl styrene)-POSS. Citing specific values, incorporating 1.1mol% POSS they observed a T_{dec} of 378-383 °C for 10 % wt loss, while in our case for the same POSS content we observe a T_{dec} of 394 °C (5 % wt loss) and 402 °C (10 % wt loss). This slight increase could arise from the semi-crystalline nature of polymer matrix influencing the aggregration of the inorganic POSS component of the copolymers.[68] The char yield recorded under nitrogen increases considerably from 1.1% (sPS-POSS-1) to 17.2% (sPS-POSS-4). The TGA experiments were also carried out in the presence of air as the carrier gas. It was noted that the T_{dec} remained the same for both sPS and sPS-POSS-1 at 307 °C and then increased with increasing POSS content to 344 °C for sPS-POSS-4, while the char yield increased from 2.1% for sPS-POSS-1 loading to 21.8 % for sPS-POSS-4. This improvement of thermal oxidative stability is attributed to the formation of a silica layer on the surface of the polymer melt in the presence of oxygen, which serves as a barrier preventing further degradation of the underlying polymer.[52]

4.4 Conclusions

In summary, a straightforward synthetic route for preparing syndiotactic polystyrene POSS copolymers has been described. Copolymerizations of styrene and POSS-styryl **4** afforded a novel nanocomposite of syndiotactic polystrene and POSS. The activity of the copolymerizations is much slower compared to radical polymerization

presumably due to the consideration of a coordination polymerization mechanism. The ^{13}C NMR data reveal the moderately high syndiotacticity of polystyrene backbone consistent with the $CpTiCl_3$ catalyst used and a POSS loading as high as 24 wt%, 3.2 mol%. Thermogravimetric analysis of the sPS-POSS copolymers under both nitrogen and air show improved thermal stability with higher degradation temperatures and char yields.

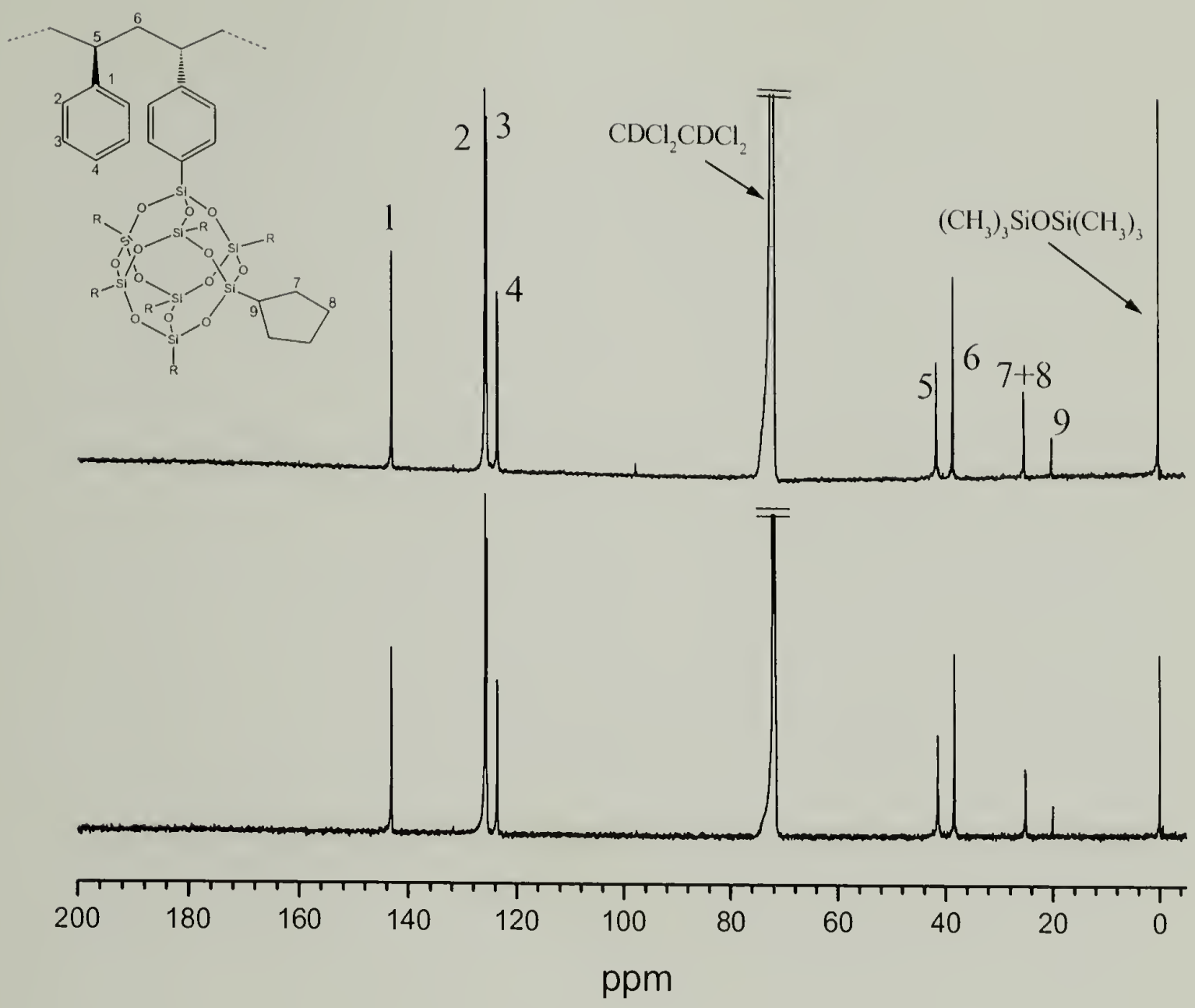

Figure 4.3 ^{13}C NMR Spectra of the Copolymers (sPS-POSS-3) before (top) and after (bottom) Soxhlet Extraction

Table 4.1 Copolymerization of Styrene and POSS-styryl using $CpTiCl_3$[a]

Sample	[styrene]: [POSS] (mol ratio)	Reaction Time (hr)	Yield (g)	POSS wt %[b]	POSS mol %[b]	M_w[c] $\times 10^{-3}$ (g/mol)	PDI[c]	MEK Insoluble[d] (%)
sPS	100:0	0.5	2.23	0	0	33	1.76	90
sPS-POSS-1	100:1	1	1.57	3.3	0.36	37	1.45	89
sPS-POSS-2	100:3	1	1.15	9.9	1.1	35	1.51	~ 80
sPS-POSS-3	100:5	1	0.90	16	1.9	18	1.50	~ 60
sPS-POSS-4	100:10	3	0.47	24	3.2	32	1.58	~ 40

[a] Experimental Conditions: 10 μmol $CpTiCl_3$, 8mmol MAO (Al:Ti = 800), 0.03 mol styrene and 20 mL toluene, 50 °C.

[b] As determined by ^{13}C-NMR.

[c] As determined by GPC coupled with light scattering detectors in TCB at 135 °C.

[d] As calculated from polymer insoluble in 2-butanone (MEK) after 24h Soxhlet extraction.

Table 4.2 Summary of Thermal Characterization of sPS-POSS Copolymers[a]

Sample	T_g[b] (°C)	T_m[b] (°C)	Heat of Fusion[b] ΔH_f (J/g)	5% wt. Loss under N_2[c] (°C)	Char Yield under N_2 (%)	5% wt. Loss under Air[c] (°C)	Char Yield under Air (%)
sPS	98	259	28.7	387	0	307	0
sPS-POSS-1	99	255	25.1	398	1.1	307	2.1
sPS-POSS-2	101	245	20.1	394	2.6	300	5.8
sPS-POSS-3	100	237	15.1	397	4.3	321	8.9
sPS-POSS-4	102	--[d]	--[d]	387	17.2	344	21.8

[a] Data were collected on the samples before extraction.
[b] Data were gathered on the second melt using a heating and cooling rate 10 °C/min.
[c] Temperature ramp 20°C /minute
[d] Not detectable.

CHAPTER 5

X-RAY CHARACTERIZATIONS OF POLYETHYLENE POLYHEDRAL OLIGOMERIC SILSESQUIOXANE COPOLYMERS

5.1 Introduction

Organic-inorganic nanocomposite materials[2-4,6-8] have attracted a great deal of attention recently due to their potential as candidate materials for bridging the gap between organic polymers and inorganic ceramics. In particular, the use of polyhedral oligomeric silsesquioxane (POSS™)[1] nanoparticles has been demonstrated to be an efficient method in the design of hydrid materials.[6,8-19] A typical POSS macromonomer has an inorganic Si_8O_{12} core surrounded by seven organic groups (e.g. cyclopentyl or cycylohexyl) on the corners, which promote solubility in conventional solvents, and one unique group at the final corner which is used as the site of polymerization with an assorted array of comonomers (Figure 5.1). Copolymers obtained in this manner include copolymers of polysiloxane,[9,16] poly(methyl methacrylate),[10] poly(4-methyl styrene),[11,13] epoxy,[12,14] polynorbornene,[15] and polyurethane.[18,19] They represent a new category of polymers characterized by the presence of bulky POSS nanoparticles.

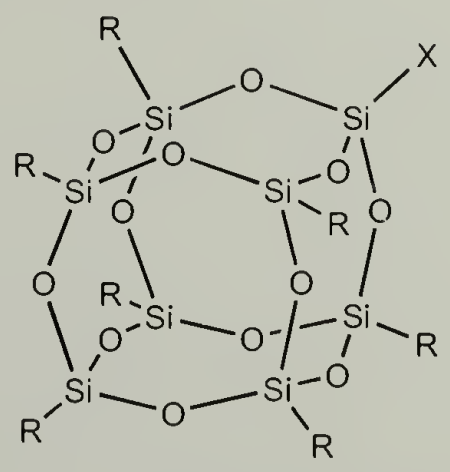

Figure 5.1 POSS Macromonomer Structure

In general, POSS containing copolymers have higher mechanical and thermal properties than the polymers without POSS side-units. However, neither the microstructure of this category of polymers nor the mechanism of reinforcement is well understood. Such reinforcement may, in principle, arise either from isolated POSS nanoparticle units, or from aggregates of these units into larger POSS clusters. The degree of aggregation may be expected to depend on the mole fraction of POSS nanoparticles, the lattice energy of POSS crystals, the degree of compatibility of the POSS with the host polymer component and the tendency for this host component to form a separate crystalline phase. There are literature reports ascribing mechanical reinforcement to both isolated POSS nanoparticles and to POSS aggregates. For example, the increase and broadening of glass transition temperature with increasing POSS loadings in a POSS epoxy crosslinked system was attributed to the nanoscopic size of individual POSS nanoparticles which hindered the motion of molecular chain network junctions.[12] Rheological measurements on amorphous linear poly(4-methyl styrene)-co-POSS copolymers found a high temperature rubbery plateau, suggesting that associative interactions between POSS nanoparticles were responsible for retarding polymer chain motion.[13] Mechanical relaxation measurements and WAXS of amorphous polynorbornene-co-POSS copolymers with different pendant R groups on POSS nanoparticles indicated that ordering in POSS aggregates at the nanometer scale was better in cyclopentyl substituted POSS than cyclohexyl substituted POSS.[15] On the other hand, a report based on atomistic molecular dynamics simulation of the same system concluded that aggregation of the POSS nanoparticles was not required for reinforcement effects, such as the increase in glass transition temperature and retardation of chain

dynamics. The lack of mobility of individual POSS nanoparticles, with an approximate spherical diameter of 1.5 nm (comparable to that of polymer segments), was reasoned to be the primary source for the beneficial effects.[46] Conceptionally, the reinforcement of a copolymer by aggregates of POSS should be distinguished from any reinforcement caused simply by the bulky nature of individual POSS nanoparticles in cases where the POSS units do not crystallize.

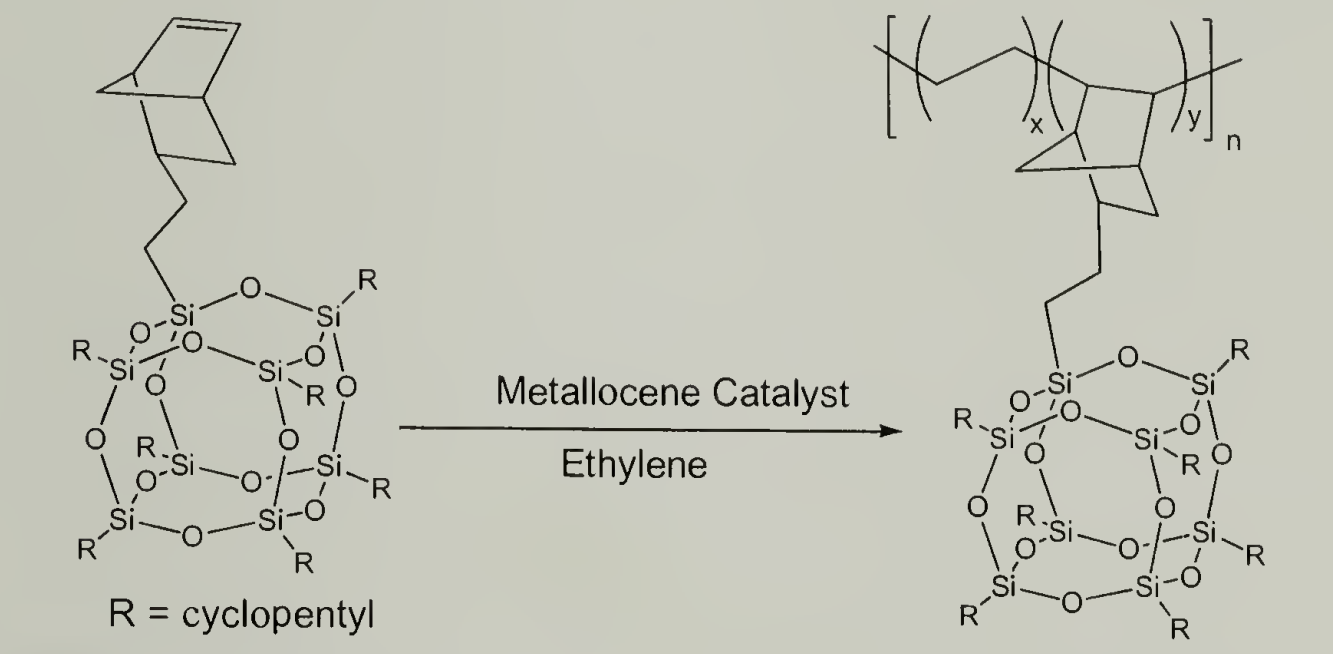

Figure 5.2 Synthesis of PE-co-POSS Copolymer

A body of work has shown that octa-substituted alkyl substituted POSS nanoparticles $R_8Si_8O_{12}$ with various R groups (R = hydrogen, methyl, ethyl, isopropyl, cyclohexyl or phenyl) form rhombohedral (hexagonal) crystal structures with similar WAXS "finger-prints".[76-80] POSS nanoparticles can also form crystalline aggregates when attached as pendant groups to a host chain by copolymerization. This occurs with a variety of copolymers ranging from random to block.[13,15,81] The POSS component in all these copolymers showed similarities in their X-ray diffraction patterns. Moreover, these

patterns were similar to those from crystals of unattached POSS nanoparticles (described above), suggesting that in POSS containing copolymers, POSS aggregates may also crystallize in a similar rhombohedral geometry. However, detailed study is needed to fully determine the structures.

Most previous work, with some exceptions,[19] has focused on amorphous host polymers which are inherently uncrystallizable. The present work now extends this to a fundamentally different class of materials in which the host polymer is itself highly crystallizable in the homopolymer state. In the copolymers there is, of course, a strong tendency for ordered aggregation and crystallization of the host polymer segment, which therefore competes with POSS aggregation and crystallization. Recently we reported a novel class of copolymers of this type. These polyethylene-co-POSS (PE-POSS) copolymers with bulky POSS nanoparticles covalently attached to the polyethylene backbone were synthesized using metallocene catalyzed polymerization (Figure 5.2).[71] These polymers displayed enhanced thermal properties and dimensional stability. The microstructure of this new class of materials is undetermined and presents an interesting and also practically important problem. This work addresses this issue.

5.2 Experimental

Polymer samples were synthesized according to our previous report.[71] The precipitated polymers were pressed into films on a Carver press at 180 °C for 10 minutes between two Kapton® films. They were then cooled to room temperature by circulating water through the hot plates. The transparent films were roughly 0.2 mm thick. The POSS content varied from 19 wt % (0.64 mol %) to 56 wt % (3.4 mol %). Attention is

drawn to the fact that, at even very small mole fractions, the weight fraction of POSS is substantial. An example material (37 wt%, 1.6 mole %) was oriented by drawing in the solid state at 90 °C to a draw ratio of ~3 using an Instron 5564 equipped with an environmental chamber.

Table 5.1 Molecular Weight Data of PE-POSS Copolymers

Sample	POSS in Copolymers (wt %)	POSS in Copolymers (mol %)	M_w $\times 10^{-3}$ (g/mol)	Polydispersity Index
PE	0	0	328	1.26
PE-POSS1	19	0.64	315	1.43
PE-POSS2	27	1.0	315	1.67
PE-POSS3	37	1.6	516	1.73
PE-POSS4	56	3.4	446	2.07

WAXS images were obtained using an evacuated Statton camera with a 10cm × 15cm Fuji image plate. Cu-Kα radiation (wavelength 1.54 Å) was used with a nickel filter. The X-rays were collimated into a fine beam of circular cross-section using a pin hole collimator. Calcite was used to calibrate the camera length. The scattering patterns were scanned on a Fuji BAS-2500 image plate scanner. Intensity profiles were obtained from radial averages of the scattering pattern intensities. The drawn film was examined with the beam both normal and edge-on to the plane of the film.

5.3 Results

The X-ray scattering profiles of PE-POSS1-4 are shown in Figure 5.3, b-e. For comparison, traces of homo polyethylene and the POSS macromonomer are also shown, a and f, respectively. The pure PE shows reflections at 2θs of 21.4° (4.10 Å), 24.2° (3.68

Å) and 36.5° (2.46 Å), corresponding to the 110, 200 and 020 reflections of the usual orthorhombic PE crystal structure. A weaker reflection at 2θ = 19.6° (4.52 Å) is the 010 reflection from the commonly observed but minor component of the monoclinic crystal structure of PE. The pure POSS macromonomer shows strong reflections at 2θs of 8.2° (10.8 Å), 11.0°(8.03 Å) and 19.0° (4.66 Å).

It is clear that the copolymers show crystalline features which are characteristic of the structures of the two separate components. The PE-co-POSS sample with lowest POSS content in this series is dominated by the PE crystal component. However, two additional broad peaks at 8.4° (10.5 Å) and 19.4° (4.57 Å) also appear. These clearly correspond to the strongest of the POSS reflections (trace f). As the POSS content increases, the reflections from the POSS component increase in intensity and sharpness, while the PE reflections weaken and broaden. At the highest POSS content, 56% wt.% (3.4 mol %), the sample shows only weak PE crystal peaks, leading to the conclusion that the PE component (which forms ~44 wt% and 97 mole% of the material) must be primarily disordered. It is also notable that, with progressive increase in POSS content, although the PE crystallinity is much lower, where there are PE crystals, the PE peak positions remain constant, therefore indicating that the crystal lattice is not expanded.

The progressive intensification and sharpening of the POSS reflections clearly show the progressive development of a distinct ordered POSS lattice at the expense of the crystallinity of PE. Simple estimation of the apparent crystallite size dimensions (L), based on the half-widths of reflections (β) at 10.5 Å using Scherrer's Equation ($L= \lambda/(\cos\theta\beta)$), indicates a gradual increase in the POSS crystallite size and/or order with POSS content (PE-POSS1 ~40 Å to PE-POSS4 ~100 Å). We especially draw attention to

the difference in line broadening between the POSS peaks at 4.57 Å and 10.5 Å. The difference in the width of the 10.5 Å peak compared with that at 4.57 Å is far greater in the copolymers than in the macromonomer, indicating an anisotropy in apparent crystallite size in the copolymers which is not displayed in the POSS macromonomer, Figure.5.3.

The diffraction pattern of the film drawn at 90 °C is shown in Figure 5.4. With the beam normal to the sample plane two crystalline components, originating from the PE and the POSS, can again be identified. Both PE_{110} and PE_{020} appear as two arcs above and below the equator (plus or minus ~16°). The large apparent equatorial spread of PE_{200} is also considered to be due to separating into two reflections above and below the equator. The near meridional reflection (at 2.23 Å) is identified as PE_{011}. Turning to the POSS component, the POSS reflection at 10.5 Å appears meridionally, while the broad POSS reflection at 4.57 Å, forms a continuous ring. With the beam edge-on, the POSS 10.5 Å reflection is again meridional, while both PE_{110} and PE_{200} are equatorial.

5.4 Discussion

Most previous work on polymeric materials containing POSS nanoparticles included as pendant groups has concerned host polymers which are themselves inherently uncrystallizable. In such copolymers, aggregation and crystallization of POSS is limited primarily by the topology of the host chain. The system of PE-POSS in this study is distinct from these other systems in that crystallization of both POSS and PE chain segments may occur, and the final microstructure may be controlled not only by host chain topology but also by the competition between the two crystallization processes. In these PE-POSS copolymers the PE crystallinity and apparent crystal sizes become

progressively smaller with increasing POSS concentration. This is presumably because POSS nanoparticles disrupt the crystallization of polyethylene crystals, by virtue of their size (~1.5 nm for each POSS group). It is clearly impossible for such large units to be accommodated within the PE crystal structure. And, in this respect, it is noted that the PE lattice parameter appear to be essentially unchanged over the entire range of loading. Nevertheless, the crystallization of PE is evidently limited by the presence of POSS groups along the chain, even at low POSS mole fractions.

With increasing POSS mole fraction, it is also seen that the amount of POSS crystallization increases. The *d*-spacing values for our POSS nanocrystals (10.5-, 7.96- and 4.57 Å) are very similar to those reported in other polymer systems containing POSS nanoparticles, such as the homopolymer of POSS-styryl[13] and the block copolymer of poly(methylacrylate)-*block*-POSS.[81] In these reports, the most intense reflection was at a spacing of approximately 10-11 Å, and this sharpened with increasing POSS concentration. However, the peak at 4-5 Å seemed relatively broad and diffuse. In spite of the different polymer host, it is reasonable to conclude that the POSS crystallites in all these copolymers have similar packing structures or unit cells. Moreover, the patterns from the copolymers are very similar to those from the POSS macromonomer, leading to conclude that the packing in the copolymers is very similar to the rhombohedral (hexagonal) packing of the POSS macromonomer crystal in the absence of a host polymer. Such differences as there are between POSS structures in different host systems may reasonably be explained by differences in spatial and topological constraints.

Consideration of the crystallization of large units of POSS which are attached as side groups to a polymer chain, quickly leads to the realization that there are considerable

spatial constraints imposed on the crystal shape. In particular, it becomes clear that the development in three dimensions is impossible and that crystals will necessarily form either a columnar (1-dimensional) nano-crystal, with the polymer chain decorating the outside of the crystal, or, at best, a lamellar (2-dimensional) nano-crystal, again with the polymer lying on the external faces of the lamellac, Figure 5.5. This, of course, is entircly consistent with the preferential broadening of selected WAXS signals with others remaining noticeably sharper. Specifically, the signals at 4.57 and 10.5 Å in the copolymers can therefore be associated with planes approximately perpendicular to the short and long dimensions of the nanocrystal, respectively.

The distance between two POSS particles in the lattice of the copolymers is slightly smaller than that of the macromonomer on the basis of diffraction peak positions (i.e. larger 2θ) (8.4° vs. 8.2°, 11.1° vs. 11.0° and 19.4° vs.19.0°, Figure 5.3; e vs. f). Again this can be explained by our proposed constrained lattice in copolymers. In a three-dimensional lattice of POSS particles the lattice accommodates the substituted norbornylene group, which is slightly larger than the cyclopentyl groups on the remaining corners; in a dimensionally constrained crystal lattice of POSS copolymers the large norbornylene groups, which are connected to the polymer backbones, are likely to be excluded from the lattice, (Figure.5.2 and 5.5).

Further information is obtained from the oriented WAXS from the drawn material, Figure 5.4. The texture is consistent with the 10.5 Å spacing in the POSS crystal (considered to be the long axis in the crystallites) lying parallel to the draw direction. The PE WAXS component does not show simple chain orientation; rather this appears consistent with a texture with c_{PE} lying in the planc of the film but inclined at a

slight angle to the draw direction, and in which a_{PE} and b_{PE} are randomized about c_{PE}. Therefore, hk0s appear equatorial in the edge-on projection in WAXS (Fig. 5.4b) and the inclination of c_{PE} to the draw direction is only revealed in the normal projection (Fig. 5.4a). Moreover, the angle of inclination of c_{PE} was found to be variable. Clearly, as opposed to orientation of chains, drawing has rather promoted orientation of the crystallites. It is important to note that drawing was carried out below the melting point of both crystal components. The oriented pattern indicates that POSS crystallites have aligned parallel to the drawing direction while the PE crystals are inclined at some variable angle to this direction. The variability of the alignment of PE crystalites with respect to the draw direction (and therefore to the alignment of the POSS crystals) suggests that the two crystalline components are not directly in contact and that they must be separated by a region of uncrystallized material (hence providing a location for the considerable quantity of uncrystallized PE). The POSS crystallites are clearly the features primarily aligning along the draw direction and these, in turn, "pull" and "rotate" the PE crystallites with them. The absence of chain orientation, even at a relatively high draw ratio of ~3, may also be explained by the covalent connectivity between the PE and POSS. Such chain orientation would require the PE crystallites to "pull-out" and fragment and, accordingly, would also require the POSS crystallites to fragment. The POSS crystals can then be regarded as a source of reinforcement for the PE crystallites.

This, of course, has implications for other properties. The observed improvement of dimensional stability, with retention of shape well above the melting temperature of polyethylene, can also be attributed to POSS nano-crystals acting as physical cross-linking points. The observed extension of the rubbery plateau above the melting

temperature of polyethylene in mechanical tests, is also explicable in these terms.[71] Such a POSS structure may also be expected to play a role in the improved oxidative stability seen in PE-POSS nanocomposites, facilitating the formation of an effective protective coating of SiO_2.[52] Indeed, the formation of POSS nano-crystals readily explains the change in rheological properties and the increase of glass transition temperature observed in many other POSS copolymers.

Finally, the interfacial property of POSS nanoparticles can be tuned by changing the substitution groups R at the corners of each POSS unit (Figure. 5.1), to increase or decrease the compatibility between the POSS and polymer matrix. In our specific system, with cyclopentyl groups on POSS and a PE matrix, we found very clear separation of the two components into different crystal domains.

5.5 Conclusion

Polyethylene-co-POSS random copolymers of 0.64-3.4 mol % (corresponding to 19-56 wt %) have been characterized using WAXS. Crystallites of both polyethylene and pendant POSS nanoparticles were found to coexist in the copolymers. This leads to a "mutually dependent" microstructure in which no one component can be said to be controlling. The presence of POSS nanoparticles lowers the crystallinity of the PE component and results in smaller/disordered PE crystallites. On the other hand, POSS crystallites do not show full three dimensional development but rather grow within spatial constraints imposed by the presence of the polymer chain, leading to an anisotropic crystallite shape. The anisotropic shape of the POSS crystallites was particularly displayed during mechanical drawing at elevated temperature (but below the melting point). The anisotropic POSS crystallites were found to be the primary component

responding to the draw, aligning with their major dimension parallel to the draw direction. The PE crystallites (of course, covalently attached to the POSS crystallites) were less responsive to the draw. This leads us to conclude that the surfaces of the PE and POSS crystals cannot be connected directly and that disordered material must lie within this interfacial region.

The POSS lattice formed shows very similar diffraction characteristics to both crystals of unpolymerized POSS macromonomer and to those reported in POSS crystals formed in other POSS containing copolymers. Consequently, it was concluded that very similar crystal structures were formed in all these cases.

An important conclusion from this study is that an anisotropically shaped, inorganic structure is formed from isotropic POSS nanoparticles covalently bonded to polymer chains (which are the source of the limitation of POSS crystal growth). The use of POSS as assembling blocks of aggregated structures may open the door for the design and synthesis of novel type of nanocomposites. Many physical properties observed in clay polymer nanocomposites, such as low gas permeability, can also be envisaged in polymer systems containing anisotropic nanostructures of POSS.

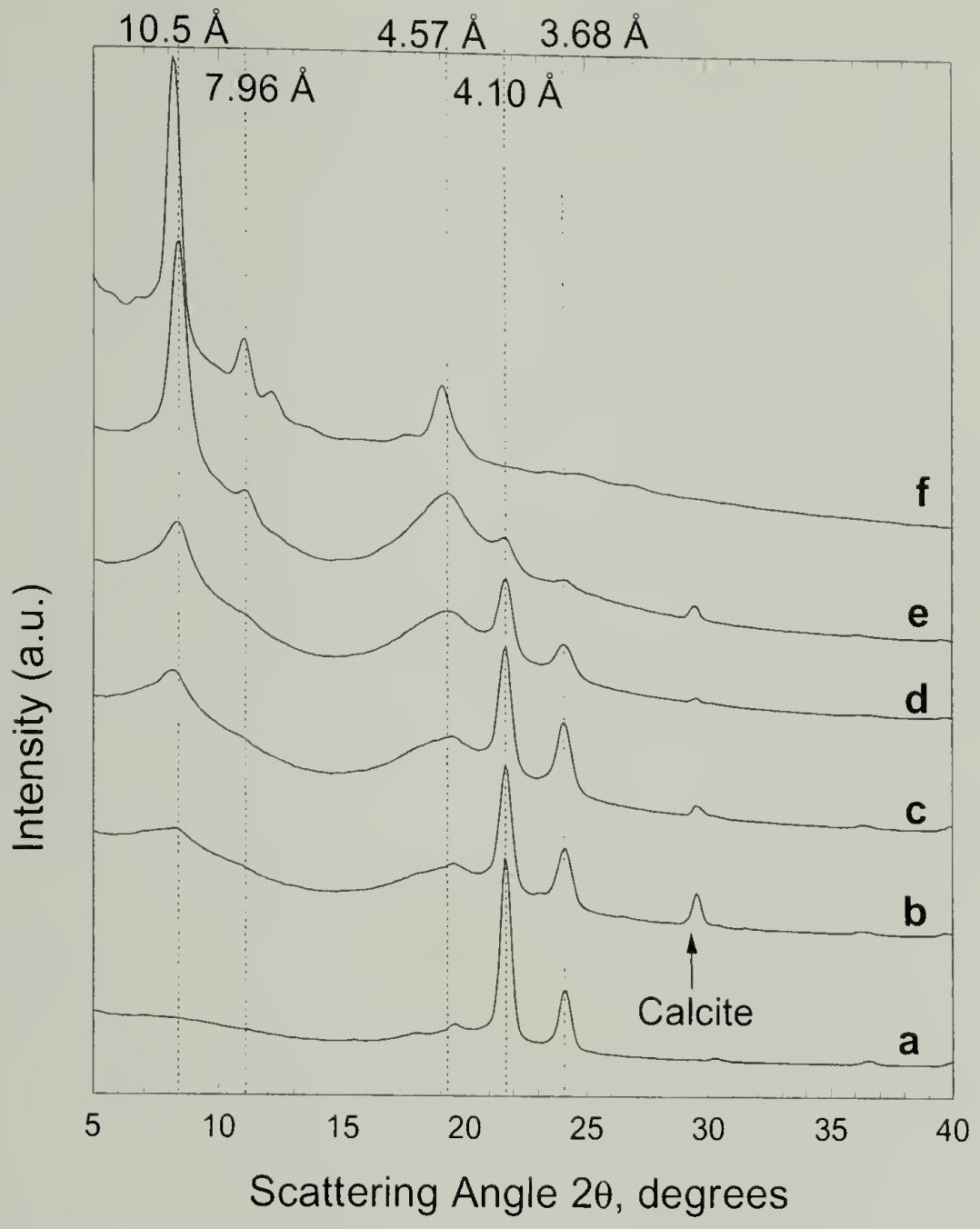

Figure 5.3 Line Profiles of WAXS Data of PE-co-POSS Copolymers. (a) PE, (b) PE-POSS 19wt% (0.64 mol%), (c) PE-POSS 27wt% (1.0 mol%), (d) PE-POSS 37wt% (1.6 mol%), (e) PE-POSS 56wt% (3.4 mol%), (f) POSS-norbornylene Macromonomer.

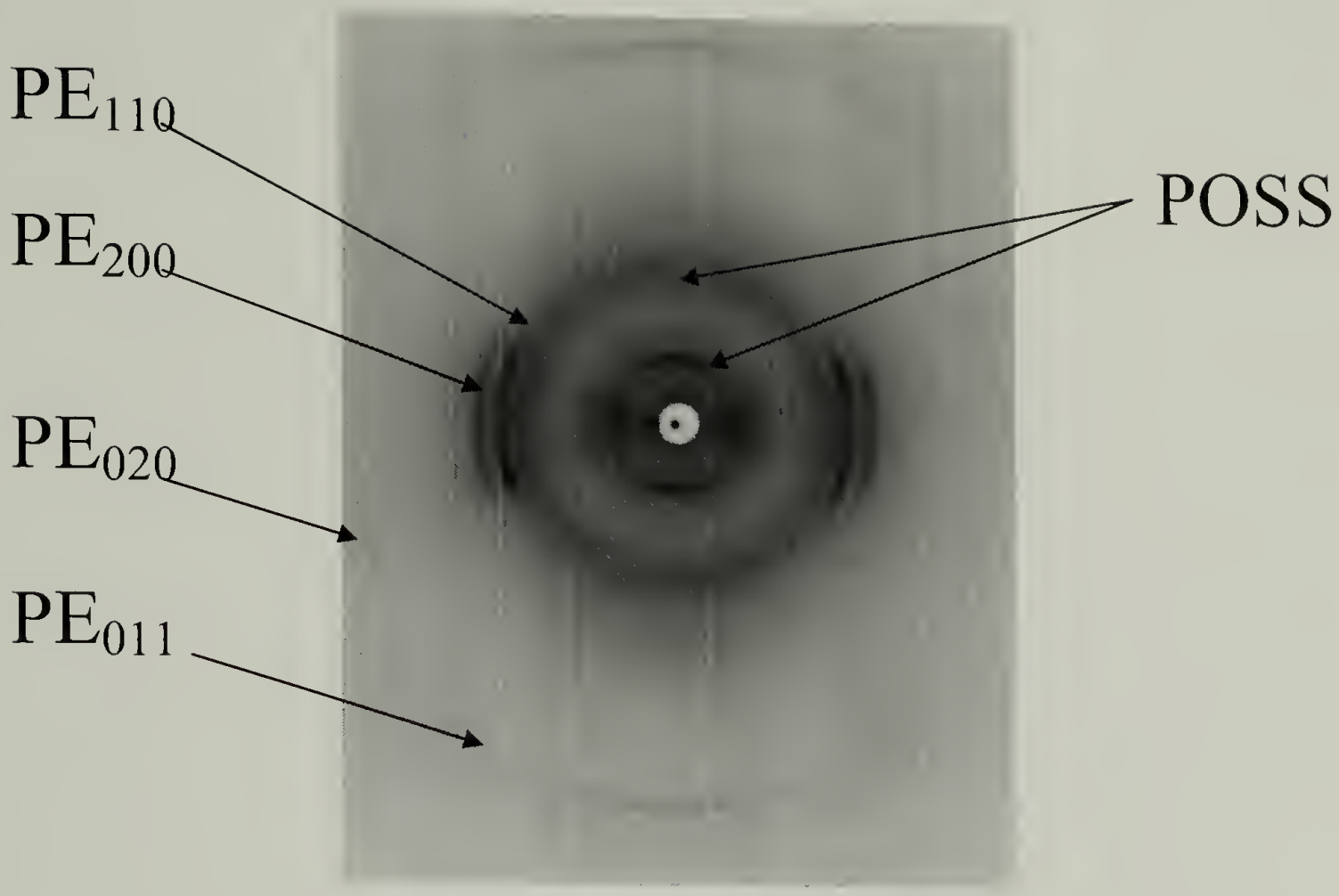

Figure 5.4 WAXS Pattern of PE-POSS37wt% Copolymer. (drawing direction is vertical, 3X). (a, top) X-ray Beam Was Normal to the Film, (b, bottom) X-ray Beam Was Edge-on to the Film.

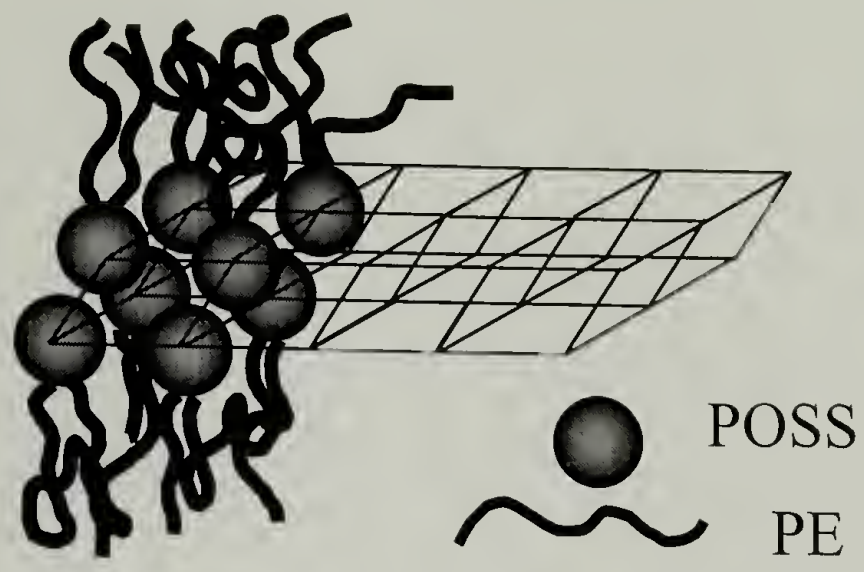

Figure 5.5 Schematic Drawing of a Two-Dimensional POSS Lattice Formed in PE-POSS Copolymers.

CHAPTER 6

POLYMER NANOCOMPOSITES BY CONTROLLED SELF-ASSEMBLY OF CUBIC SILSESQUIOXANES

6.1 Introduction

One of the most challenging goals of nanoscience and nanotechnology is to efficiently fabricate desirable nanostructures. Self-assembly has been extensively utilized for this purpose to generate ordered supramolecular architectures based on a variety of non-covalent interactions.[82,83] Two main schemes have been used to achieve the hierarchical assembly of polymeric structures. Based on the volume fraction, molecular weight, and block incompatibility, using organic diblock copolymers to generate a range of differing morphologies is well known.[84,85] Comparable nanoscale morphological structures have been obtained for inorganic polymeric structures using sol-gel preparative methods utilizing an amphiphilic surfactant.[34-36] In either synthetic method, the fundamental principles that dictates aggregation and consequently ordering is based on a driving force of reducing surface energy between chemically linked, yet incompatible, blocks. To design organic-inorganic hybrid polymeric materials using these phenomena can be viewed as an indirect approach, in which block copolymers or surfactants are used as templating agents to seed nanostructures. While certain success has been observed using this approach, the long annealing time needed to achieve thermodynamically favorable structures and the problem of maintaining structure upon removal of the templates afterward have hindered its further applications.[38] In contrast, the approach of

building nanostructured material directly using suitable building blocks by controlling associative interactions of scaffolds, while still at early stage of development, shows great promise. Nevertheless, a considerable challenge lies in the understanding of specific interactions and the ability to manipulate them in order to design a polymeric structure with suitable primary chemical sequences which is amenable to secondary ordering at longer length scales.

Polymer nanocomposites are one of the first successful demonstrations to emerge from the rapidly expanding field of nanoscale science.[2-4] Combining the thermal stability and strength from the inorganic component and the easy of processing from organic polymer component, it holds the potential to bridge the performance gap between ceramics and organic polymeric materials. Specifically, the substantial improvements in tensile strength, and heat distortion temperature achieved at relatively low loadings of inorganic layered clays within a host polymer matrix permits structural components to be fabricated for use at elevated temperatures such as those found under the hood in an automobile. The morphology of polymer clay nanocomposites is composed of well dispersed individual mineral clay layers, with a thickness of 1 nm and an aspect ratio of 100-2000, within a polymer matrix. Preparations of nanocomposites of silicate clay and polymeric materials often times encounter the problem of unfavorable interactions between the hydrophilic surface of clays and hydrophobic polymers. This results in an incomplete dispersal or limited exfoliation. As a result, true polymer clay nanocomposites are successful only in selected systems despite the numerous attempts have been extended to most polymer materials. It presents an interesting and practically important challenge to find alternative approaches to obtain polymer nanocomposites.

Generally speaking, the approach to obtain polymer clay nanocomposites typically involves a top-down strategy with a goal of separating macroscopic mineral clays into nanometer sized individual layer. An alternative approach pursued in this work is to build the inorganic layered nanostructure using suitable self-assembly building blocks through a bottom-up approach.

Polyhedral oligomeric silsesquioxanes (POSS) are a family of molecularly precise isotropic particles with diameters of 1-3 nm depending on the sizes of the cage and their substitution groups.[6] Cubic silsesquioxanes have an inorganic cubic core comprised of Si_8O_{12} surrounded by eight tunable substitution groups, i.e. cycloaliphatic groups (Figure 6.1A). It has an approximate spherical diameter of 1.5 nm when R is cyclopentyl group. Efficient synthetic methods have been developed whereby one of the corner groups is substituted by a functional group capable of undergoing polymerization.[10] This has provided the possibility to incorporate inorganic POSS cages into organic polymer chains. On the basis of previous work,[68] it has been realized that cubic silsesquioxanes can self-recognize and assemble into hexagonal crystalline lattice similar to a structure obtained from close packed hard spheres. Upon connection to the polymer backbone, which serves as the source of confinement, the crystalline lattice from these isotropic particles will be forced to adopt an anisotropic two-dimensional lattice. A new model of layered inorganic clay-like structure has been designed based on this observation. In this design, cubic silsesquioxane particles are used as self-recognition assembly blocks to build a layered nanostructure (Figure 6.1C).

6.2 Results and Discussion

To demonstrate the concept, a series of random copolymers comprising polybutadiene (PBD) and cubic silsesquioxane was designed. The copolymers were synthesized by ring-opening metathesis copolymerization (ROMP) of 1,5-cyclooctadiene and cubic silsesquioxane bearing a polymerizable norbornene group using a catalyst $RuCl_2(=CHPh)(PCy_3)_2$ (Figure 6.1B). ROMP of cyclooctadiene provides 100% 1,4-polybutadiene as polymer backbones. Samples with different incorporation of POSS (12 - 53 wt %) were obtained simply by changing the feed ratio between cyclooctadiene and POSS. The weight average molecular weights of these copolymers are in the range of 67-88 kg/mol, with polydispersity indices around 1.7-2.0 (Table 6.1). The POSS are randomly distributed along the polymer backbone based on NMR data (see the support information). The physical appearance of the copolymers changes dramatically from viscous liquid of 0 % POSS to elastomeric material with 23 wt% or greater POSS loadings. According to the design, the morphology of these materials is predetermined through the specific interactions between cubic silsesquioxanes.

Table 6.1 Summary of Molecular Weight Data of PBD- POSS Copolymers

Sample	POSS (wt %) in Feed	POSS in Copolymer[a]		M_w[b] (kg/mol)	PDI[b]	trans/cis[c]
		wt%	mol%			
PBD	0	0	0	68	1.7	61 : 39
PBD-POSS1	10	12	1.4	67	1.7	56 : 44
PBD-POSS2	20	23	3.0	71	1.8	53 : 47
PBD-POSS3	30	33	5.0	74	1.8	57 : 43
PBD-POSS4	40	43	7.5	79	1.9	55 : 45
PBD-POSS5	50	53	10.8	88	2.0	51 : 49

[a] As determined by ^{1}H-NMR in $CDCl_3$.

[b] Weight average molecular weight as determined by GPC in THF, versus narrow molecular weight polystyrene standards.

[c] Trans/cis ratio of backbone unsaturations as determined by ^{13}C-NMR of olefin region in $CDCl_3$.

Wide angle X-ray diffraction (WAXS), which is used to characterize crystalline structure, can provide evidence of POSS aggregation and precise information of crystalline lattice of POSS nanostructure. Shown in figure 6.2A are the diffraction profiles of PBD-POSS1 to PBD-POSS5. For comparison, traces of PBD and POSS are also drawn respectively. The pure PBD shows a broad peak at 2θs of 19.5° (4.55 Å), corresponding to the amorphous halo. The pure POSS shows strong reflections at 2θs of 8.2° (10.8 Å), 11.0° (8.03 Å), 12.1° (7.31 Å) and 19.0° (4.66 Å). These are associated with the hexagonal crystalline structure of POSS from 101, 110, 111 and 300/113 diffraction planes with a hexagonal unit cell of a = 16.06 Å and c = 17.14 Å. It is clear that the copolymers show features which are characteristic of the structures of the two separate components. The PBD-POSS1 sample with lowest POSS content in this series is dominated by the PBD amorphous halo. However, an additional peak at 8.3° (10.6 Å) also appears. The next sample PBD-POSS2 shows a third peak at 11.1° (7.96 Å). These clearly correspond to the strong POSS reflections. As the POSS content increases, the reflections from the POSS component increase in intensity compared with PBD. At the highest POSS content, 53% wt.% (10.8 mol %), the sample shows only a weak PBD halo and strong 101 and 110 diffractions from POSS , leading to the conclusion that more and more POSS particles aggregate and form crystalline structure with increasing of POSS concentrations. The strong diffraction from POSS 300/113 diffraction planes at 19° is shown to be a broad peak overlapping with the peak from PBD due to close peak positions. In contrast to the sharp diffractions in the POSS, the broadening was attributed to the anisotropic shape of crystals.[68] The crystallization of POSS which are attached as

side groups to a polymer chain, can easily lead to the realization that there are considerable spatial constraints imposed on the crystal shape. In particular, it becomes clear that the crystal development in three dimensions is impossible and that crystals will necessarily form either a columnar (1-dimensional), or, most likely, a lamellar (2-dimensional) lattice, with the polymer lying on the external faces of the lamellae. In a constrained crystal lattice, the diffraction planes associated with long dimensions (length and width in a lamellar structure) show sharp diffraction, while the one with short dimension (thickness) shows broad peaks.

Although WAXS data indicated anisotropic crystalline aggregation of POSS nanoparticles in PBD-POSS random copolymers, it could not unambiguously prove the nanoscaled morphology formed by POSS particles. As a result, transmission electron microscopy (TEM) studies were carried out. The contrast in a TEM micrograph is originates from diffraction and mass-thickness contrast. POSS, due to its silicon contents, are heavier than PBD chains which are comprised solely of hydrocarbon. In addition, the crystalline POSS domains as observed by WAXS diffract electrons more effectively than amorphous PBD. Both effects will render POSS darker in TEM imaging. Shown in Figure 6.3 are two TEM micrographs of PBD-POSS random copolymers with 12 and 43 wt% POSS incorporation. In Figure 6.3A, POSS were found to aggregate into short randomly oriented lamellae with the lateral dimensions of approximately 50 nm. The thickness of the lamellae was found to be approximately 3 ~ 5 nm and corresponded roughly to twice the diameter of a POSS nanoparticles. The morphology observed here is comparable to that of fully exfoliated nylon clay nanocomposites.[4] Increasing the incorporation ratio of POSS to 43wt%, the lamellae were found to be able to form

continuous morphology with lateral length on the order of microns (Figure 6.3C). The irregular lamellar spacing shown is possibly a combination of both POSS lamella twisting and the random nature of the copolymers. The morphology bears similarity to the lamellar morphology formed by precise diblock copolymers.

The lamellar morphology formed *via* controlled self-assembly of POSS particles is further supported by small-angle X-ray diffractions (SAXS, Figure 6.2B), where broad maxima were observed for all samples except PBD-POSS1. The peak positions correspond to the spacing between lamellae. The value can be simply calculated by $2\pi/q$, where $q = 4\pi/\lambda\sin(\theta/2)$ is the scattering factor. For example, the average distance between POSS layers is ~12 nm in the PBD-POSS4 sample. The lack of higher order reflections is a result of the random nature of the copolymers. The shift of broad maxima indicates the spacing changes on the basis of the POSS concentrations. In a high POSS concentration sample, such as PBD-POSS5, the inter-lamellar distance is much smaller due to the relatively lower PBD contents between two layers. These results indicate the possibility to control the length scale of fillers/matrix simply by changing their relative ratio.

Interestingly, the nanostructure of the PBD-POSS at high concentration resembles that of the nacre of abalone shell with alternating inorganic crystalline hard layers and soft organic rubbery layers.[7,23] This method, through self-assembly of POSS nanoparticles, is the first direct synthetic approach to obtain this type of layered organic-inorganic nanocomposite structure in bulk materials. This controlled self-assembly process is noteworthy considering the random nature of the copolymers and broad molecular weight distribution (Polydispersity Index ~ 2). Other assembly methods, specifically surfactant and block copolymer approaches, require the use of well defined

molecules or polymers. This work demonstrates it is possible to obtain ordered nanostructure from a random copolymer system, if specific interactions between chains are understood. In this specific case, it is utilizing a controlled/limited crystallization process of inorganic particles attached to polymer chains.

It should be noted that by switching the synthetic approach from top-down to bottom-up, the unfavorable behavior of phase separation has been changed into a favorable factor. Compared with the strategy to obtain polymer clay nanocomposites, this approach can easily achieve a "homogenous" organic-inorganic composite with an inorganic clay-shape filler uniformed distributed at the nanaometer range. The novel properties shown in the polymer clay system, such as flame retardance and reduced gas permeability associated with the anisotropic shape, are expected to be observed in assembled POSS systems.

In conclusion, we have shown it is possible to achieve nanocomposites through a bottom-up approach using cubic silsesquioxane nanoparticles. The morphology of the copolymers has been characterized by WAXS, TEM, and SAXS and clearly shows the formation of lamellar nanostructure of POSS aggregates, which bears the similarity, at low POSS loadings, to the morphology of exfoliated polymer clay nanocomposites. Taking advantage of controlled interactions between polymer chains, we open the door to the design of polymer materials at the important nanometer length scale beyond their primary sequences. Ultimately, this may provide materials with properties bridging the performance gap between polymer and ceramics.

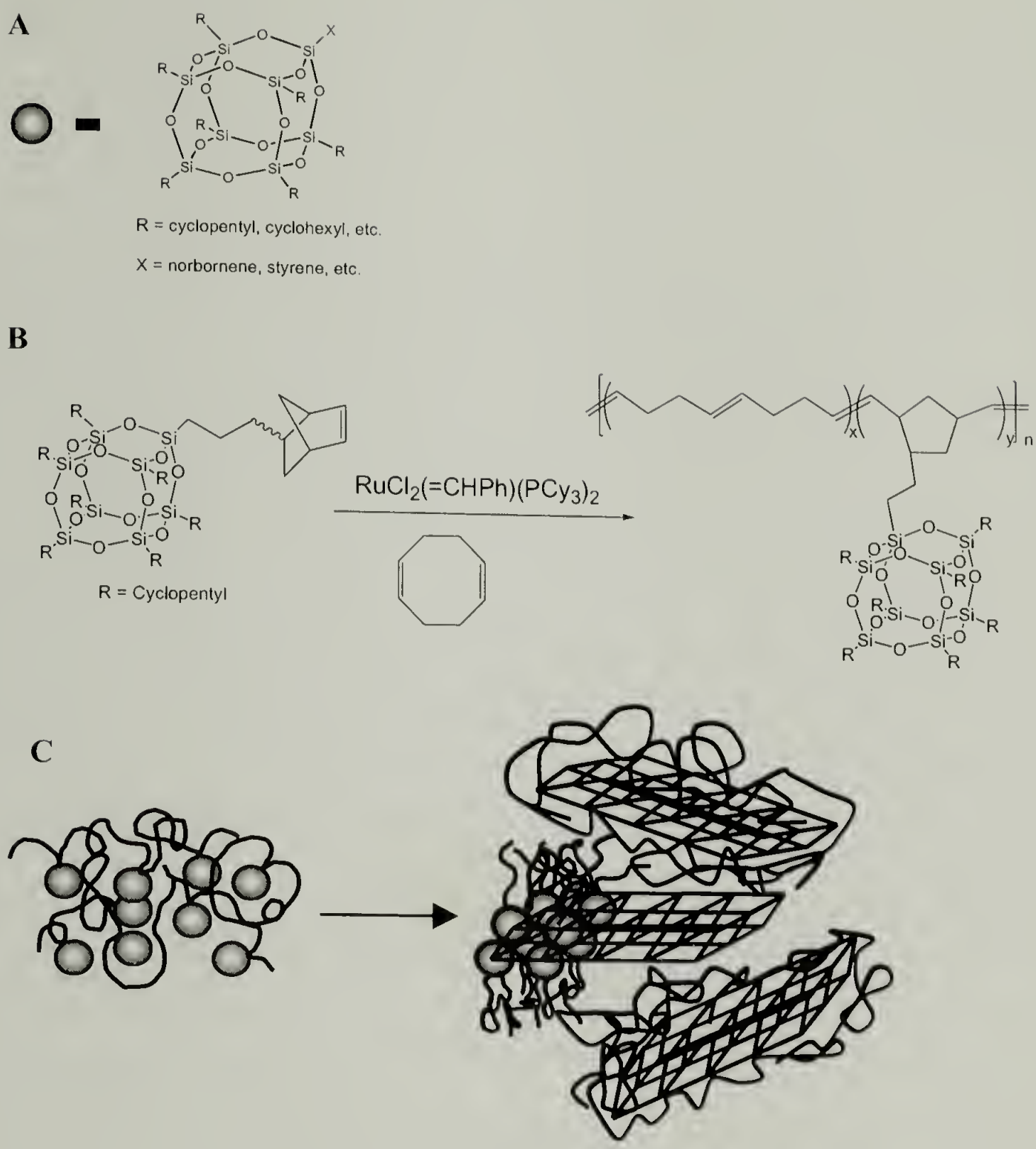

Figure 6.1 (A) Structure of POSS nanoparticles. (B) Synthesis of PBD-POSS copolymers. (C) Synthesis of Polymer Nanocomposites through Controlled Self-assembly of Cubic Silsesquioxane (POSS) Nanoparticles

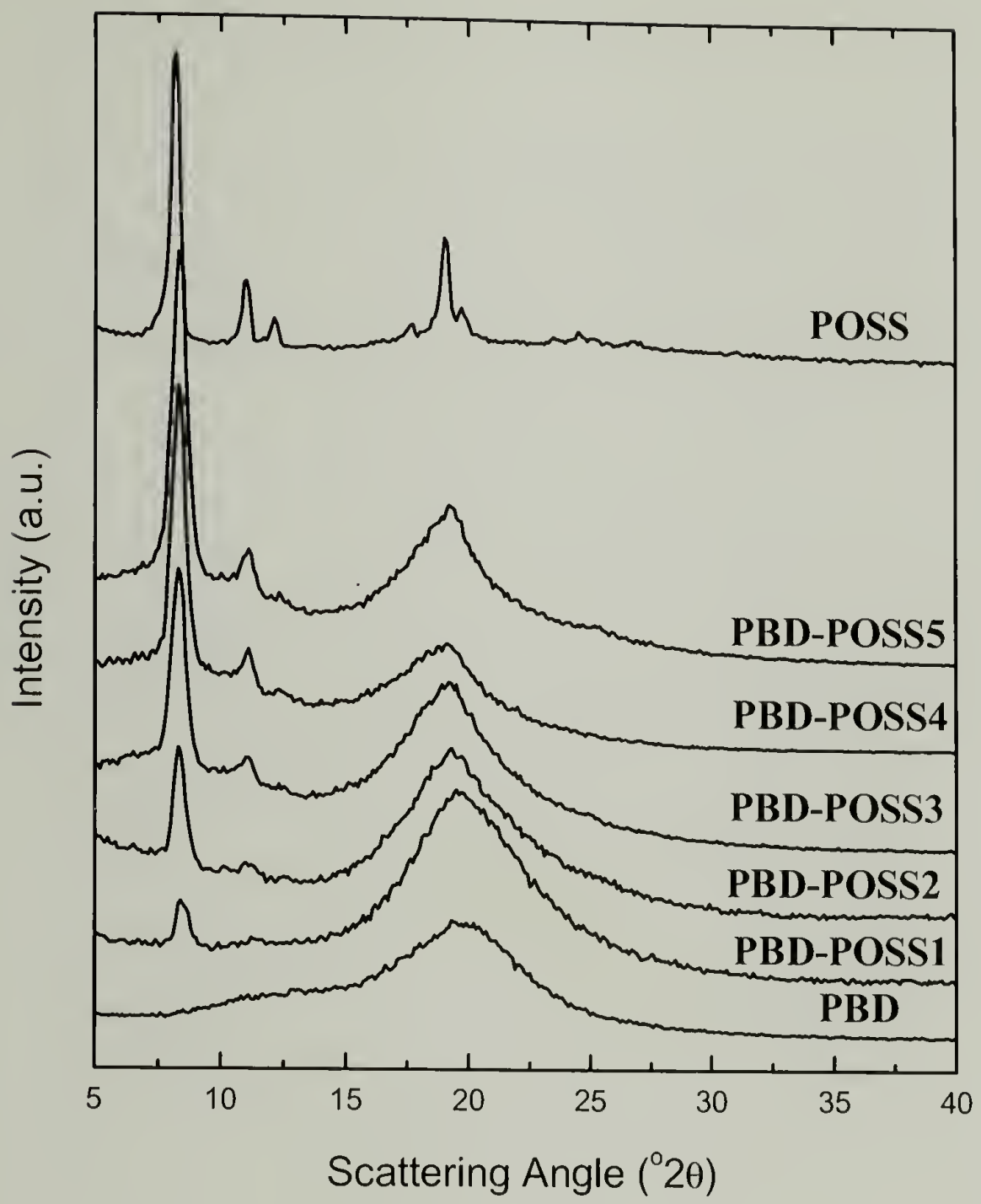

Figure 6.2 (A) WAXS of PBD-POSS

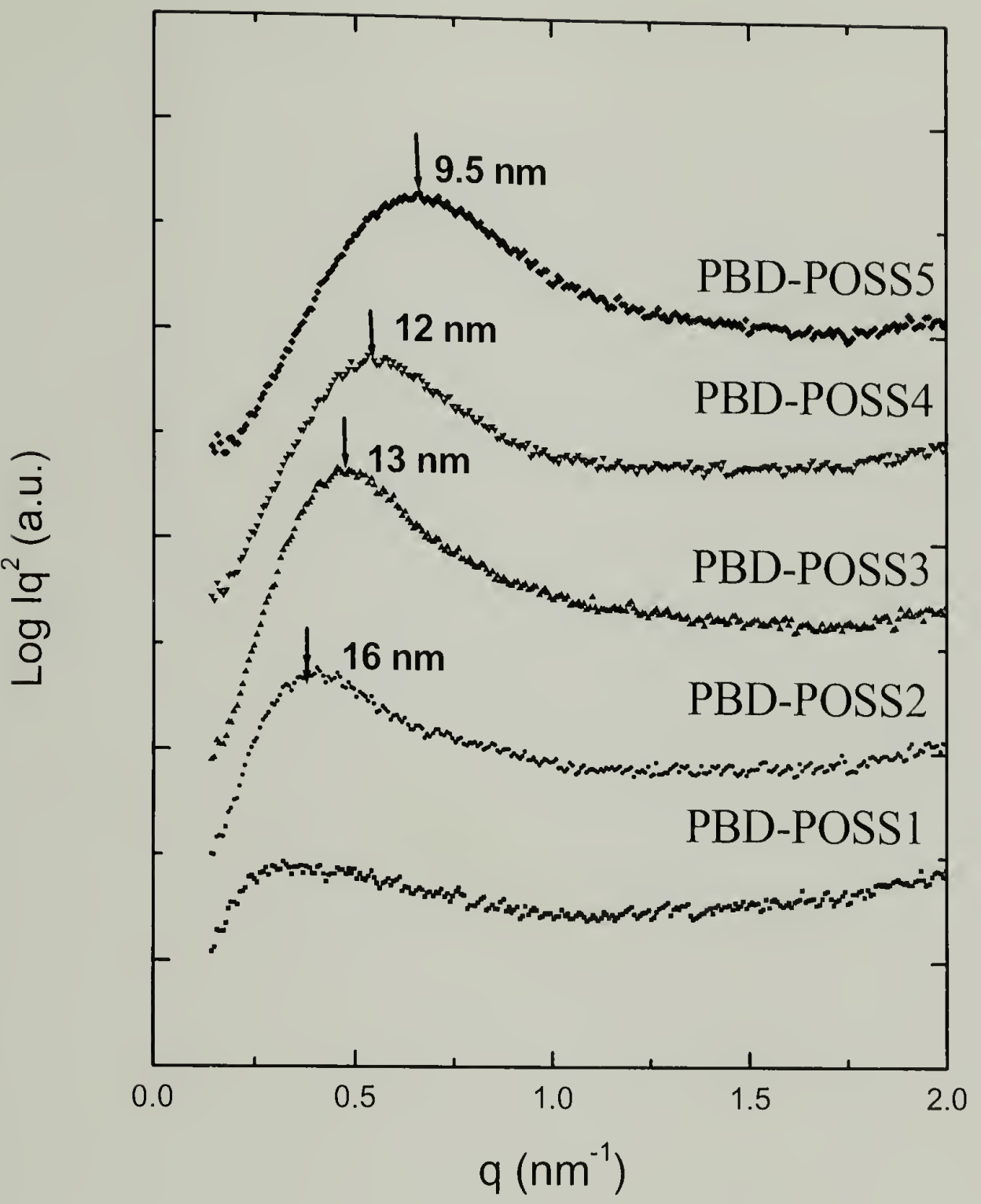

Figure 6.2 (B) SAXS of PBD-POSS

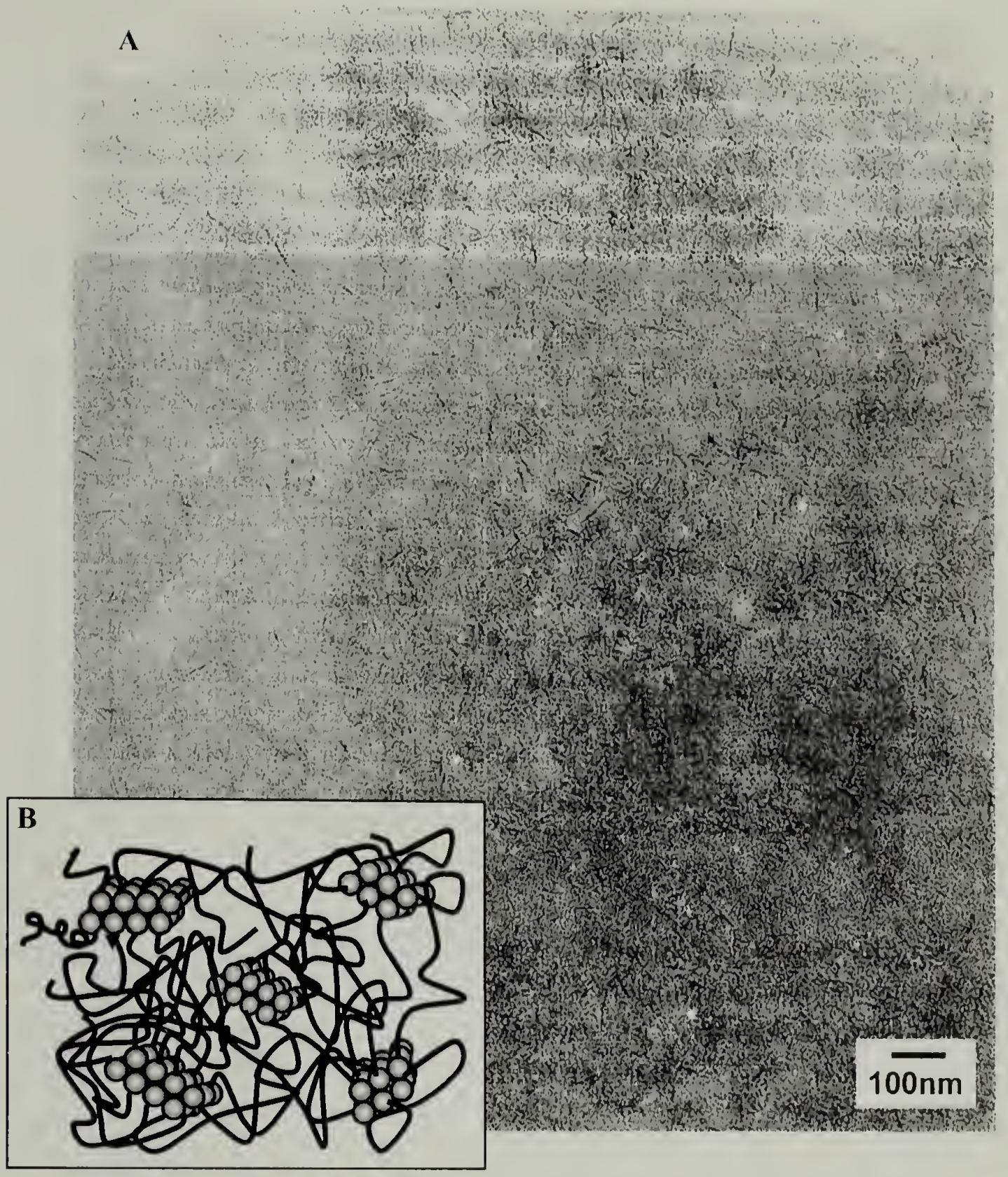

Figure 6.3 (A) TEM of PBD-POSS1. (B) Schematic drawing of PBD-POSS Assembly at Low POSS Concentration

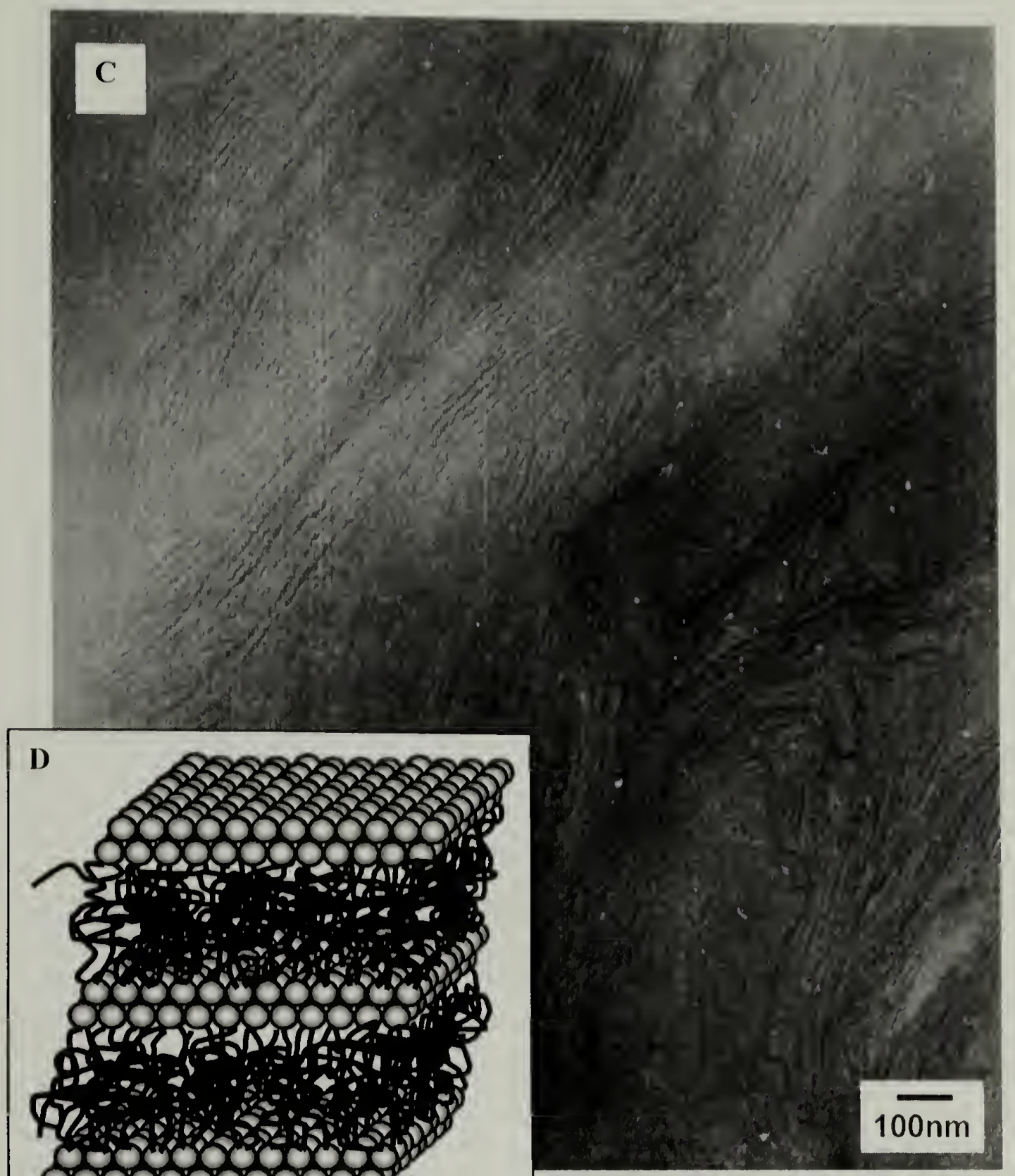

Figure 6.3 (C) TEM of PBD-POSS4. (D) Schematic Drawing of PBD-POSS Assembly at High POSS Concentration

6.3 Supporting Information

6.3.1 Materials

Cyclopentyl-POSS-norbornylene macromonomer 1-[2-(5-norbornen-2-yl)ethyl]-3,5,7,9,11,13,15-heptacyclopentylpentacyclo[9.5.1.1^{3,9}.1^{5,15}.1^{7,13}]octasiloxane (POSS-norbornylene) was provided by the Air Force Research Laboratory, Propulsion Directorate, AFRL/PRSM, Edwards Air Force Base, California. Other reagents were obtained from Aldrich. The catalyst $RuCl_2(=CHPh)(PCy_3)_2$ was purchased from Strem Chemical. Cyclooctadiene and methylene chloride were vacuum transferred from CaH_2 prior to use.

6.3.2 Polymerization Procedures for Polybutadiene-POSS Copolymers

9.74 mg (12 μmol) of $RuCl_2(=CHPh)(PCy_3)_2$ was dissolved in 1 mL of CH_2Cl_2 and added to a solution of 0.65 g cyclooctadiene (6 mmol, 500 equiv.) and 0.072 g POSS-norbornylene (0.070 mmol, 10 wt%) in 4 mL of CH_2Cl_2 in the glovebox. The reaction mixture was stirred for 24 hours under nitrogen at room temperature. The reaction was stopped by injection of 1 mL CH_2Cl_2 with a trace amount of ethyl vinyl ether and 2,6-di-tert-butyl-4-methylphenol. The copolymers were precipitated in 100 mL methanol, recovered by decanting the solvent and dried overnight under vacuum at room temperature. The polymerizations were repeated using varying amounts of , 0-50 wt%, to prepare a range of copolymers. The isolated yields were generally above 80%.

6.3.3 Polymer Characterization

^{1}H speetra were obtained at 300 MHz using a Bruker DPX-300 FT-NMR speetrometer. ^{13}C NMR speetra were reeorded in ehloroform-*d* with a Bruker DPX-300 FT-NMR speetrometer operating at 75 MHz. High temperature NMR were reeorded in tetrachloroethane-d_2 with a Bruker AMX-500 FT NMR speetrometer operating at 125 MHz. Gel permeation ehromatography was performed using a Polymer Lab LC1120 HPLC pump equipped with a Waters differential refraetometer deteetor. The mobile phase was THF with a flow rate of 1 mL/min. Separations were performed using 10^5 Å, 10^4 Å and 10^3 Å Polymer Lab eolumns. Moleeular weights were ealibrated versus narrow moleeular weight polystyrene standards.

6.3.4 Polymerization Results and Discussion

The eopolymerization between 1,5-eyelooetadiene and eyelopentyl-POSS-norbornylene maeromonomer 1-[2-(5-norbornen-2-yl)ethyl]-3,5,7,9,11,13,15-heptacyelopentylpentacyelo[9.5.1.1^{3,9}.1^{5,15}.1^{7,13}] oetasiloxane was employed to make polybutadiene POSS copolymers using Grubbs' eatalyst,[48] $RuCl_2(=CHPh)(PCy_3)_2$ (Figure 6.1B). The mole ratio of eyelooetadiene to eatalyst was fixed at 500:1 to yield moderately high moleeular weight polybutadiene. For the various eopolymerizations, POSS-norbornylene was added in the range of 10-50 wt%, relative to eyelooetadiene, to the reaetion mixture prior to addition of the eatalyst. The solutions remained homogenous throughout the entire reaetion. The polymers were reeovered by preeipitation in methanol and dried in vaeuum oven overnight.

Using ^{1}H NMR to determine the level of ineorporation of POSS maeromonomer in the copolymers revealed a steady inerease as the amount of POSS in the feed was

increased (Table 6.1). It also revealed no residual POSS-norbornenyl macromonomer. The conversion of cyclooctadiene was not complete (~ 80%) due to its low ring stain. In the relatively dilute solution polymerization condition (0.65 g cyclooctadiene/5 mL CH_2Cl_2), the thermodynamic equilibrium between copolymer, cyclic oligomer and residue monomer resulted in the maximum conversion to be roughly 80%. Dilute solution polymerization was chosen instead of neat bulk polymerization or concentrated condition simply due to the limited solubility of POSS macromonomer (~100 mg/mL). The wt% and mol% of POSS obtained from ^{1}H-NMR agreed with the feeding ratio if the conversion of cyclooctadiene was considered. The molecular weight characterization data of the polybutadiene POSS copolymers are also listed in Table 6.1. All of them are in the range of 67-88 kg/mol and molecular dispersity around 1.7-2.0. We believe the backbone sequences of copolymers are random, not block, based on the cross-metathesis mechanism between polymer chains as we described in previous report.[57] Although the POSS-norbornylene has much higher activity than cyclooctadiene, sufficiently long reaction time (24 hours) was chosen to allow for significant inter-chain cross metathesis to occur to ultimately afford random copolymers. The evidence for efficient cross metathesis comes from ^{1}H NMR studies of the final copolymers. The ^{1}H NMR of the copolymer with 53 wt% POSS at 100 °C in $C_2D_2Cl_4$ does not show any characteristic olefinic peaks from homopolymer of POSS-norbornylene (Figure 6.4) and therefore no significant amount of POSS-norbornenyl block segments are present in the copolymer. It was further supported by the olefin trans/cis ratio >1 since the maximum trans concentration possible is 50% due to the fact that one of two cis double bonds of

cyclooctadiene does not participate ROMP, and higher trans percentages can only be achieved through cross-metathesis.

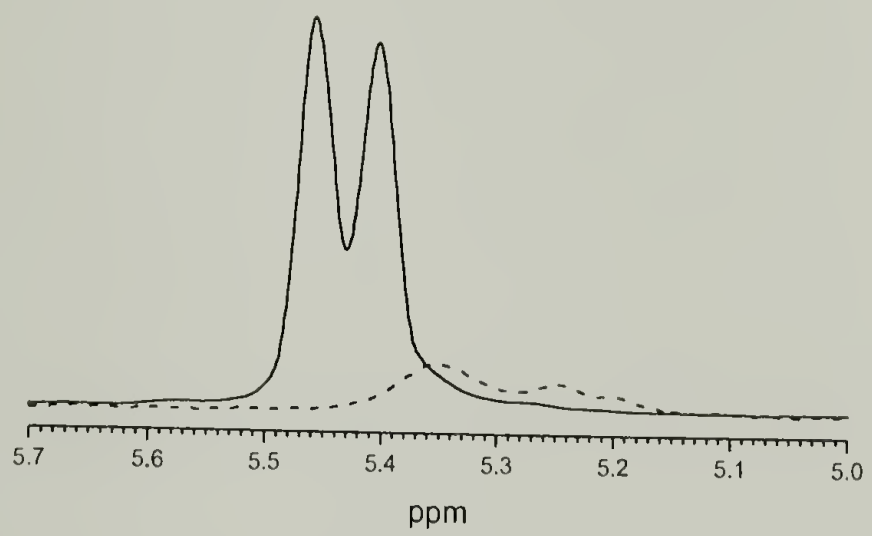

Figure 6.4 Olefinic Region ^{1}H NMR Spectra of PBD-POSS5 (Table 6.1, solid line) and Poly(POSS-norbornylene) (dashed line) at 100 °C in $C_2D_2Cl_4$

BIBLIOGRAPHY

(1) POSS(R) is a trademark of Hybrid Plastics www.hybridplastics.com.

(2) Giannelis, E. P. *Adv. Mater.* **1996**, *8*, 29-35.

(3) Pinnavaia, T. J.; Beal, G. W., Eds. *Polymer Clay Nanocomposites*; John Wiley & Sons: New York, 2001.

(4) Kojima, Y.; Usuki, A.; Kawasumi, M.; Okada, A.; Kurauchi, T.; Kamigaito, O. *J. Polym. Sci., Part A: Polym. Chem.* **1993**, *31*, 983-986.

(5) Novak, B. M. *Adv. Mater.* **1993**, *5*, 422-433.

(6) Lichtenhan, J. D. In *Polymeric Materials Encyclopedia*; Salamone, J. C., Ed.; CRC Press: Boca Raton, 1996; pp 7768-7777.

(7) Sellinger, A.; Weiss, P. M.; Nguyen, A.; Lu, Y. F.; Assink, R. A.; Gong, W. L.; Brinker, C. J. *Nature* **1998**, *394*, 256-260.

(8) Schwab, J. J.; Lichtenhan, J. D. *Appl. Organometal. Chem.* **1998**, *12*, 707-713.

(9) Lichtenhan, J. D.; Vu, N. Q.; Carter, J. A.; Gilman, J. W.; Feher, F. J. *Macromolecules* **1993**, *26*, 2141-2142.

(10) Lichtenhan, J. D.; Otonari, Y. A.; Carr, M. J. *Macromolecules* **1995**, *28*, 8435-8437.

(11) Haddad, T. S.; Lichtenhan, J. D. *Macromolecules* **1996**, *29*, 7302-7304.

(12) Lee, A.; Lichtenhan, J. D. *Macromolecules* **1998**, *31*, 4970-4974.

(13) Romo-Uribe, A.; Mather, P. T.; Haddad, T. S.; Lichtenhan, J. D. *J. Polym. Sci., Part B: Polym. Phys.* **1998**, *36*, 1857-1872.

(14) Lee, A.; Lichtenhan, J. D. *J. Appl. Polym. Sci.* **1999**, *73*, 1993-2001.

(15) Mather, P. T.; Jeon, H. G.; Romo-Uribe, A.; Haddad, T. S.; Lichtenhan, J. D. *Macromolecus* **1999**, *32*, 1194-1203.

(16) Shockey, E. G.; Bolf, A. G.; Jones, P. F.; Schwab, J. J.; Chaffee, K. P.; Haddad, T. S.; Lichtenhan, J. D. *Appl. Organometal. Chem.* **1999**, *13*, 311-327.

(17) Fu, B. X.; Zhang, W. H.; Hsiao, B. S.; Rafailovich, M.; Sokolov, J.; Johansson, G.; Sauer, B. B.; Phillips, S.; Balnski, R. *High Perform. Polym.* **2000**, *12*, 565-571.

(18) Hsiao, B. S.; White, H.; Rafailovich, M.; Mather, P. T.; Jeon, H. G.; Phillips, S.; Lichtenhan, J.; Schwab, J. *Polymer* **2000**, *49*, 437-440.

(19) Fu, B. X.; Hsiao, B. S.; Pagola, S.; Stephens, P.; White, H.; Rafailovich, M.; Sokolov, J.; Mather, P. T.; Jeon, H. G.; Phillips, S.; Lichtenhan, J.; Schwab, J. *Polymer* **2001**, *42*, 599-611.

(20) Nalwa, H. S., Ed. *Handbook of Nanostructured Materials and Nanotechnology*; Academic Press: San Diego, CA, 2000.

(21) Edelstein, A. S.; Cammarata, R. C., Eds. *Nanomaterials : Synthesis, Properties and Applications*; Bristol, Philadelphia : Institute of Physics Pub., 1996.

(22) Heuer, A. H.; Fink, D. J.; Laraia, V. J.; Arias, J. L.; Calvert, P. D.; Kendall, K.; Messing, G. L.; Blackwell, J.; Rieke, P. C.; Thompson, D. H.; Wheeler, A. P.; Veis, A.; Caplan, A. I. *Science* **1992**, *255*, 1098-1105.

(23) Mann, S. *Nature* **1993**, *365*, 499-505.

(24) Jackson, A. P. *P. Roy. Soc. Lond. B. Bio* **1988**, *234*, 415-425.

(25) Schubert, U. *Chem. Mat.* **2001**, *13*, 3487-3494.

(26) Schollhorn, R. *Chem. Mat.* **1996**, *8*, 1747-1757.

(27) Akporiaye, D. E. *Angew. Chem. Int. Ed.* **1998**, *37*, 2456-2457.

(28) Moller, K.; Bein, T. *Chem. Mat.* **1998**, *10*, 2950-2963.

(29) Ogawa, M.; Kuroda, K. *Bull. Chem. Soc. Jpn.* **1997**, *70*, 2593-2618.

(30) Sarikaya, M.; Aksay, I. A., Eds. *Biomimetics: Design and Processing of Materials*; Am. Inst. of Phys., New York, 1995.

(31) Heywood, B. R.; Mann, S. *Adv. Mater.* **1994**, *6*, 9-20.

(32) Tarasevich, B. J.; Rieke, P. C.; Liu, J. *Chem. Mat.* **1996**, *8*, 292-300.

(33) Bunker, B. C.; Rieke, P. C.; Tarasevich, B. J.; Campbell, A. A.; Fryxell, G. E.; Graff, G. L.; Song, L.; Liu, J.; Virden, J. W.; McVay, G. L. *Science* **1994**, *264*, 48-55.

(34) Aksay, I. A.; Trau, M.; Manne, S.; Honma, I.; Yao, N.; Zhou, L.; Fenter, P.; Eisenberger, P. M.; Gruner, S. M. *Science* **1996**, *273*, 892-898.

(35) Yang, H.; Kuperman, A.; Coombs, N.; MamicheAfara, S.; Ozin, G. A. *Nature* **1996**, *379*, 703-705.

(36) Lu, Y. F.; Ganguli, R.; Drewien, C. A.; Anderson, M. T.; Brinker, C. J.; Gong, W. L.; Guo, Y. X.; Soyez, H.; Dunn, B.; Huang, M. H.; Zink, J. I. *Nature* **1997**, *389*, 364-368.

(37) Keller, S. W.; Kim, H. N.; Mallouk, T. E. *J. Am. Chem. Soc.* **1994**, *116*, 8817-8818.

(38) Ogawa, M. *J. Am. Chem. Soc.* **1994**, *116*, 7941-7942.

(39) Jordan, J. W.; Williams, F. J. *Kolloid-Z.* **1954**, *138*, 40-48.

(40) Fukushima, Y.; Inagaki, S. *J. Inclusion Phenom.* **1987**, *5*, 473-482.

(41) LeBaron, P. C.; Wang, Z.; Pinnavaia, T. J. *Appl. Clay Sci.* **1999**, *15*, 11-29.

(42) Hasegawa, N.; Kawasumi, M.; Kato, M.; Usuki, A.; Okada, A. *J. Appl. Polym. Sci.* **1998**, *67*, 87-92.

(43) Brown, J. F.; Vogt, L. H. *J. Am. Chem. Soc.* **1965**, *87*, 4313-4317.

(44) Feher, F. J.; Newman, D. A.; Walzer, J. F. *J. Am. Chem. Soc.* **1989**, *1111*, 1741-1748.

(45) Pyun, J.; Matyjaszewski, K. *Macromolecules* **2000**, *33*, 217-220.

(46) Bharadwaj, R. K.; Berry, R. J.; Farmer, B. L. *Polymer* **2000**, *41*, 7209-7221.

(47) *http://www.hybridplastics.com/NanotechComp.htm*.

(48) Schwab, P.; Grubbs, R. H.; Ziller, J. W. *J. Am. Chem. Soc.* **1996**, *118*, 100-110.

(49) Hahn, S. F. *J. Polym. Sci. Part A:Polym. Chem.* **1992**, *30*, 397-408.

(50) Buchmeiser, M. R. *Chem. Rev.* **2000**, *100*, 1565-1604.

(51) Hillmyer, M. A.; Benedicto, A. D.; Nguyen, S. T.; Wu, Z.; Grubbs, R. H. *Macromol. Symp.* **1995**, *89*, 411-419.

(52) Gonzalez, R. I.; Phillips, S. H.; Hoflund, G. B. *J. Spacecraft and Rockets.* **2000**, *37*, 463-467.

(53) Loy, D. A. *Mrs Bulletin* **2001**, *26*, 364-365.

(54) Schmidt, H. *Polymer Based Molecular Composites*; Mater. Res. Soc.: Pittsburgh, PA, 1990.

(55) Kawasumi, M.; Hasegawa, N.; Kato, M.; Usuki, A.; Okada, A. *Macromolecules* **1997**, *30*, 6333-6338.

(56) Heinemann, J.; Reichert, P.; Thomann, R.; Mulhaupt, R. *Macro. Rapid Comm.* **1999**, *20*, 423-430.

(57) Zheng, L.; Farris, R. J.; Coughlin, E. B. *J. Polym. Sci., Part A: Polym. Chem.* **2001**, *39*, 2920-2928.

(58) Tsuchida, A.; Bolln, C.; Sernetz, F. G.; Frey, H.; Mulhaupt, R. *Macromolecules* **1997**, *30*, 2818-2824.

(59) dn/dc values are obtained from Wyatt. They agree well with the previously reported values (Horska, J.; Stejskal, J.; Kratochvil, P. *J. Appl. Polym. Sci.* **1983**, *28*, 3873.) at different wavelengths.

(60) Amiard, Y.; Bellissent, J.-P.; Marie, G. US Patent, 3,723,399, Mar. 27, 1973.

(61) Bergstrom, C. H.; Seppala, J. V. *J. Appl. Polym. Sci.* **1997**, *63*, 1063-1070.

(62) Bergstrom, C. H.; Vaananen, T. L. J.; Seppala, J. V. *J. Appl. Polym. Sci.* **1997**, *63*, 1071-1076.

(63) Brekner, M.-J.; Rohrmann, J.; Antberg, M. US Patent, 5,087,677, Feb. 11, 1992.

(64) Kaminsky, W.; Kulper, K.; Brintzinger, H. H.; Wild, F. R. W. P. *Angew. Chem. Int. Ed. Engl.* **1985**, *24*, 507-508.

(65) Resconi, L.; Cavallo, L.; Fait, A.; Piemontesi, F. *Chem. Rev.* **2000**, *100*, 1253-1345.

(66) Landrock, A. H. *Handbook of Plastics Flammability and Combustion*; Noyes Publication: Park Ridge, NJ, 1983.

(67) Jordens, K.; Wilkes, G. L.; Janzen, J.; Rohlfing, D. C.; Welch, M. B. *Polymer* **2000**, *41*, 7175-7192.

(68) Zheng, L.; Waddon, A. J.; Farris, R. J.; Coughlin, E. B. *Macromolecules* **2002**, *35*, 2375-2379.

(69) Voronkov, M. G.; Lavrent'yev, V. I. In *Topics in Current Chemistry*; Boschke, F. L., Ed.; Springer-Verlag: Berlin, 1982; Vol. 102, pp 199-236.

(70) Costa, R. O. R.; Vasconcelos, W. L.; Tamaki, R.; Laine, R. M. *Macromolecules* **2001**, *34*, 5398-5407.

(71) Zheng, L.; Farris, R. J.; Coughlin, E. B. *Macromolecules* **2001**, *34*, 8034-8039.

(72) Ishihara, N.; Kuramoto, M.; Uoi, M. *Macromolecules* **1988**, *21*, 3356-3360.

(73) Ishihara, N.; Seimiya, T.; Kuramoto, M.; Uoi, M. *Macromolecules* **1986**, *19*, 2464-2465.

(74) Pangborn, A. B.; Giardello, M. A.; Grubbs, R. H.; Rosen, R. K.; Timmers, F. J. *Organometallics* **1996**, *15*, 1518-1520.

(75) Po, R.; Cardi, N. *Prog. Polym. Sci.* **1996**, *21*, 47-88.

(76) Barry, A. J.; Daudt, W. H.; Domicone, J. J.; Gilkey, J. W. *J. Am. Chem. Soc.* **1955**, *77*, 4248-4252.

(77) Larsson, K. *Ark. Kemi* **1960**, *16*, 203-228.

(78) Larsson, K. *Ark. Kemi* **1960**, *16*, 209-214.

(79) Larsson, K. *Ark. Kemi* **1960**, *16*, 215-219.

(80) Auf der Heyde, T. P. E.; Burgi, H.-B.; Burgy, H.; Tornroos, K. W. *Chimia* **1991**, *45*, 38-40.

(81) Mather, P. T.; Chun, S. B.; Pyun, J.; Matyjaszewski, K. *Polymer Preprint (Am. Chem. Soc.)* **2000**, *41(1)*, 582.

(82) Whitesides, G. M.; Mathias, J. P.; Seto, C. T. *Science* **1991**, *254*, 1312-1319.

(83) Ikkala, O.; ten Brinke, G. *Science* **2002**, *295*, 2407-2409.

(84) Matsen, M. W.; Bates, F. S. *Macromolecules* **1996**, *29*, 1091-1098.

(85) Muthukumar, M.; Ober, C. K.; Thomas, E. L. *Science* **1997**, *277*, 1225-1232.